

Spin-Torsion, Braneworlds and Changing Symmetry in the Universe From the Beginning to the End

Leong Chung Wei Bernard

Darwin College

Cavendish Laboratory

Preface

This dissertation is the result of work carried out in the Astrophysics Group (formerly Radio Astronomy Group) of the Cavendish Laboratory, Cambridge between October 1999 and September 2002. Except where explicit reference is made to the work of others, the work contained in this dissertation is my own and is not the outcome of work done in collaboration. No part of this dissertation has been submitted for a degree or diploma or other qualification at this or any other university. The total length of this dissertation does not exceed sixty thousand words.

Bernard Leong
October 2002

Acknowledgements

The subject is a very much difficult and intricate one than at first one is inclined to think and I feel that I have not succeeded in catching the keynote. When that is found, the various results here given will no doubt appear in their real connection with one another, perhaps even as immediate consequences of a thoroughly adequate conception of the question.

- **Tait**

Our whole problem (in theoretical physics) is to make the mistakes as fast as possible.

- **J.A. Wheeler**

There are many people who I like to thank in the process of making this thesis a reality. First and foremost, I thank my supervisor, Professor Anthony Lasenby for the guidance and encouragement which he has given me over the past three years of my Ph.D. Of equal importance, I express my thanks to Dr Anthony Challinor, who I have benefitted from his guidance and ideas over the course of the past three years. I am also indebted to Dr Peter Dunsby, Professor Roy Maartens and Professor William Saslaw whom I have benefitted for their time and guidance with the exposure to the many facets of the subject in cosmology. The results of their guidance have led to the writing of this thesis. I thank D. Baumann, C. Doran, S. Gull, M. Hobson, Y. L. Loh, C. Martins, C. Van de Bruck and A. Sinha and my many colleagues in the Cavendish Astrophysics Group for many illuminating discussions and assistance.

Finally, I thank my parents, relatives, friends and teachers for their support and encouragement.

I gratefully acknowledge financial support from Overseas Research Studentship (ORS), Cambridge Commonwealth Trust (CCT) and Lee Foundation, Singapore.

Abstract

In this thesis, we explore three alternatives to the current paradigm of the standard inflationary big bang scenario. The three alternative themes are spin torsion (or Einstein-Cartan-Kibble-Sciama) theories, extra dimensions (braneworld cosmology) and changing global symmetry. In the spin torsion theories, we found new cosmological solutions with a cosmological constant as alternative to the standard scalar field driven inflationary scenario and we conclude that these toy models do not exhibit an inflationary phase. In the theme of extra dimensions, we discuss the dynamics of linearized scalar and tensor perturbations in an almost Friedmann-Robertson-Walker braneworld cosmology of Randall-Sundrum type II using the 1+3 covariant approach. We derive a complete set of frame-independent equations for the total matter variables, and a partial set of equations for the non-local variables, which arise from the projection of the Weyl tensor in the bulk. The latter equations are incomplete since there is no propagation equation for the non-local anisotropic stress. For the scalar perturbations, we found solutions that reveal the existence of new modes arising from the two additional non-local degrees of freedom (extra dimensions) under the assumption that the non-local anisotropic stress vanishes. Our solutions should prove useful in setting up initial conditions for numerical codes aimed at exploring the effect of braneworld corrections on the cosmic microwave background (CMB) power spectrum. For the tensor perturbations, we set out the framework of a program to compute the tensor anisotropies in the CMB that are generated in braneworld models. In the simplest approximation, we show the braneworld imprint as a correction to the power spectra for standard temperature and polarization anisotropies and similarly show that the tensor anisotropies are also insensitive to the high energy effects. Finally in the theme of changing global symmetry, we constructed a bounded isothermal solution embedded in an expanding Einstein de Sitter universe and showed that there is a possible phase transition in the far future.

Contents

1	Prologue	1
§1.1	Introduction	1
§1.2	The Standard Inflationary Big Bang Cosmology	3
§1.3	Three Alternatives to Standard Cosmology	6
§1.3.1	Spin-Torsion Theory	8
§1.3.2	Extra Dimensions	10
§1.3.3	Changing Global Symmetry	13
I	Spin-Torsion Theories	17
2	Spin-Torsion Cosmology	19
§2.1	Introduction	19
§2.2	Geometric Algebra and Gauge Theory of Gravity	21
§2.2.1	Geometric Algebra	21
§2.2.2	Gauge Theory of Gravity	22
§2.3	The Self-Consistent Dirac Field and the Field equations	24
§2.4	Massive Non-Ghost Solutions to ECKS theory	25
§2.4.1	Cosmological implications	30
§2.4.2	Massive Non-Ghost Solution	36
§2.5	Discussion	37
II	Braneworld Cosmology	41
3	Braneworld Cosmology I: Formalism	43
§3.1	Introduction to Braneworld Cosmology	43
§3.2	(1+3)-Covariant Approach in Cosmological Perturbation Theory	45
§3.3	Field Equations of Braneworld Cosmology	48

§3.4	Linearised perturbation equations for the total matter variables . . .	52
§3.4.1	Local and non-local conservation equations	53
§3.4.2	Propagation and constraint equations	54
§3.5	Cosmological Perturbations on the Brane	56
§3.5.1	Scalar Perturbations	56
§3.5.2	Vector Perturbations	61
§3.5.3	Tensor Perturbations	62
§3.6	A covariant expression for the temperature anisotropy	65
4	Braneworld Cosmology II: Initial Conditions and CMB Anisotropies	69
§4.1	From Perturbation Theory to CMB Anisotropies in Braneworlds . . .	70
§4.2	Perturbation dynamics and Initial Conditions of Scalar Modes . . .	72
§4.2.1	The CDM Frame	72
§4.2.2	The Energy Frame	85
§4.2.3	Discussion on the Scalar Modes	89
§4.3	Braneworld Tensor Anisotropies in the CMB	89
§4.3.1	A Local Approximation to the Nonlocal Anisotropic Stress .	91
§4.3.2	Discussion on the Tensor Power Spectra	94
III	Changing Global Symmetry	99
5	Changing Global Symmetry	101
§5.1	Introduction	102
§5.2	The Isothermal Universe	103
§5.2.1	The Isothermal Metric	103
§5.2.2	Properties and Implications of the Isothermal solution with a Global Phase Transition of the Universe	104
§5.2.3	Generalization of the Isothermal Metric to Finite Spheres . .	106
§5.3	The Isothermal Approximation	109
§5.4	Thermodynamic Consequences implied by the Generalised Equation of State	113
§5.5	A Solution of an Expanding, Centrally Isothermal Universe	115
§5.5.1	The derivation of the hybrid metric	117
§5.5.2	The validity of the matching of the metric	120
§5.6	Evolution of the Isothermal Universe - A Sequence of Hybrid Solutions	124
§5.7	Discussion	127

IV	Epilogue	129
6	Discussion	131
A	Conventions, Units, Sign Manifesto and Table of Symbols	137
§A.1	Conventions	137
§A.2	Units	138
§A.2.1	Conversion Factors	138
§A.2.2	Fundamental Constants	138
§A.3	Physical Parameters	138
§A.3.1	Cosmological parameters	138
§A.4	Sign Manifesto	139
§A.5	Table of Symbols	139
B	Identities in Geometric Algebra	143
§B.1	Multivectors	143
§B.2	Geometric Calculus	144
§B.3	Linear Algebra	145
C	Identities in Cosmological Perturbation Theory	147
§C.1	Differential Identities in the PSTF Approach	147
§C.2	The identities for the harmonics	149
§C.2.1	Scalar Harmonics	149
§C.2.2	Vector Harmonics	150
§C.2.3	Tensor Harmonics	151

List of Figures

1.1	A diagram (not drawn to scale) illustrating the history of the standard inflationary big bang cosmology.	7
1.2	A diagram (not drawn to scale) illustrating how the three alternative themes to the standard inflationary big-bang cosmology is altered with respect to fig.1.1.	9
1.3	A diagram depicting the Kaluza-Klein concept of compactification of extra dimensions: (a) Compactifying a 3-D Universe with two space dimensions and one time dimension which simplifies the picture of Kaluza and Klein. (b) The Lorentz symmetry of the large dimension is broken by the compactification and what remains is the 2-D space plus the U(1) symmetry represented by the arrow. (c) On large scales we see only a 2-D Universe (one space plus one time dimension) with the “internal” U(1) symmetry of electromagnetism. The diagram is reproduced from the article “The search for extra dimensions” by Abel and Russell in [1].	12
1.4	The matter fields (the electromagnetic, strong and weak nuclear forces) in the standard model are confined on the 3-brane (our observable Universe). Only gravity is allowed to propagate into the extra dimensions (i.e. the bulk). A collision between a proton and an antiproton can produce, for example, a single jet of matter particles plus graviton emission into the bulk. Such collisions might be seen in high-energy physics experiments. The diagram is reproduced from the article “The search for extra dimensions” by Abel and Russell in [1].	15

- 2.1 A sketch of the equation (2.55) with \dot{y}^2 vs y for both particle and anti-particle respectively, i.e. $\pm m$. This is for the case, $4m^2 \gg 3\Lambda$. The three regions of interest : (i) an expanding Universe with particle from an initial singularity (for $t > 0$) or a Universe contracting to a singularity in some finite time (for $t < 0$), (ii) an anti-particle Universe which expands to a finite value and contracts to a singularity (for $t > 0$), and (iii) an expanding anti-particle Universe (for $t > 0$) and a contracting Universe which bounces at $t = 0$ and expands indefinitely (for $t < 0$). 31
- 2.2 A sketch of the equation (2.55) with \dot{y}^2 vs y for both particle and anti-particle respectively, i.e. $\pm m$. This is for the extremal case: $4m^2 = 3\Lambda$. Like 2.1, we have three regions of interest : (i) an expanding Universe with particle from an initial singularity (for $t > 0$) or a Universe contracting to a singularity in some finite time (for $t < 0$), (ii) an anti-particle Universe which expands to a finite value and contracts to a singularity (for $t > 0$), and (iii) an expanding anti-particle Universe (for $t > 0$) and a static Universe which smoothly matches from $-t$ to t (for $t < 0$). 33
- 2.3 Graph of the scale factor $a(\tau)$ vs conformal time (in units of $H_0\tau$) for the particle and anti-particle solutions for the extremal Universes at $t > 0$ i.e. $4m^2 = 3\Lambda$ for $\Omega_\Lambda = 0.7$. The scale factor for flat Universe (with and without the cosmological constant) are plotted for comparison. Note that the scale factor for an extremal particle solution is similar to a flat universe with positive Λ , whereas the scale factor for an extremal anti-particle asymptotes towards a constant. 35
- 4.1 A figure which depict history of the different modes for the braneworlds. The KK mode, the CDM and the neutrino isocurvature modes will trail from the high energy to the low energy regime, after inflation. In the high energy regime, where $\rho/\lambda \gg 1$, there are 4 degenerate modes in the case of the braneworld. When the instantaneous transition from high to low energy regime ($\rho/\lambda \ll 1$) at $\rho/\lambda = 1$, the modes will be split up from four modes to two modes which correspond to the case in general relativity and the other remaining two modes which are the non-local isocurvature modes. The two remaining non-local isocurvature modes from the high energies are redshifted by approximately 10^4 if there is no dark energy term. Hence the only effect on the CMBR anisotropies is induced only by the KK mode. 90

4.2	The temperature power spectrum for tensor perturbations in braneworld models using the approximation in Eq. (4.151), with ζ the dimensionless KK parameter. Models are shown with $\zeta = 0.0, 0.1, 0.25, 0.5$ and 1.0 . The initial tensor power spectrum is scale invariant and we have adopted an absolute normalisation to the power in the primordial gravity wave background. The background cosmology is the spatially flat Λ CDM (concordance) model with density parameters $\Omega_b = 0.035, \Omega_c = 0.315, \Omega_\Lambda = 0.65$, no massive neutrinos, and the Hubble constant $H_0 = 65 \text{ km s}^{-1} \text{ Mpc}^{-1}$	96
4.3	The electric polarization power spectrum for tensor perturbations for the same braneworld models as in Fig. 4.2.	97
4.4	The magnetic polarization power spectrum for tensor perturbations for the same braneworld models as in Fig. 4.2.	98
5.1	Contour plot of j . Here $x \equiv (r/r_b)$. For $j \ll 1$, which characterizes almost all combinations of α and x , the deviation of the generalised metric from the ideal isothermal form is negligible.	110
5.2	Contour plot of the deviation term Δ . The plot gives the characteristic core region where the deviation from the perfect isothermal equation of state is less than a particular contour value. Note that although the ratio of the core radius to the boundary radius $x_c = (r_c/r_b)$ decreases with increasing α (and hence with step number), both r_c and r_b are monotonically increasing with each step. The decreasing x_c merely reflects their relative rates of increase. . .	111
5.3	Contour plot of the derivative of the deviation term ($d\Delta/dx$). The plots gives the core region (small $\alpha, r \ll r_b$) where the derivative is less than a particular value and the ratio of pressure to density is therefore nearly independent of position.	112
5.4	Surface plot of r_b – the model’s future laid out before us: It is interpreted as a map of the future scale of the generalised isothermal universe for particular values of α and A . The radius of the generalised isothermal sphere, r_b , is in units of centimeters, A is measured in $[cm^{-\frac{4\alpha}{1+\alpha}}]$ and α is dimensionless. r_b and A are plotted on a logarithmic scale. The hypothetical present size of the isothermal sphere is taken to be $r_b \sim 10^{25} \text{ cm}$ (the size of the Coma cluster).	126

Chapter 1

Prologue

I want to know how God created this world. I am not interested in this or that phenomenon, in the spectrum of this or that element. I want to know His thoughts; the rest are details.”

- **Albert Einstein**

“The future of the empirical world (or of the phenomenal world) is completely predetermined by its present state, down to its smallest detail.”

- **Karl Popper, “Conjectures and Refutations”**

“There is a coherent plan in the universe, though I don’t know what it’s a plan for.”

- **Fred Hoyle**

§1.1 Introduction

How did our Universe begin? Where did it come from and where is it heading to? How will our Universe end? These questions about the origin and the end of our observable Universe have fascinated many great thinkers from the ancient Greeks to the dawn of the 21st century. There is, perhaps, no question other than that of the origin of our Universe, which so transcends cultural and temporal divides, inspiring the ancient and modern philosophers, and the modern cosmologists. At a fundamental level, we yearn to find an explanation of why there is a Universe, how it has come to assume the form which we observe it to take, and what are the fundamental laws and principles that govern its evolution. Although some of the above questions are philosophical and metaphysical, there are still

others which are within the boundaries of scientific enquiry. Of course, we are interested here in the latter rather than the former.

How do we describe our physical universe? The global description of the observable Universe rests on two important attributes, namely the **cosmological parameters** from a physical theory and the **irregularities or inhomogeneities** which we observe. The cosmological parameters describe quantitatively the various features of the Universe, for example, the baryon density, Ω_b and the age of the Universe, t_0 . The irregularities or **density perturbations** describe the physics of the evolution of the matter components and how they are distributed irregularly throughout the Universe. Einstein's theory of general relativity is a theory of gravity which is used to study cosmology, and is thought to be an effective low energy theory from a more fundamental theory that we have no grasp of. The dynamics of the expanding Universe are characterized by the Hubble parameter that describes the expansion rate, H_0 , and the spatial curvature, Ω_K . The cosmological parameters are obtained from experiments, for example, the measurement of the cosmic microwave background (CMB) radiation, which can be characterized by a thermal distribution at a temperature of about 2.728 K. However, not all the cosmological parameters are measured accurately by one type of experiment. For example, there are experiments such as large galactic surveys and measurement of type I supernova that can give us other accurate cosmological parameters to compare to the CMB experiments. For the matter content of our Universe, we observe the visible baryonic matter. However, there is circumstantial evidence which suggest that there exists a large and dominant amount of nonbaryonic matter (or dark matter) in our Universe. To explain the issue of how the large scale structure of clusters and galaxies has emerged, we assume the existence of cold dark matter which comprises particles with negligible velocity. There could be other possibilities such as hot dark matter (particles that decouple when their velocities are relativistic) or something exotic. The final possibility with increasing support is that our Universe possesses a nonzero positive cosmological constant, Λ .

With these features, we have a reasonable description of our Universe. It remains a question how these features come to be the way they are. The answer lies in the search for an underlying theory of gravity which works from the Planck scale to the present size of our observable Universe. At present, there exists no theory of gravity which could work at the Planck scale although there are many candidates for these theories, namely **M/string-theory** and **loop quantum gravity**. On the other hand, an effective description beyond the Planck scale is expressed elegantly with Einstein's general relativity. General relativity provides an reasonable idea of how the cosmological parameters and the density perturbations come about. The resulting cosmology from general relativity is the standard **inflationary big bang cosmology** which assumes that there is a beginning of our Universe. In the

next section, we will summarize the central tenets of the standard inflationary big bang cosmology.

§1.2 The Standard Inflationary Big Bang Cosmology

In this section, we briefly sketch the theory of the standard hot big bang cosmology which is presented in many standard texts [109, 127, 131, 153, 154, 155]. The central premises of the theory are:

1. The Universe is isotropic and homogeneous on large scales based on the **Copernican** or **cosmological principle** which states that *there are no privileged observers in the Universe*. In general relativity, the observable Universe is described by the Friedmann-Robertson-Walker (FRW) metric* :

$$ds^2 = -dt^2 + a(t)^2 \left[\frac{dr^2}{1 - Kr^2} + r^2(d\theta^2 + \sin^2\theta d\phi^2) \right], \quad (1.1)$$

where K is the curvature constant which is $+1$ for a closed Universe, -1 for an open Universe and 0 for a flat Universe.

2. The Universe is expanding and obeys an empirical relation known as the Hubble law. An example of the Hubble law is the relationship between the “distance” to a galaxy[†], d_L and the observed redshift of a galaxy, z , which can be expressed by the following power series:

$$z = H_0 d_L + \frac{1}{2}(q_0 - 1)(H_0 d_L)^2 + \dots, \quad (1.2)$$

where H_0 is the present value of the Hubble constant ($H = (\dot{a}/a)$) which characterizes the age of the Universe, and q_0 is the deceleration parameter which measures the rate of slowing of the expansion[‡].

3. The Universe began from a state of infinite (or near infinite) density and temperature and then cooled with the expansion of the Universe.

*In this thesis, we adopt the choice of natural units and set $\hbar = c = G = 1$.

[†]An example of a distance indicator is the absolute luminosity L , which is defined as the energy per unit time produced by the source in its rest frame.

[‡] q_0 is defined in terms of the scale factor of the FRW metric to be:

$$q_0 = -\frac{\ddot{a}(t_0)}{a(t_0)H_0^2} \quad (1.3)$$

where t_0 denotes the present age of the Universe.

The big bang model makes accurate and scientifically testable hypotheses. The agreement with data from astronomical observations has given us considerable confidence in the model. The four key observational successes of the standard Hot Big Bang model are the following:

- **Expansion of the Universe:** Our Universe began about fifteen billion years ago in violent “explosions” at every point of spacetime. In an early super-dense phase, every particle started rushing apart from every other particle. At lower redshifts $z \lesssim 1$, the linear relationship between d_L and z is clear and convincing. One may determine H_0 from this linear relationship by making use of galaxies at relatively low redshifts. This linear relation at low redshifts was first discovered by Hubble [94].
- **Origin of the cosmic background radiation:** About 3×10^5 years after the Big Bang, the temperature of the Universe had dropped sufficiently for electrons and protons to combine into hydrogen atoms. This is known as the **recombination era**. After the recombination era, the cosmic microwave background photons just stream toward the observer at the present. Hence the temperature differences on this surface of last scattering become the anisotropies in the CMB temperature we see today. Since the recombination era, the radiation has propagated freely as it is unable to interact with the electrically neutral background matter (hydrogen atoms). The radiation constantly loses energy because its wavelength is stretched by the expansion of the Universe. The radiation temperature has fallen to approximately 2.728 K in the present day. This background temperature was discovered by Penzias and Wilson [157] in 1965. Subsequently, the temperature anisotropies ($(\Delta T/T) \sim 10^{-5}$) were discovered by the COBE satellite in 1992 [177]. The large angle CMB anisotropies probe the fluctuations in the early Universe, possibly due to the result of quantum mechanical processes during an epoch of inflation. The large scale structures of our present Universe are generated by these primordial fluctuations due to gravitational instability. A detailed description of the physics of these CMB anisotropies is given in [92, 93].
- **Nucleosynthesis of the light elements:** After the big bang occurred, the matter which consisted of free neutrons and protons, was very dense and hot. The temperature of the matter fell and some of the nucleons combined to form the light elements, for example, deuterium[§], helium-3, and helium-4. Theoretical calculations predicted that 25 per cent of the matter should be in the form of helium-4, a result which is in good agreement with current stellar observations. The heavier elements, of which we are partly made,

[§]The formation of deuterium depends crucially on the baryon/photon ratio.

were created later in the interiors of stars and spread widely in supernova explosions.

- **Formation of galaxies and large-scale structure:** The formation of galaxies and large-scale structure of our observable Universe, can be understood in the framework of the hot big bang model. At about 10,000 years after the big bang, the temperature had fallen to the point at which massive particles dominate the energy density of the Universe. The matter content of the Universe can affect structure formation by different processes which modify any primordial perturbations, for example, growth under self gravitation and effects of pressure and dissipative processes. As a result, we observe the large-scale structure of our Universe today.

Although the Big Bang model is successful, it is also plagued by various problems. Since there is no quantum theory of gravity, there exist the problem of initial conditions for the standard big bang cosmology. It does not explain why the Universe we observe is nearly flat (the flatness problem). Another interesting question, is that the comoving distance over which causal interactions can occur before the release of the cosmic microwave background is considerably less than the comoving distance that the radiation traverses after decoupling. It would imply that the microwaves arriving from regions separated by more than the horizon scale at last scattering which typically subtends about a degree, cannot have interacted before decoupling. The big bang model does not offer a satisfactory explanation for the nearly homogeneous temperature of the cosmic microwave background in the Universe. It requires that the homogeneity must be part of the initial conditions and this is known as the horizon problem. Finally, for the big bang to begin at a very high temperature, there are possible unwanted relics forbidden by observation which would survive till today, for example, the gravitino in supergravity theories or the moduli fields in superstring theory.

To deal with these inherent problems, an inflationary phase is incorporated into the standard big bang cosmology. The inflationary cosmology was proposed by Guth [78], Albrecht and Steinhardt [3] and Linde [129, 130]. It assumes that there is an epoch during which the scale factor of the Universe is accelerating. It is often described as a rapid superluminal expansion driven by a source, for example, a scalar field (or the **inflaton field**). A physical characterization of inflation is given by the following expression

$$\frac{d}{dt} \frac{1}{aH} < 0, \quad (1.4)$$

where $1/(aH)$ is the comoving Hubble length which is the most important characteristic scale of the expanding Universe. The condition for inflation is that the comoving Hubble length is decreasing with time. With inflation, the above mentioned

problems of the big bang cosmology are more or less cured (see [109, 127, 153, 155]). In the case of the flatness problem, inflation requires the condition that the critical density Ω is driven towards 1 rather than away from it. It would explain why the Universe is nearly flat. As for the horizon problem, we can allow our present observable Universe to emerge from a tiny region which was well inside the Hubble radius early on during inflation because of the large reduction in the comoving Hubble length during the inflationary phase. Finally, the relic abundances can be reduced by the expansion during inflation if they are produced before the inflationary epoch.

Another example of the many successes of inflation is that it provides the mechanism for setting the scale-invariant spectrum of density perturbations present in the CMB anisotropies. The discovery of the acoustic peaks in CMB anisotropies came from the recent balloon-based experiments such as BOOMERANG [115] and MAXIMA [14]. These acoustic peaks probe the information of the early Universe, since they depend mainly on the spectrum of initial fluctuations and fundamental cosmological parameters. Although inflation is a successful phenomenological theory that accounts for the large scale structure and various other features of the observable Universe, the inflaton field (or the scalar field) is not related to the Standard Model which has unified electromagnetism, strong and weak nuclear interactions in high energy theories. As a result, there are many different models of inflation (see [109, 127, 132]). The future experiments in the CMB and gravitational waves will be able to constrain the possible type of inflationary models that give us the present description of our observable Universe.

Of course, the above summary does not do enough justice to the development of cosmology for the last few decades. However, we can formulate an updated picture of the history of our Universe (see fig. 1.1). In the picture, we could see that considering the period after inflation, we can account for most of the features of our Universe with the present standard inflationary big bang cosmology.

§1.3 Three Alternatives to Standard Cosmology

The central aim of this thesis is to look at three alternative themes to the present cosmology. Although there exist recent alternative models of inflation [7, 13, 17, 72, 90, 104] which are constructed in a top-down approach from a plausible theory of quantum gravity, the focus of this thesis is taking the themes in alternative cosmologies from the bottom-up approach (or phenomenological theories) after the Planck scale. We adopt a modest approach in the subject and would like examine not all but some of these alternative models and their implications.

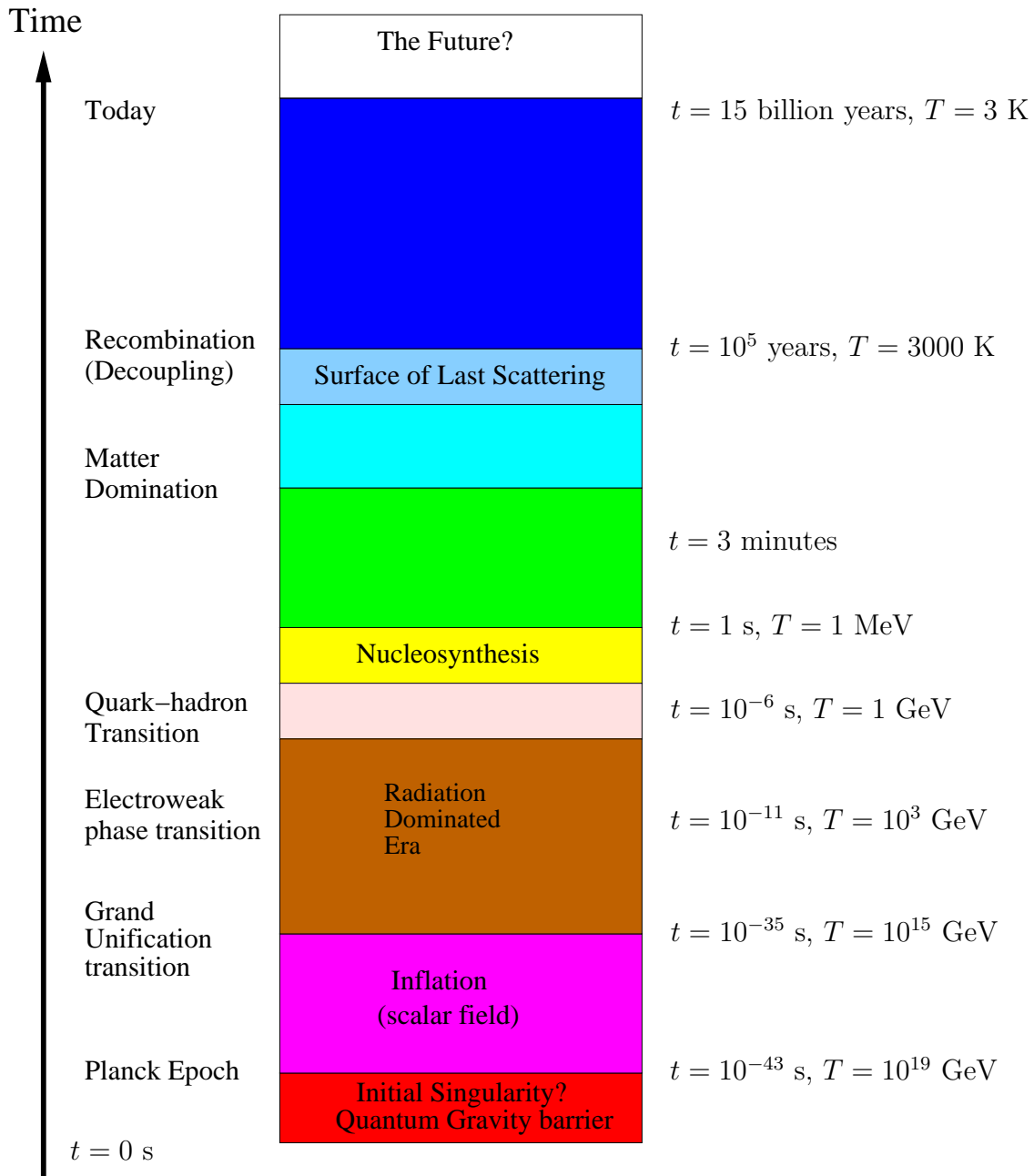


Figure 1.1: A diagram (not drawn to scale) illustrating the history of the standard inflationary big bang cosmology.

We hope to explore phenomenological possibilities in these alternative models if possible. There are reasons why these alternative themes would be an interest of study (see fig. 1.2 to see how they fit into the big picture). The first reason is

to explore alternative mechanisms to the standard inflationary big bang cosmology. One could ask whether we could substitute other possible inflationary driven fields that might give us an alternative to the standard scalar fields, for example, this theme will be explored in the **spin-torsion** or **Einstein-Cartan-Kibble-Sciama** (ECKS) theories. The second reason is that some of these alternative themes are required as basic premises to be integrated into theories which are plausible candidates for quantum gravity theories. For example, the premise of **extra-dimensions** is an essential feature in M/String theory. Finally, we explore the topic of **changing global symmetry** where we look at the possibility of our Universe undergoing a phase transition. We will discuss these topics in detail in the following sections.

§1.3.1 Spin-Torsion Theory

The concept of torsion is introduced as an extension to Einstein's theory of relativity for various reasons [70]. These theories of gravitation included with torsion are built upon Cartan's earlier suggestion in [28] that the torsion (the anti-symmetric part of the connection) should be identified as a possible physical field. The first reason, perhaps a historical one, is that it creates an analogy of general relativity with the theory of dislocations for the study of materials in continuum mechanics. Yet, there is no reason to believe that the structures are inherently similar for both general relativity and continuum mechanics. The next and perhaps more plausible reason is that torsion theories are good candidates to formulate gravity as a gauge theory, for e.g. [38, 56, 81, 97, 98, 105, 142, 185]. Proceeding from the premise that torsion theories are possible candidates of a gauge theory of gravity, one possible extension of general relativity, known as **spin-torsion** theory can be found by the gauge-theoretic approach in [82]. In spin-torsion theory, the connection between torsion and quantum spin was identified in [105, 173, 192] when it was realised later that the stress energy tensor for a massive fermion field was not symmetric [43, 193].

In the presence of torsion, the standard cosmology would be significantly altered. The first results were discussed in [83, 103, 194]. The singularity theorems in the presence of torsion may be suppressed in a wide class of models [82]. In addition, Kerlick [102] has shown that if a Dirac field provides the source of matter, then the energy condition in the singularity theorems is weakened by the presence of torsion, leading to an enhanced singularity formation rate. Hence it is of considerable interest to study cosmological solutions and their implications in such scenarios.

Recently, a gauge theory of gravity (GTG) has been developed by Lasenby, Doran and Gull [121]. The gauge theory of gravity is based on the reformulation of physics in Clifford algebra pioneered by Hestenes and his collaborators in [85,

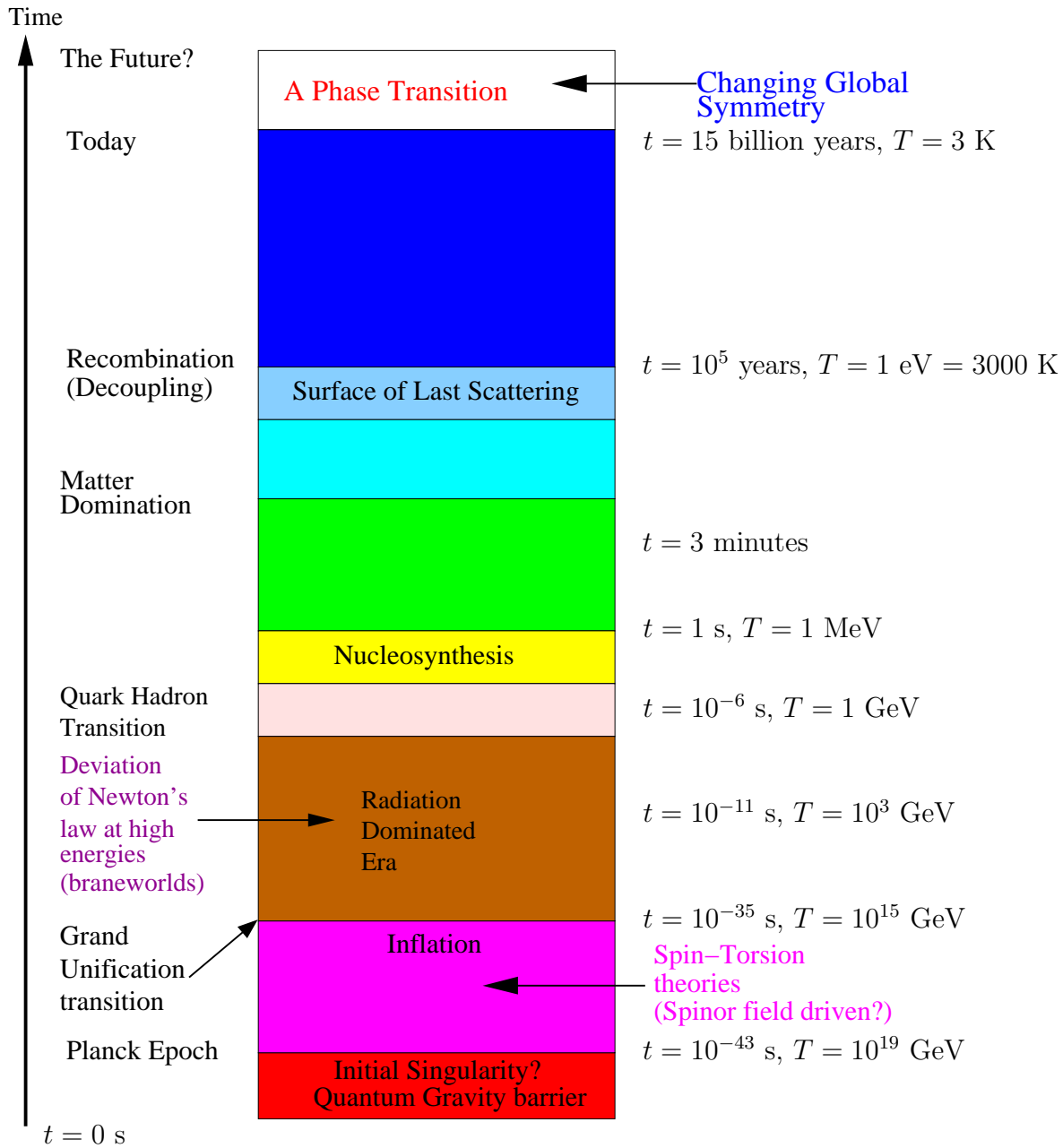


Figure 1.2: A diagram (not drawn to scale) illustrating how the three alternative themes to the standard inflationary big-bang cosmology is altered with respect to fig.1.1.

86, 87, 88]. In the GTG approach, the gravitational effects are described by a pair of gauge fields defined over a flat Minkowski background spacetime. These

gauge fields ensure the invariance of the theory under arbitrary local displacements and rotations in the background spacetime, and the physical predictions are all extracted in a gauge invariant manner, i.e. the background spacetime does not play any dynamic role in the physics. In [121], the torsion sector was set to zero; generally, the GTG then reproduces most of the standard results in general relativity, but differs in the interpretation of global issues such as the role of topology and horizons.

Further work has been done in [35, 49] to explore the torsion sector of GTG. One of the motivations was to look at spinor-driven inflationary models and see the comparisons with possible experiments and observations. Unlike in general relativity where torsion is interpreted as a property of a non-Riemannian manifold, the torsion in GTG is a physical field which is derived from the gravitational gauge fields. The added feature of GTG is that it constrains physically the form which the torsion can take. This constraint is a consequence of the demanding minimally coupled equations for the matter fields when derived from a minimally-coupled, gauge-invariant action. The spin-torsion theory in GTG led to interesting developments in the problem of finding cosmological solutions for a Dirac field coupled to gravity in a self consistent model. A new exact solution to spin torsion theory (or Einstein-Cartan-Dirac equations) was found in [35] that describes a homogeneous Universe with spin induced anisotropy.

In Chapter 2, we extend the work in [35] to find the cosmological solutions for a Dirac field coupled self-consistently to gravity with a cosmological constant. We also discuss the implications of these cosmological solutions.

§1.3.2 Extra Dimensions

The holy grail of modern physics is to unify the four fundamental forces namely, gravity, electromagnetism, the strong and weak nuclear forces. Unfortunately, the two great pillars of theoretical physics, namely general relativity which is the theory of gravitation and quantum theory which describes the sub-atomic regime of matter, are mutually incompatible. The search for the theory of quantum gravity is still ongoing.

The early Universe provides a testing ground for theories of gravity. The standard cosmological model, based on general relativity with an inflationary era, is very effective in accounting for a broad range of observed features of the Universe. However, the lack of a consistent theoretical framework for inflation, together with the ongoing puzzles on the nature of dark matter and dark energy, indicate that cosmology may be probing the limits of validity of general relativity.

M-theory (or superstring theory) is considered to be a promising potential path to quantum gravity. It assumes the basic premise that matter is made up of strings instead of point particles at the Planck scale (i.e. the scale where all the four forces

are unified). However, in order for M-theory to be a theory of quantum gravity, there are two pre-requisites, namely supersymmetry and extra dimensions. Both pre-requisites have not been experimentally verified. The Large Hadron Collider (LHC) in CERN (which will run in 2006) would test the possibility of finding supersymmetric particles at high energies. The question is whether we can find experiments that could demonstrate the existence of extra dimensions [¶].

As such, it is an important candidate for cosmological testing. In the absence of a sufficiently general M-theoretic model of cosmology, we can use phenomenological models that share some of the key features of M-theory, including branes. In brane cosmology, the observable Universe is a 1+3-dimensional “brane” surface moving in a higher-dimensional “bulk” spacetime. Standard-model fields are confined to the brane, while gravity propagates in the bulk. The simplest, and yet sufficiently general, phenomenological braneworld models are those based on the Randall-Sundrum II scenario [160]. These models have the additional advantage that they provide a framework for investigating aspects of holography and the AdS/CFT correspondence.

The idea of using extra dimensions to unify fundamental forces was first explored by Kaluza [99] and Klein [106] in the 1920s. Kaluza proposed that one can start from a five dimensional theory of general relativity, and assume that one of the dimensions is being curled up into a circle, leading to a theory that unifies gravity and electromagnetism. Klein took a step further after rediscovering Kaluza’s theory, he noted the quantisation of the electric charge and hoped that Kaluza’s theory would underlie quantum mechanics. He came close to the modern point of view in his discussion of higher harmonics and the size of the small circle, and insisted that the 5th dimension should be treated seriously. He assumed that the coordinate of the 5th dimension is periodic. It is difficult to envisage a 5D spacetime with such a topology. However, one can use a simple analogy provided by a hosepipe: at large distances, the hosepipe looks like a line but close inspection reveals at every point on the line, there is a circle (see Fig. 1.3). The Kaluza Klein picture requires the dimensions to be compact and essentially homogeneous. In this picture, it is the compactness which ensures that the spacetime is effectively 4-dimensional at distances exceeding the compactification scale, i.e. the size of the extra dimensions. As a result, the size of the extra-dimensions must be very small, and the size was of the order of the Planck scale. With the Planck length $l_P \sim 10^{-35}\text{m}$ and the corresponding Planck energy scale $M_P \sim 10^{19}\text{GeV}$, it remains almost impossible to probe the extra dimensions with present technology.

In recent years, much attention has been focused on **brane world scenarios**. They are based on the idea that the standard model of particle physics (which

[¶]For a more technical review on the subject of extra dimensions in the high energy physics framework, see [163].

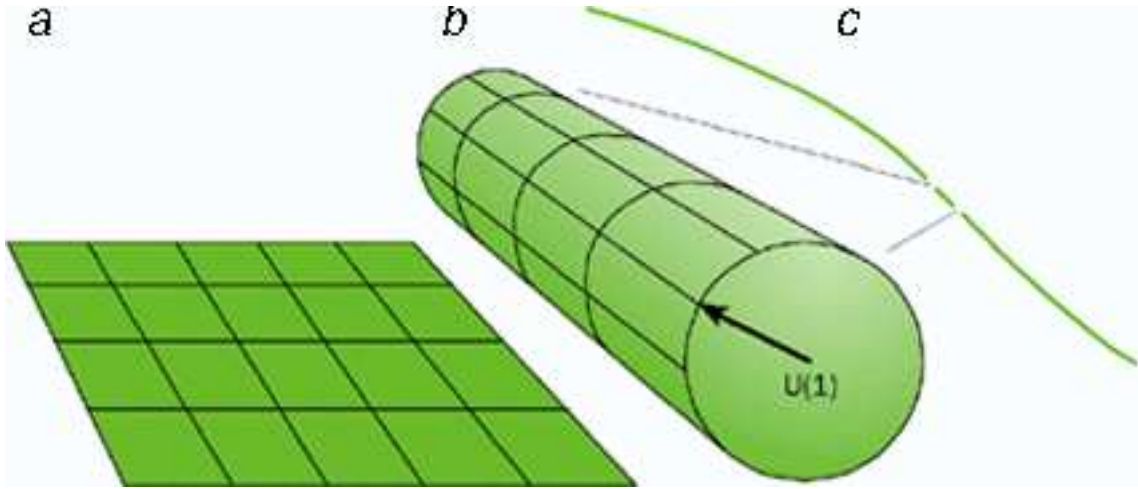


Figure 1.3: A diagram depicting the Kaluza-Klein concept of compactification of extra dimensions: (a) Compactifying a 3-D Universe with two space dimensions and one time dimension which simplifies the picture of Kaluza and Klein. (b) The Lorentz symmetry of the large dimension is broken by the compactification and what remains is the 2-D space plus the $U(1)$ symmetry represented by the arrow. (c) On large scales we see only a 2-D Universe (one space plus one time dimension) with the “internal” $U(1)$ symmetry of electromagnetism. The diagram is reproduced from the article “The search for extra dimensions” by Abel and Russell in [1].

unifies the electromagnetic, strong and weak nuclear forces) is confined to a 3-brane (an object or membrane which is a solution in string theory that corresponds to our observable Universe) and only gravity lives in the higher dimensional bulk. In general, the spatial dimensions transverse to the branes must be very small in order to avoid large deviations from Newton’s law of gravitation (see 1.4). One interesting suggestion was put forward in [6] that two of the extra dimensions are large (mm scale). Since the four dimensional effective gravitational constant is related to the fundamental higher dimensional gravitational constant through the size of the extra dimensions, the fundamental gravitational constant can be reduced to the TeV scale, provided that the large extra dimensions have a size of ~ 1 mm. The connection to superstring theory was made in [5]. This new proposal allows us to deal with the mass hierarchy problem in elementary particle physics without invoking supersymmetry.

By projecting the brane world models to an effective 4D theory, we can study how the extra dimensions may affect the standard observational cosmology. Such an approach is the first step to understanding these new models and seeing whether

one can find any new features in them that may show up in future experiments in observational cosmology. In Chapter 3, we will set up the formalism of the (1+3)-covariant approach for studying cosmological perturbations in these braneworld models. Subsequently, in Chapter 4, we will explore the effects of the extra dimensions on the cosmic microwave background for both scalar and tensor perturbations.

§1.3.3 Changing Global Symmetry

In standard general relativity, the Friedmann-Robertson-Walker (FRW) metric is a well-defined metric describing an expanding, homogeneous, isotropic Universe. The symmetry of a FRW spacetime is both translational and rotational about every point and there is no preferred centre (Copernican).

However, local inhomogeneities grow to form galaxies and clusters of galaxies and hence generate the large scale structure which we observe today. In an Einstein-de Sitter (flat, dust dominated) Universe, these clustered structures would grow continuously, leading to the merger of galaxy clusters to form superclusters. Subsequently, this leads to the formation of an ever-changing hierarchical structure. Such an astrophysical mechanism results in a changing equation of state from a pressure-free expansion to a transition state where gravitational clustering induces a cosmologically significant pressure which feeds back into the metric. At this stage, the symmetry of the metric alters, and depends on the exact form of the equation of state. Extrapolating this picture into the future, we can envisage the following possible development. By taking the clustering model to the extreme, one could imagine a time in the far future when the whole Universe is basically one large cluster. The internal constituents of this cluster exchange energy. The whole Universe virializes on the largest possible scale and we get an asymptotic state represented approximately by an isothermal Universe. For such a state, the metric is well-defined, as the final symmetry is rotational about one point only and translational nowhere and there is a definite centre (Anti-Copernican).

The effectiveness of gravitational clustering is related to the global structure of the standard Einstein-Friedmann Universes. There exist three general cases mentioned earlier for the future evolution of the Universe, and they depend on the total energy density. In a closed geometry the Universe will eventually recollapse into a singularity and all large-scale structure will be destroyed in the big crunch. In an open geometry the rate of universal expansion is too great to allow complete clustering. In a flat geometry (Einstein-de Sitter) the expansion timescale is comparable to the clustering timescale. Gravitational clustering grows continuously. Therefore, although gravitational clustering of galaxies occurs in all Einstein-Friedmann cosmological models, only in the Einstein-de Sitter model does it grow continuously. Only the Einstein-de Sitter model allows the formation of

the isothermal asymptotic state. However, the existence of a cosmological constant would change this evolution.

Saslaw and his collaborators[169, 171, 172] have found a solution to Einstein's field equations, which corresponds to a class of isothermal inhomogeneous Universes in which the nonzero pressure balances gravity and discussed whether the infinite and unbounded isothermal sphere could provide a possible state of our Universe. They suggested various arguments which demonstrate the possibility that such spherical and static models might represent the ultimate state of an Einstein-de Sitter Universe (with $\Lambda = 0$). If that is the case, the Einstein-de Sitter Universe will undergo a dynamical symmetry breaking into the isothermal Universe, i.e. from Copernican to anti-Copernican, which may correspond to a possible phase transition in the far future. This is (at least to our knowledge) the first time the question has been asked about what happens when a local condensation with one symmetry grows to eventually fill a Universe with another symmetry.

In Chapter 5, we examine the changing global symmetry of the Einstein-de Sitter Universe and see how it could lead to a possible phase transition in the future.

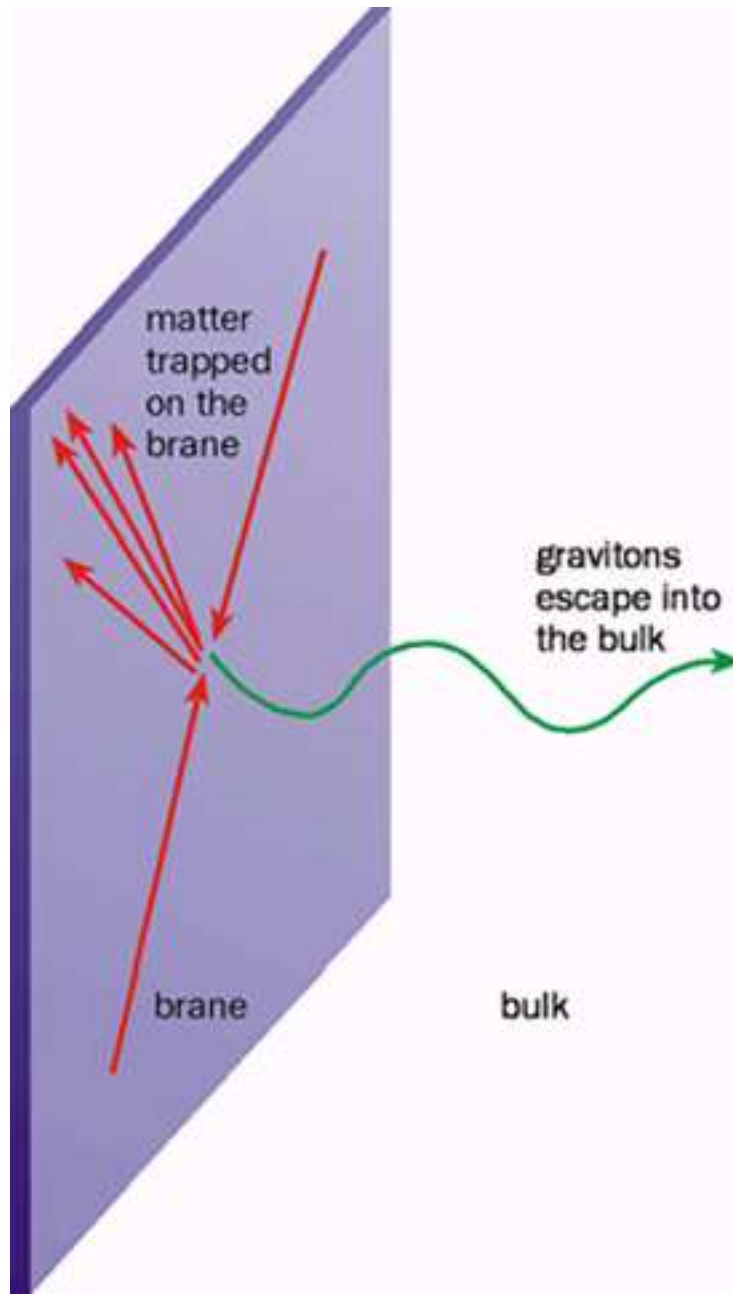


Figure 1.4: The matter fields (the electromagnetic, strong and weak nuclear forces) in the standard model are confined on the 3-brane (our observable Universe). Only gravity is allowed to propagate into the extra dimensions (i.e. the bulk). A collision between a proton and an antiproton can produce, for example, a single jet of matter particles plus graviton emission into the bulk. Such collisions might be seen in high-energy physics experiments. The diagram is reproduced from the article “The search for extra dimensions” by Abel and Russell in [1].

Part I

Spin-Torsion Theories

Chapter 2

Spin-Torsion Cosmology

“There could be no fairer destiny for any ... theory than that it should point the way to a more comprehensive theory which it lives on as a limiting case. ”

- Albert Einstein

In this chapter, we extend the gauge theory of gravity (GTG) approach of finding cosmological solutions in spin-torsion theories to include a cosmological constant. We find a new anti-particle solution in addition to the two solutions found in [35]. We also discuss the cosmological implications of these solutions.

§2.1 Introduction

The gauge theory of gravity (GTG) provides an alternative formulation to the standard spin-torsion or Einstein-Cartan-Kibble-Sciama theories. In the GTG approach developed in [49, 120, 121], one can identify the torsion with the spin of the matter field that follows naturally from the gauge-theoretic approach to gravity (see [83]). Fundamentally in GTG, the gravitational effects are described by a pair of gauge fields which are defined over a flat Minkowski background spacetime. The gauge fields ensure the invariance of the theory under arbitrary local displacements and rotations in the background spacetime. All the physical predictions are extracted in a gauge-invariant manner, thus ensuring that the background spacetime plays no dynamical role in the physics. In [49], the equations describing the Dirac field coupled self-consistently to gravity were given, and the analogues of the Einstein-Cartan-Dirac (ECD) equations were derived from a minimally-coupled, gauged-invariant action. It is known that the Einstein-Dirac equations, which describe a Dirac field coupled to gravity through the (symmetrised) stress-energy tensor only, cannot be derived from a minimally coupled action. Hence this serves as a compelling reason to regard the ECD equations as being more fundamental.

One of the main applications of GTG is in finding cosmological solutions for a Dirac field coupled to gravity in a self-consistent model. This problem was considered by several authors [2, 37, 46, 47, 84, 96, 152, 158, 159, 174] in the past. One of the main motivations was to see whether the Dirac field could offer an alternative type of inflationary model over standard scalar field models. However, the solutions found by these authors either solve the Einstein-Dirac equations [2, 37, 84, 152, 159] which do not include the effect of torsion induced by the spin of the Dirac field, or they do include the spin-induced torsion (i.e. they solve the Einstein-Dirac-Cartan equations) but only for massless fields [84, 96, 174] or for ghost solutions [46, 47, 158]. (A ghost solution has a vanishing stress energy tensor for the Dirac field.) The first massive, non-ghost solution was recently found for a Dirac field coupled self-consistently to gravity in [35].

The origin of a cosmological constant, Λ , is a mystery in gravitation and modern particle physics. It was introduced originally by Einstein to allow static homogeneous cosmological solutions to the field equations in the presence of matter. The discovery of the expanding Universe by Hubble, made it unnecessary, but it did not change its status as a legitimate addition to the gravitational field equations, or as a parameter constrained by observation. In particle physics, the cosmological constant turns out to be a measure of the energy density of the vacuum i.e. the state of the lowest energy. This identification becomes crucial in dealing with two present unsolved problems: firstly, why the vacuum energy is so small and secondly, to understand why it is comparable to the present day density of the Universe. It turns out that there are compelling reasons to believe why our Universe should have a non-zero Λ in both theory and experiment.* Recent results from the cosmic microwave background, supernova data and large scale structure seem to favour a cosmological constant with $\Omega_\Lambda = 0.7$.

In this chapter, we will extend the work in [35] to find a massive non-ghost solution for a Dirac field coupled self-consistently to gravity with the inclusion of a cosmological constant. We will briefly summarize the geometric algebra formalism and the gauge theory of gravity in §2.2. Subsequently, we will introduce the minimally coupled Einstein-Cartan-Dirac (ECD) action in §2.3, and the GTG analogue of the field equations. We will derive the cosmological solutions in §2.4 and discuss their implications in §2.4.1.

*A good review of the cosmological constant is given by Carroll [27].

§2.2 Geometric Algebra and Gauge Theory of Gravity

To find the cosmological solutions for a Dirac field coupled to gravity in a self consistent model with a cosmological constant, we shall employ the tools of Geometric Algebra (GA), which was originally developed from the spacetime algebra (STA) approach by Hestenes (see [85, 86, 87, 88]). We briefly summarize the geometric algebra formalism in §2.2.1 and the gauge theory of gravity in §2.2.2. Note that only in this chapter, we will use the other metric signature convention (+, −, −, −).

§2.2.1 Geometric Algebra

We start with the definition of a geometric (or Clifford) product in [39] that combines both symmetric inner product and antisymmetric outer product which is defined as follows:

$$ab = a \cdot b + a \wedge b \quad (2.1)$$

where both a and b are vectors.

In general, an arbitrary real superposition of the basis elements (2.7) is called a *multivector*. A multivector can be decomposed into sums of elements of different grades, for example, scalars are grade zero objects, vectors grade one, bivectors grade two and etc. These elements inherit the associative Clifford product of the $\{\gamma_\mu\}$ generators. For a grade- r multivector A_r and a grade- s multivector B_s , we define the inner and out products via

$$A_r \cdot B_s \equiv \langle AB \rangle_{|r-s|} , \quad (2.2)$$

$$A_r \wedge B_s \equiv \langle AB \rangle_{r+s} , \quad (2.3)$$

where $\langle M \rangle_r$ denotes the grade- r part of M . The subscript 0 will be left implicit when taking the scalar part of a multivector. We shall make use of the commutator product

$$A \times B \equiv \frac{1}{2}(AB - BA) . \quad (2.4)$$

The operation of reversion, denoted by a tilde, is defined by

$$(AB)^\sim \equiv \tilde{B}\tilde{A} , \quad (2.5)$$

and the rule that vectors are unchanged under reversion. We adopt the convention that in the absence of brackets, inner, outer and commutator products take precedence over Clifford products.

The geometric algebra of spacetime is familiar to physicists in the form of the algebra generated from the Dirac- γ matrices. The spacetime algebra (STA) is generated by four vectors, $\{\gamma_\mu\}$, $\mu = 0\dots 3$, equipped with an associative (Clifford) product, denoted by juxtaposition. The symmetrised and antisymmetrised products define the inner and outer products between vectors, and are denoted by a dot and a wedge respectively:

$$\begin{aligned}\gamma_\mu \cdot \gamma_\nu &\equiv \frac{1}{2}(\gamma_\mu \gamma_\nu + \gamma_\nu \gamma_\mu) = \eta_{\mu\nu} = \text{diag}(+ \ - \ - \ -), \\ \gamma_\mu \wedge \gamma_\nu &\equiv \frac{1}{2}(\gamma_\mu \gamma_\nu - \gamma_\nu \gamma_\mu).\end{aligned}\tag{2.6}$$

The outer product of two vectors defines a bivector — a directed plane segment including the two vectors.

The full basis for a 16-dimensional STA is provided by

1	$\{\gamma_\mu\}$	$\{\sigma_k, \mathcal{I}\sigma_k\}$	$\{\mathcal{I}\gamma_\mu\}$	\mathcal{I}
1 scalar	4 vectors	6 bivectors	4 trivectors	1 pseudoscalar

(2.7)

where $\sigma_k \equiv \gamma_k \gamma_0$, $k = 1\dots 3$, and $\mathcal{I} \equiv \gamma_0 \gamma_1 \gamma_2 \gamma_3 = \sigma_1 \sigma_2 \sigma_3$. The pseudoscalar \mathcal{I} squares to -1 and anticommutes with all odd-grade elements. The $\{\sigma_k\}$ generate the geometric algebra of Euclidean 3-space, and are isomorphic to Pauli-matrices.

We denote vectors in lower case Latin, a , or Greek for a set of basis vectors. A (coordinate) frame of vectors $\{e_\mu\}$ is generated from a set of coordinates $\{x^\mu(x)\}$ via $e_\mu \equiv \partial_\mu x$, where $\partial_\mu \equiv \frac{\partial}{\partial x^\mu}$. The reciprocal frame, denoted by $\{e^\mu\}$, satisfies $e_\mu \cdot e^\nu = \delta_\mu^\nu$. The vector derivative $\nabla (\equiv \partial_x)$ is then defined as

$$\nabla \equiv e^\mu \partial_\mu.\tag{2.8}$$

More generally, the vector derivative with respect to a is denoted ∂_a . Further details concerning geometric algebra and the STA may be found in [86, 88] and a summary of useful identities is given in appendix B.

§2.2.2 Gauge Theory of Gravity

The language of geometric algebra is used by Lasenby, Doran and Gull [121] to develop an alternative theory of gravity based on gauge principles alone. The theory is known as **Gauge Theory of Gravity** (GTG). The key ideas in GTG are summarized as follows:

1. The gravitational effects are described by a pair of gauge fields, defined over a flat Minkowski spacetime namely, the position gauge field, $\bar{h}(a)$ and the rotation gauge field, $\Omega(a)$.

- (a) The first of these, the position gauge field, $\bar{h}(a)$ describes a position dependent linear function mapping the vector a to vectors. The overbar serves to distinguish the linear function, $\underline{h}(a)$ from its adjoint, $\bar{h}(a)$, where

$$\underline{h}(a) \equiv \partial_b \bar{h}(b) \cdot a . \quad (2.9)$$

The gauge-theoretic purpose of $\bar{h}(a)$ is to ensure covariance of the equations under arbitrary local displacements of the matter fields in the background spacetime.

- (b) The second gauge field, the rotation gauge field, $\Omega(a)$, is a position dependent linear function mapping the vector a to bivectors. The purpose of this gauge field is to ensure covariance under local (Lorentz) rotations of fields at a point in the background spacetime [121]. A gauge field $\omega(a)$ is introduced to map vectors to bivectors and is defined as

$$\omega(a) = \Omega \underline{h}(a) . \quad (2.10)$$

2. Physical predictions are extracted in a gauge invariant manner which ensures that the background spacetime plays no dynamical role in the physics.
3. The two gauge fields are minimally coupled to the Dirac field to enforce invariance under local displacements and both spacetime and phase rotations[†]. One can formulate the Dirac action in a way that it ensures that the internal phase rotations and spacetime rotations assume equivalent forms.
4. In the process, one can construct a Lagrangian density for gravitational fields. The first surprise of adopting such an approach is that the demand of the minimally-coupled Dirac equation restricts us to a single action integral. There is no freedom except for the inclusion of a cosmological constant.
5. This leads to a set of field equations which are completely independent of how we choose to label the position of fields by a vector x .

The resulting theory based on the above key ideas is a first order theory which is consistent with quantum mechanics at the first quantized level. One can develop additional and alternative insight to the general theory of relativity from the GTG. The ideas are applied in the context of black holes, collapsing matter and cosmology in the second part of [121].

[†]This requires a vector gauge field for electromagnetism.

The covariant derivative \mathcal{D} is assembled from the (flat space) vector derivative ∇ and the gravitational gauge fields. The action of \mathcal{D} on a general multivector M is given by

$$\begin{aligned}\mathcal{D}M &\equiv \partial_a a \cdot \mathcal{D}M \\ &\equiv \partial_a [a \cdot \bar{h}(\nabla)M + \omega(a) \times M],\end{aligned}\quad (2.11)$$

where we have introduced the rotational gauge field $\omega(a)$ defined in (2.10).

The covariant derivative contains a grade-raising and lowering component, so that we may write

$$\mathcal{D}M = \mathcal{D} \cdot M + \mathcal{D} \wedge M, \quad (2.12)$$

where

$$\mathcal{D} \cdot M \equiv \partial_a \cdot (a \cdot \mathcal{D}M), \quad \mathcal{D} \wedge M \equiv \partial_a \wedge (a \cdot \mathcal{D}M). \quad (2.13)$$

The single-sided transformation law of spinors under rotations requires us to introduce a separate spinor covariant derivative $D\psi \equiv \partial_a a \cdot D\psi$, where

$$a \cdot D\psi \equiv a \cdot \bar{h}(\nabla)\psi + \frac{1}{2}\omega(a)\psi. \quad (2.14)$$

The field strength corresponding to the $\Omega(a)$ gauge field is defined by

$$R(a \wedge b) \equiv a \cdot \nabla\Omega(b) - b \cdot \nabla\Omega(a) + \Omega(a) \times \Omega(b). \quad (2.15)$$

From this, we define the covariant Riemann tensor

$$\mathcal{R}(a \wedge b) \equiv R\underline{h}(a \wedge b). \quad (2.16)$$

The Ricci tensor, Ricci scalar and Einstein tensor are then given by

$$\mathcal{R}(a) = \partial_b \cdot \mathcal{R}(b \wedge a), \quad (\text{Ricci tensor}) \quad (2.17)$$

$$\mathcal{R} = \partial_a \cdot \mathcal{R}(a), \quad (\text{Ricci scalar}) \quad (2.18)$$

$$\mathcal{G}(a) = \mathcal{R}(a) - \frac{1}{2}a\mathcal{R}. \quad (\text{Einstein tensor}) \quad (2.19)$$

§2.3 The Self-Consistent Dirac Field and the Field equations

The equations of motion for the Dirac field and the gauge fields are derived from a form of the minimally coupled action from [49, 121]:

$$S_{\mathcal{E}\mathcal{C}\mathcal{D}} = \int |d^4x| \det(\underline{h})^{-1} \left[\frac{\mathcal{R}}{2} - \kappa^2 \langle D\psi i\gamma_3 \tilde{\psi} - m\psi \tilde{\psi} \rangle - \Lambda \right]. \quad (2.20)$$

Varying Eq. (2.20) with respect to $\Omega(a)$, $\bar{h}(a)$ and ψ respectively (refer to the procedure in [121]), the following equations describe a Dirac field of mass m coupled self-consistently to gravity [49] with the inclusion of the cosmological constant in this paper.

$$\mathcal{D} \wedge \bar{h}(a) = \kappa^2 \mathcal{S} \cdot \bar{h}(a) + \frac{\kappa^2}{2} [\partial_b \cdot \mathcal{S}(b)] \wedge \bar{h}(a), \quad (\text{'wedge'}) \quad (2.21)$$

$$\mathcal{G}(a) - \Lambda a = \kappa^2 \mathcal{T}(a), \quad (\text{Einstein}) \quad (2.22)$$

$$D\psi i\sigma_3 = m\psi\gamma_0, \quad (\text{Dirac}) \quad (2.23)$$

where we set $\kappa^2 = 8\pi G$, Λ is the cosmological constant. The term $\mathcal{S}(a)$ is the covariant spin tensor, and is defined by

$$\mathcal{S}(a) = S\bar{h}^{-1}(a), \quad (2.24)$$

and \mathcal{S} is the spin trivector and is defined by,

$$\mathcal{S} = \frac{1}{2} \psi i\gamma_3 \tilde{\psi}, \quad (2.25)$$

and the matter stress-energy tensor is defined to be

$$\mathcal{T}(a) = \left\langle a \cdot D\psi i\gamma_3 \tilde{\psi} \right\rangle_1. \quad (2.26)$$

The above equations are the GTG analogue of the **Einstein-Cartan-Dirac** equations. The second term on the RHS in Eq. (2.21) is set to zero because the minimally-coupled equations for the matter fields are obtained from a minimally-coupled Lagrangian only if the contraction of the spin tensor vanishes, i.e. $\partial_a \cdot \mathcal{S}(a) = 0$. One could include cases for non-vanishing spin tensor since the spin tensor vanishes for scalar fields and Yang-Mills gauge fields. For spin-1/2 fields, we can use the form $\mathcal{S}(a) = \mathcal{S} \cdot a$, where \mathcal{S} is the spin trivector. Further results for a non-vanishing tensor are given in [49].

The wedge equation in the spin-torsion theory is algebraic in $\omega(a)$, and may be solved for a vanishing spin tensor to give

$$\omega(a) = -\bar{h}[\nabla \wedge \bar{h}^{-1}(a)] + \frac{1}{2} a \cdot \{ \partial_b \wedge \bar{h}[\nabla \wedge \bar{h}^{-1}(b)] \} + \frac{1}{2} \kappa^2 a \cdot \mathcal{S}. \quad (2.27)$$

§2.4 Massive Non-Ghost Solutions to ECKS theory

In this section, we derive a self-consistent solution for a massive Dirac field ψ , which is both homogeneous and isotropic at the level of classical fields, with the

inclusion of a cosmological constant. We note that the classical fields do not feel the anisotropy of the ω -function which arises due to the spin of the Dirac field, as the classical fields couple to gravity via the \bar{h} -function only. We first summarize the procedure in [35] which we adopt and then extend the solutions to the case with a cosmological constant.

We begin by introducing a set of polar coordinates,

$$\begin{aligned} t &\equiv x \cdot \gamma_0, & \cos \theta &\equiv \frac{x \cdot \gamma^3}{r}, \\ r &\equiv \sqrt{(x \wedge \gamma_0)^2}, & \tan \phi &\equiv \frac{x \cdot \gamma^2}{x \cdot \gamma^1}. \end{aligned} \quad (2.28)$$

We also make use of the following vectors which are members of the polar coordinate frame:

$$e_t \equiv \gamma_0, \quad e_r \equiv \frac{x \wedge \gamma_0 \gamma_0}{r}. \quad (2.29)$$

We choose the gauge based on the assumed symmetry for the \bar{h} -function for a vector b , and giving [121]:

$$\bar{h}(a) = b \cdot e_t e_t + a(t) \left(1 + \frac{kr^2}{4} \right) b \wedge e_t e_t, \quad (2.30)$$

where $a(t)$ is the scale factor of the Universe, and the curvature constant $k = -1, 0, +1$ defined for open, flat and closed Universes respectively. Note that $\bar{h}(a)$ is globally defined for all k .

The isotropic line element is generated by the \bar{h} -function

$$ds^2 = dt^2 - [a(t)]^{-2} \left(1 + \frac{kr^2}{4} \right)^{-2} [dr^2 + r^2(d\theta^2 + \sin^2 \theta d\phi^2)]. \quad (2.31)$$

In this gauge, the fundamental observers have covariant velocity e_t where t is the cosmic time, and their surfaces of homogeneity are $t = \text{constant}$ surfaces.

From Eq. (2.27), we obtain $\omega(b)$ in the following form :

$$\omega(b) = H(t)b \wedge e_t - \frac{1}{2}kra(t)e_r(b \wedge e_t e_t) + \frac{1}{2}\kappa^2 b \cdot \mathcal{S}, \quad (2.32)$$

where $H(t)$ is the Hubble parameter in cosmic time, i.e. $H(t) \equiv \dot{a}(t)/a(t)$ and \dot{a} is the derivative of the scale factor with respect to cosmic time, t .

We can cast the Dirac equation from Eq. (2.23) in the following form

$$\left[e_t \partial_t + a(t) \left(1 + \frac{kr^2}{4} \right) e_t e_t \wedge \nabla + \frac{3}{2} H e_t + \frac{1}{2} kra(t) e_r + \frac{3}{4} \kappa^2 \mathcal{S} \right] \psi i \sigma_3 = m \psi \gamma_0. \quad (2.33)$$

Following Isham and Nelson [96], if the gauge invariant observables (for example, the the projection of the Dirac current onto the velocity of the fundamental observers constructed from ψ) are to be homogeneous, we must have $\psi = \psi(t)$. Then the only term with any dependence on the spatial coordinates would be $(k/2)a(t)e_r\psi i\sigma_3$ in Eq. (2.33). We thus arrive at the conclusion that the Universe must be spatially flat (i.e. $k = 0$), if we require the observables associated with the Dirac field to be homogeneous [‡] [96]. The motivation for the above gauge choice is attributed to the fact that \bar{h} must be globally defined, for all choices to k .

From now onwards, we specialize to the flat Universe ($k = 0$). It is then convenient to work in a new gauge reached by the displacement,

$$x' = f(x) = x \cdot e_t e_t + a(t)x \wedge e_t e_t, \quad (2.34)$$

which turns \bar{h} -function to the simple form

$$\bar{h}(b) = b + rH(t)b \cdot e_r e_t. \quad (2.35)$$

This generates the line-element

$$ds^2 = (1 - r^2 H^2) dt^2 + 2Hr dt dr - [dr^2 + r^2(d\theta^2 + \sin^2 \theta d\phi^2)]. \quad (2.36)$$

The above gauge choice is known as the **Newtonian gauge**, and has an analogue in GR which employs the description of a set of geodesic clocks in a radial freefall, comoving with the fluid.

The $\omega(a)$ transforms to give

$$\omega(b) = H(t)b \wedge e_t + \frac{\kappa^2}{2}(b \cdot \mathcal{S}), \quad (2.37)$$

which leaves the homogeneous Dirac field, ψ unchanged. The surfaces of homogeneity still have $t = \text{constant}$. The covariant velocity of the fundamental observers remains e_t , but their radial coordinates are proportional to the scale factor $a(t)$.

We now consider the spin-torsion Universe with a non-zero cosmological constant Λ . The Riemann tensor evaluates to be

$$\mathcal{R}(B) = -\dot{H}B \cdot e_t e_t - H^2 B + \frac{1}{4}\kappa^4 B \cdot \mathcal{S}\mathcal{S} - \frac{1}{2}\kappa^2(B \cdot \mathcal{D}) \cdot \mathcal{S}, \quad (2.38)$$

for any arbitrary bivector B , and the Einstein tensor $\mathcal{G}(b)$ is found to be

$$\mathcal{G}(b) = 2\dot{H}b \wedge e_t e_t + 3H^2 b - \frac{1}{4}\kappa^2 b \cdot (\mathcal{D} \cdot \mathcal{S}) + \frac{1}{2}\kappa^4 (b \cdot \mathcal{S})\mathcal{S} - \frac{3}{4}\kappa^4 \mathcal{S}^2 b, \quad (2.39)$$

[‡]One can arrive at the same conclusion if one attempts to solve the Dirac equation non-self-consistently on a homogeneous gravitational background. The reason is due to the fact that the only change to the equation (2.33) would be that \mathcal{S} is now the torsion trivector of the background rather than the spin of the Dirac field.

The stress energy tensor of the self-consistent Dirac field evaluates to

$$T(a) = \left\langle b \cdot e_t \psi i \gamma_3 \tilde{\psi} + H b \wedge e_t \mathcal{S} + \frac{\kappa^2}{2} (b \cdot \mathcal{S}) \mathcal{S} \right\rangle_1, \quad (2.40)$$

where we assumed that ψ is a function of time alone. The Dirac equation reduces to

$$\left(e_t \partial_t + \frac{3}{2} H e_t + \frac{3}{4} \kappa^2 \mathcal{S} \right) \psi i \sigma_3 = m \psi \gamma_0, \quad (2.41)$$

from which we deduce

$$\begin{aligned} \dot{\mathcal{S}} &= -3H\mathcal{S} - m \left\langle \psi \tilde{\psi} \right\rangle_4 \gamma_0, \\ \mathcal{D} \cdot \mathcal{S} &= -2H e_t \cdot \mathcal{S}. \end{aligned} \quad (2.42)$$

Substituting Eq. (2.42) into Eq. (2.22), we obtain the following equation :

$$2\dot{H} b \wedge e_t e_t + 3H^2 b + \frac{3}{4} \kappa^4 \mathcal{S}^2 e_t b e_t - m \kappa^2 b \cdot e_t e_t \left\langle \psi \tilde{\psi} \right\rangle - \Lambda b = 0, \quad (2.43)$$

from which we extract the following set of scalar equations

$$2\dot{H} + 3H^2 - \frac{3}{4} \kappa^4 \mathcal{S}^2 - \Lambda = 0, \quad (2.44)$$

$$3H^2 + \frac{3}{4} \kappa^4 \mathcal{S}^2 - m \kappa^2 \left\langle \psi \tilde{\psi} \right\rangle - \Lambda = 0. \quad (2.45)$$

If we exclude torsion from the model, from Eq. (2.44), the equation becomes

$$3H^2 + 2\dot{H} - \Lambda = 0. \quad (2.46)$$

Since $\mathcal{S}^2 \leq 0$, the effect of torsion would make \dot{H} more negative for any given value of the Hubble parameter H . Consequently, torsion enhances singularity formation for a Hubble parameter at a particular instant. It follows that the Universe will be younger if we look at the singularity theorems in the presence of torsion [102]. Torsion effects become significant when the Compton wavelength of the field is larger than the Hubble radius. At earlier times, where ρ is singular, the torsion effects are dominant. However, the inclusion of a positive cosmological constant would provide a repulsive force which would dominate the late time behaviour of the Universe. The competing effects between the torsion and the cosmological constant lead to interesting consequences in the models which we are about to examine.

Suppose one sets $m = 0$, then Eqs. (2.44) and (2.45) would be solved immediately to give

$$H(t) = \sqrt{\frac{\Lambda}{3}} \coth \frac{\sqrt{3\Lambda}}{2} t. \quad (2.47)$$

The cosmological constant alters the large t behaviour dramatically, as H would tend to a finite constant, i.e. $H \rightarrow \sqrt{\frac{\Lambda}{3}}$.

We consider the case where $\psi\tilde{\psi} \neq 0$, and parametrise ψ by the following relation [86]:

$$\psi = \sqrt{\rho} \exp\left(\frac{\mathcal{I}\beta}{2}\right) R, \quad (2.48)$$

where $\rho > 0$ and β are scalar functions of t . The rotor R is even-grade (and time dependent) and satisfies $R\tilde{R} = 1$. Substituting Eq. (2.48) into Eq. (2.41), and equating grades on either side, one finds the following equations

$$\dot{\rho} = 4m \sin \beta \mathcal{I}\gamma_0 \wedge \mathcal{S} - 3\rho H, \quad (2.49)$$

$$\rho \dot{\beta} = 4(m \cos \beta + 3\pi\rho) \mathcal{I}\gamma_0 \wedge \mathcal{S}, \quad (2.50)$$

$$\rho \dot{R}\tilde{R} = -2(m e^{-\mathcal{I}\beta} + 3\pi\rho) \gamma_0 \cdot \mathcal{S}. \quad (2.51)$$

where $\dot{R}\tilde{R}$ is a bivector. We simplify the calculation by taking $\sin \beta = 0$. Since β is then constant, a non-zero and constant ρ is forbidden by Eq. (2.49), since Eq. (2.50) gives $\gamma_0 \wedge \mathcal{S} = 0$. It follows that we must solve

$$\dot{\rho} = -3\rho H, \quad (2.52)$$

$$\dot{R} = -(m \cos \beta + 3\pi\rho) \gamma_0 R \mathcal{I}\gamma_3, \quad (2.53)$$

subject to the constraint

$$3H^2 - 12\pi^2 \rho^2 - 8\pi m \rho \cos \beta - \Lambda = 0. \quad (2.54)$$

In these equations, $\cos \beta = \pm 1$. The solutions with $\cos \beta = 1$ are regarded as “particle” (positive energy) solutions and those with $\cos \beta = -1$ as “anti-particle” (negative energy) solutions in the absence of gravity [48].

To solve the Eqs. (2.52) and (2.54), we make use of the substitution $y = \frac{1}{6\pi\rho}$ to find

$$\begin{aligned} \dot{y}^2 &= 1 \pm 4my + 3\Lambda y^2 \\ &= 3\Lambda \left(y \pm \frac{2m}{3\Lambda} + \frac{\sqrt{4m^2 - 3\Lambda}}{3\Lambda} \right) \left(y \pm \frac{2m}{3\Lambda} - \frac{\sqrt{4m^2 - 3\Lambda}}{3\Lambda} \right). \end{aligned} \quad (2.55)$$

One could obtain, by solving the above equation, the density parameter ρ and the Hubble parameter, $H(t)$, for all t in both particle and anti-particle sectors.

§2.4.1 Cosmological implications

In this section, we analyze how the inclusion of a cosmological constant would modify the solutions found in [35] for a spin-torsion Universe (see table 2.1 for the classification of the solutions). Before we proceed to the solutions, we examine the discriminant $\sqrt{4m^2 - 3\Lambda}$ and the limits which these solutions can take. There are three possible cases: (i) $4m^2 \gg 3\Lambda$, (ii) $4m^2 = 3\Lambda$ and (iii) $4m^2 \ll 3\Lambda$. In natural units, the cosmological constant, $\Lambda \sim 10^{-122}$. We compare this value to the known experimental values from the masses of the fermions in natural units. The mass of the electron, $m_e \sim 10^{-23}$ and the mass of the neutrino is estimated approximately, $m_\nu \sim 10^{-7}m_e$ (see the experimental bounds for the neutrino masses in [69]). It is found that the values of m^2 for the fermions are significantly much larger than the cosmological constant, hence, the preferred model would be case (i). For case (ii), $m \sim 10^{-38}m_e$. However no such fermion is known to exist in nature, and hence case (ii) is not a plausible model. Since case (ii) is not a plausible model, case (iii) is effectively ruled out as well. In this section, we consider the solutions of interest for both case (i) and (ii).

To solve Eq. (2.55), we demand the condition $y \not\leq 0$ since $\rho > 0$. We note that these solutions would work for all values of t . We start with case (i) with $4m^2 \gg 3\Lambda$, and assume a positive cosmological constant i.e. a repulsive force. From Fig. 2.1, since $\rho > 0$, the requirement imposes an asymmetry between the particle and anti-particle solutions. For the particle case, we consider only one branch of the solution with $y > 0$ [region (i)]. On the other hand, we observe that the anti-particle case has two branches of solutions. These two branches are labelled as regions (ii) and (iii). For $\Lambda \rightarrow 0$, the solutions found in [35] would correspond to regions (i) and regions (ii), with the appropriate limit taken. The presence of the cosmological constant has introduced an additional solution.

For regions (i) and (ii), the Hubble parameter and density parameter for both particle and anti-particle respectively are:

$$\rho(t) = \frac{\alpha^2}{6\pi \sinh at(\alpha \cosh at \pm m \sinh at)}, \quad (2.56)$$

$$H(t) = \frac{\alpha(\alpha \cosh 2at \pm m \sinh 2at)}{3 \sinh at(\alpha \cosh at \pm m \sinh at)}, \quad (2.57)$$

where $\alpha = \frac{\sqrt{3\Lambda}}{2}$. The density is singular at $t = 0$ and at $t = \alpha^{-1} \coth^{-1}[\pm(m/\alpha)]$ for both particle and anti-particle cases respectively.

Starting from the particle case for $t > 0$, the solution in region (i) corresponds to an expanding Universe from an initial singularity at $t = 0$, and $H(t)$ tends to the value for a flat Universe with a cosmological constant at later times. During this epoch, the scale factor of the Universe asymptotically approaches $\exp(t\sqrt{\Lambda/3})$. If

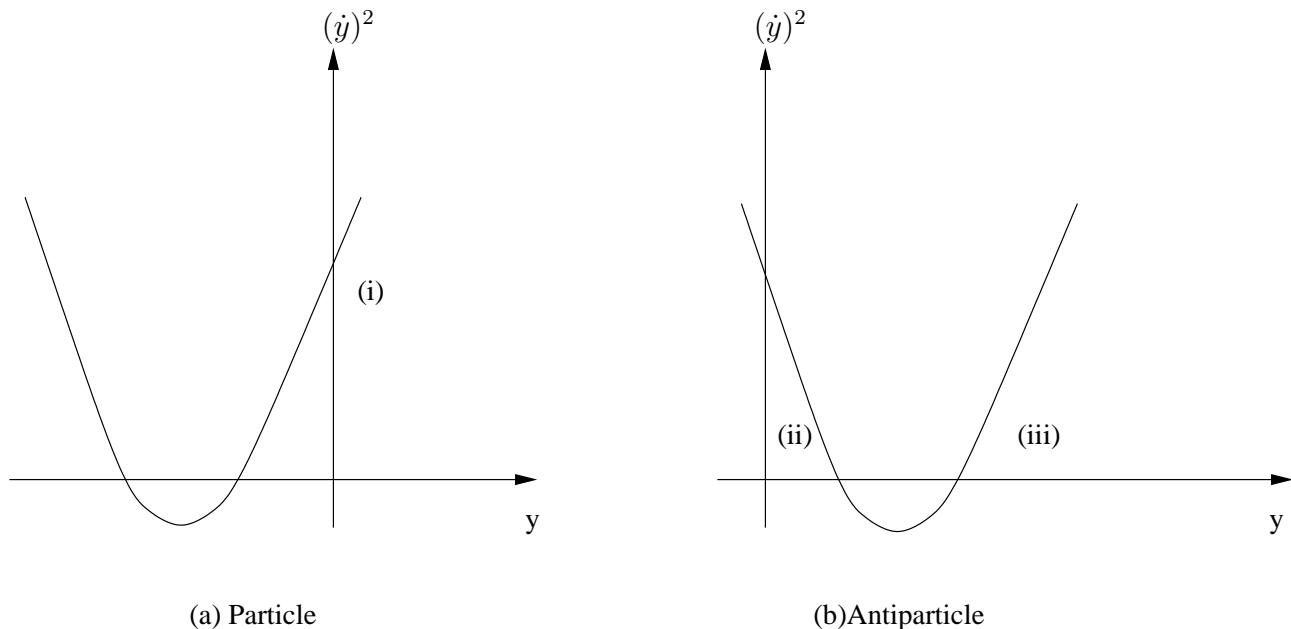


Figure 2.1: A sketch of the equation (2.55) with \dot{y}^2 vs y for both particle and anti-particle respectively, i.e. $\pm m$. This is for the case, $4m^2 \gg 3\Lambda$. The three regions of interest : (i) an expanding Universe with particle from an initial singularity (for $t > 0$) or a Universe contracting to a singularity in some finite time (for $t < 0$), (ii) an anti-particle Universe which expands to a finite value and contracts to a singularity (for $t > 0$), and (iii) an expanding anti-particle Universe (for $t > 0$) and a contracting Universe which bounces at $t = 0$ and expands indefinitely (for $t < 0$).

we move from $t \rightarrow -t$, we found $\rho(t) > 0$, but $H(t) < 0$. For $t < 0$, this solution describes a Universe contracting to a singularity in some finite time.

Next, we examine the anti-particle solution in region (ii). For $t > 0$, the Universe would expand from an initial singularity, turn around at some finite time and collapse to a singularity. A particle horizon is also present in the model which continues to exist right up to the singularity at the endpoint of the collapse. For Eqs. (2.56) and (2.57), taking the limit $\Lambda \rightarrow 0$, the solutions would be those found in [35]. For $t \rightarrow -t$, the solution describes the same cosmology as before.

From Fig. 2.1, the quadratic nature of Eq. (2.55) introduces a new anti-particle solution [region (iii)]. The Hubble parameter and density parameter for region (iii)

are found to be:

$$\rho = \frac{\alpha^2}{3\pi} \frac{1}{m + M \cosh 2\alpha t}, \quad (2.58)$$

$$H(t) = \frac{2\alpha}{3} \left[\frac{\sinh 2\alpha t}{M + \cosh 2\alpha t} \right], \quad (2.59)$$

where $M = (m/\sqrt{m^2 - \alpha^2})$. This solution satisfies Eq. (2.55) for the anti-particle case and is geodesically complete. For $t > 0$, the solution describes an expanding Universe starting from some finite y . With the inclusion of a positive cosmological constant, the Universe generated by the anti-particle sector appears to be an eternal Universe with no singularities. The $t < 0$ is an interesting case, since $\rho(-t) > 0$. This solution describes a contracting Universe from some finite $-t$, bounces at the instant at $y = 0$ and expands indefinitely like the case for $t > 0$. The solution has the property that it smoothly matches a contracting phase ($t < 0$) onto an expanding phase ($t > 0$) which is reminiscent of the pre-Big-Bang scenario [72].

In principle, we can incorporate a negative cosmological constant by switching $\Lambda \rightarrow -\Lambda$ in the above solutions. For both particle and anti-particle sectors, the solutions are similar to a closed FRW model, which corresponds to an expanding Universe starting from an initial singularity which turns around at a finite time, and collapses back into a singularity.

Another solution of interest is the extremal case where $4m^2 = 3\Lambda$. From Fig. 2.2, we note that there are three regions of interest, one solution for the particle case and two solutions for the anti-particle case. The solution is degenerate at $\rho = m/(3\pi)$.

By setting the initial conditions when $t_0 = 0$, and the initial density, $\rho_0 \rightarrow \infty$, we obtain the solutions of (2.55) for $4m^2 = 3\Lambda$. Starting from the particle case, for region (i), we obtain the density and Hubble parameter to be:

$$\rho = \frac{m}{3\pi(e^{2mt} - 1)} \quad (\text{particle}), \quad (2.60)$$

$$H(t) = \frac{2m}{3(1 - e^{-2mt})} \quad (\text{particle}). \quad (2.61)$$

From the above solutions, as $t \rightarrow \infty$, the particle Universe, $H(t)$ would tend to a finite constant $\sqrt{(\Lambda/3)}$, which is typical of a Friedmann dust model with a positive cosmological constant.

For region (ii), the solutions are:

$$\rho = \frac{m}{3\pi(1 - e^{-2mt})} \quad (\text{anti-particle}), \quad (2.62)$$

$$H(t) = \frac{2m}{3(e^{2mt} - 1)} \quad (\text{anti-particle}). \quad (2.63)$$

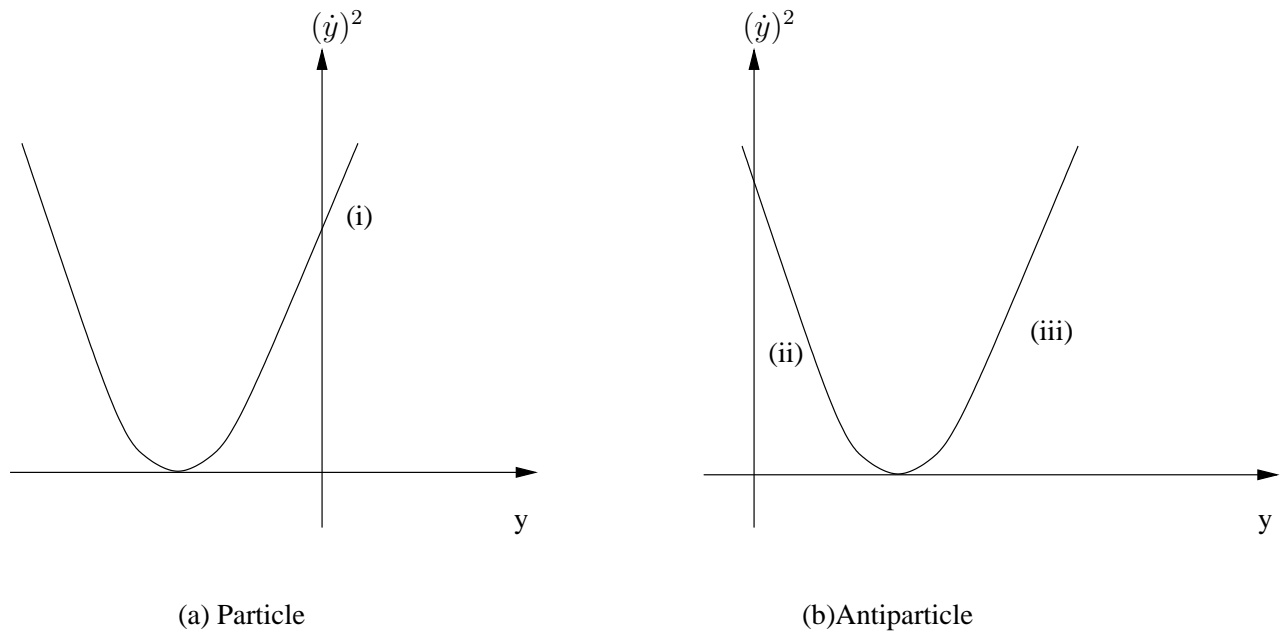


Figure 2.2: A sketch of the equation (2.55) with \dot{y}^2 vs y for both particle and anti-particle respectively, i.e. $\pm m$. This is for the extremal case: $4m^2 = 3\Lambda$. Like 2.1, we have three regions of interest : (i) an expanding Universe with particle from an initial singularity (for $t > 0$) or a Universe contracting to a singularity in some finite time (for $t < 0$), (ii) an anti-particle Universe which expands to a finite value and contracts to a singularity (for $t > 0$), and (iii) an expanding anti-particle Universe (for $t > 0$) and a static Universe which smoothly matches from $-t$ to t (for $t < 0$).

For the anti-particle Universe, $H(t)$ would tend to zero with the same limit, which suggests the scale factor of the anti-particle Universe tends asymptotically to a constant (see Fig. 2.3). In this scenario, the Universe is a Minkowski space with torsion at late times. The sole parameter of the extremal Universe is dependent on the mass of the fermion, m . Both models represent an expanding Universe with an initial singular density which decays as it evolves in time (except that the anti-particle decays to $m/3\pi$). In both cases, as we switch $t \rightarrow -t$, we get collapsing particle and anti-particle solutions which contract to a singularity.

In addition, there is an additional anti-particle solution [region (iii)] for $\rho > m/(3\pi)$ in the extremal case. The density parameter and the Hubble parameter

are found to be:

$$\rho = \frac{m}{3\pi(e^{2mt} + 1)} \quad (2.64)$$

$$H(t) = \frac{2m}{3(1 + e^{-2mt})} \quad (2.65)$$

This solution is similar to the region (iii) for the case $4m^2 \gg 3\Lambda$. For $t > 0$, it is an expanding anti-particle Universe. The $t < 0$ solution appears to be a Universe which smoothly matches a contracting phase onto an expanding phase ($t > 0$) at a finite density, with a bounce at $\rho = m/(6\pi)$. However, for the $t < 0$ solution, since the anti-particle solution starts at $t = -\infty$, indicating that $H(t) \rightarrow 0$. This means that the Universe would not be expanding, and this scenario is similar to the Einstein static Universe, but in this case, the spin-torsion has balanced against the repulsive force of the cosmological constant.

The stress-energy tensor $\mathcal{T}(a)$ is found to be

$$\begin{aligned} \mathcal{T}(e_t) &= \rho(2\pi\rho \pm m)e_t, \\ \mathcal{T}(\gamma_3) &= 0, \\ \mathcal{T}(\gamma_1) &= +\frac{1}{2}\rho H\gamma_2 - \pi\rho^2\gamma_1, \\ \mathcal{T}(\gamma_2) &= -\frac{1}{2}\rho H\gamma_1 - \pi\rho^2\gamma_2. \end{aligned} \quad (2.66)$$

As expected, e_t is a timelike eigenvector of $\mathcal{T}(a)$. The only other real eigenvector is γ_3 which is dual to the spin trivector \mathcal{S} . (Taking the dual is performed by multiplying the pseudoscalar \mathcal{I} .) The stress-energy tensor singles out the two directions in space to be algebraically special, and reflects the anisotropy of the solution at the level of the gravitational gauge fields. The energy density as measured by the fundamental observers is evaluated to be

$$\mathcal{T}(e_t) \cdot e_t = \rho(2\pi\rho \pm m). \quad (2.67)$$

From the energy density, we evaluate the density parameter which is defined by the following relation

$$\Omega = \frac{8\pi\mathcal{T}(e_t) \cdot e_t}{3H^2}, \quad (2.68)$$

which in regions (i) and (ii) evaluates to

$$\Omega = \frac{4}{3} \frac{(\alpha^2 + 3m^2 \sinh^2 \alpha t \pm 3m\alpha \sinh \alpha t \cosh \alpha t)}{(\alpha \cosh 2\alpha t \pm m \sinh 2\alpha t)^2}, \quad (2.69)$$

and in region (iii)

$$\Omega = \frac{2}{3} \left[\frac{3m^2 + 2\alpha^2 + 3mb \cosh 2\alpha t}{b^2 \sinh 2\alpha t} \right], \quad (2.70)$$

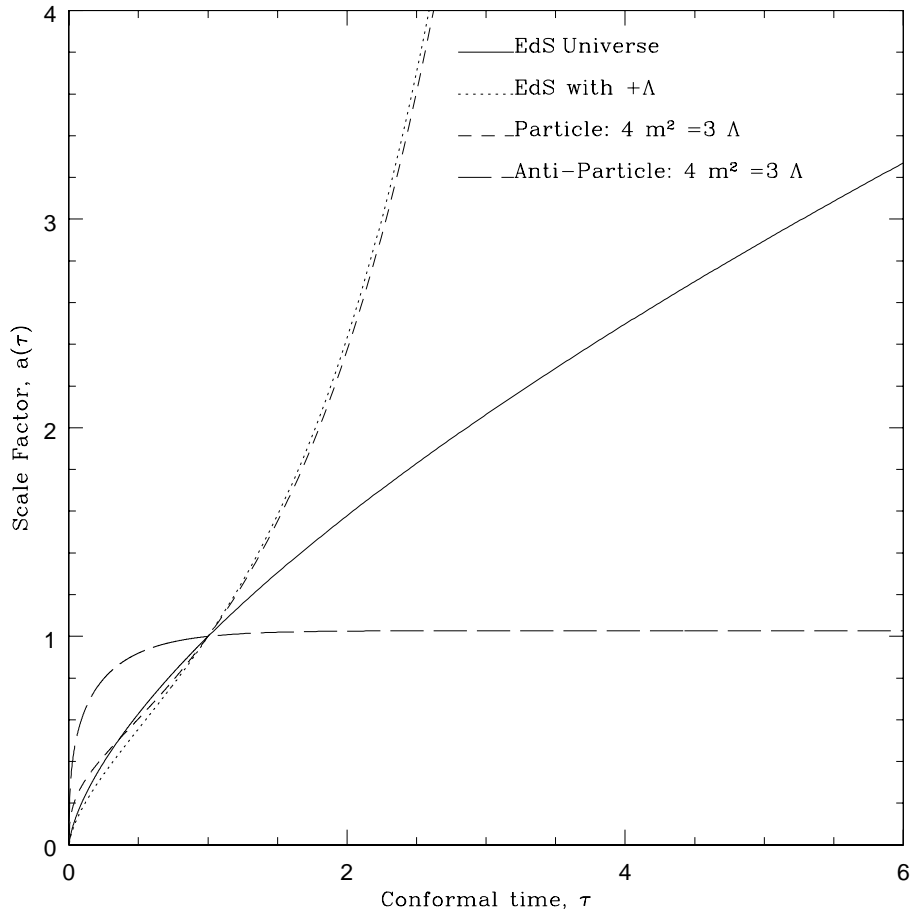


Figure 2.3: Graph of the scale factor $a(\tau)$ vs conformal time (in units of $H_0\tau$) for the particle and anti-particle solutions for the extremal Universes at $t > 0$ i.e. $4m^2 = 3\Lambda$ for $\Omega_\Lambda = 0.7$. The scale factor for flat Universe (with and without the cosmological constant) are plotted for comparison. Note that the scale factor for an extremal particle solution is similar to a flat universe with positive Λ , whereas the scale factor for an extremal anti-particle asymptotes towards a constant.

where $b = \sqrt{m^2 - \alpha^2}$. Setting $\Lambda \rightarrow 0$, we obtain the result in [35]. Hence at early times, $\Omega \neq 1$ since $4m^2 \gg 3\Lambda$.

§2.4.2 Massive Non-Ghost Solution

Finally, we arrive at the final form of the non-ghost solution. To solve the rotor equation (2.53), we would note the following result from [35]:

$$\gamma_0 \wedge \mathcal{S} = 0 \quad \Rightarrow \quad \gamma_3 \cdot (\tilde{R}\gamma_0 R) = 0 . \quad (2.71)$$

The rotor R can be decomposed into a product of rotors $R \equiv \Phi L$, where Φ and L are uniquely determined by the requirements $\Phi\gamma_0 = \gamma_0\Phi$ and $L\gamma_0 = \gamma_0\tilde{L}$. The condition in Eq. (2.71) restricts L to the form

$$L = e^{\frac{1}{2}\xi(\sin\eta\sigma_1 + \cos\eta\sigma_2)} . \quad (2.72)$$

where ξ and η are scalars. However from the rotor Eq. (2.53), we find that the vector $\tilde{R}\gamma_0 R$ is time independent. Since L is determined uniquely by this vector and γ_0 , therefore L must be constant. Now we substitute $R = \Phi L$ into Eq. (2.53), and note that L commutes with $\mathcal{I}\gamma_3$, to find that

$$\dot{\Phi} = -\dot{\chi}\Phi\mathcal{I}\sigma_3 , \quad (2.73)$$

where the scalar $\chi(t)$ is defined by

$$\dot{\chi} \equiv m \cos\beta + 3\pi\rho . \quad (2.74)$$

Hence Eq. (2.73) has the solution

$$\Phi(t) = \Phi_0 e^{-\mathcal{I}\sigma_3\chi(t)} , \quad (2.75)$$

where Φ_0 is a constant rotor which commutes with γ_0 . The rotor may be eliminated by combining the global position-gauge transformation $x' = \Phi_0 x \tilde{\Phi}_0$, with the global rotation-gauge transformation defined by the rotor $\tilde{\Phi}_0$. The solution to Eq. (2.74) is

$$\chi(t) = \pm mt + 3\pi \int \rho(t) dt , \quad (2.76)$$

where we could substitute the various forms of $\rho(t)$ found in Eqs. (2.56), (2.58), (2.60) or (2.62). The integration constant is chosen so that χ is defined for $\rho > 0$.

For regions (i) and (ii), we found that χ is evaluated to be

$$\chi(t) = \pm mt + \frac{1}{2} \ln \left[\frac{\alpha \left(1 + \tanh^2 \frac{\alpha t}{2} \right) \pm 2m \tanh \frac{\alpha t}{2}}{\tanh \frac{\alpha t}{2}} \right] , \quad (2.77)$$

Similarly, for region (iii), which only applies to the anti-particle case,

$$\chi(t) = \pm mt + \frac{1}{2} \ln \left(\frac{M + \cosh 2\alpha t}{\alpha} \right) . \quad (2.78)$$

For the extremal Universes, for both particle and anti-particle cases we find χ to be

$$\chi(t) = \pm mt + \frac{1}{2} \ln(1 - e^{-2mt}) \quad [\text{particle, region (i)}], \quad (2.79)$$

$$\chi(t) = \pm mt + \frac{1}{2} \ln(1 - e^{2mt}) \quad [\text{anti-particle, region (ii)}], \quad (2.80)$$

$$\chi(t) = \pm mt - \frac{1}{2} \ln(1 + e^{-2mt}) \quad [\text{anti-particle, region (iii)}]. \quad (2.81)$$

Hence we obtain the general self-consistent massive non-ghost solution for a Dirac field with the inclusion of a cosmological constant, ψ with $\sin \beta = 0$, with $\beta = 0$ or π to be

$$\psi(t) = \sqrt{\rho(t)} \exp\left(\frac{\mathcal{I}\beta}{2} - \mathcal{I}\sigma_3\chi(t)\right) \exp\left(\frac{\xi}{2}(\sin \eta\sigma_1 + \cos \eta\sigma_2)\right). \quad (2.82)$$

§2.5 Discussion

Finally, we examine whether the solutions for the spin-torsion Universes are inflationary or not. From (1.4) in Chapter 1, the condition for inflation is

$$\ddot{a} > 0 \quad \Rightarrow \quad \dot{H} + H^2 > 0. \quad (2.83)$$

Using (2.54), we obtain

$$\dot{H} + H^2 = \frac{\Lambda}{3} + g(\rho, \beta), \quad (2.84)$$

where

$$g(\rho, \beta) = -8\pi^2 \rho^2 \mp \frac{4\pi m\rho}{3}, \quad (2.85)$$

for the cases of particle and anti-particle respectively. For the particle case, $g(\rho, \beta) < 0$, and hence there is no inflation at earlier times since $g(\rho, \beta) \gg \Lambda$. However, at late times, there will be de-Sitter inflation induced by the cosmological constant. On the other hand, it is observed for the anti-particle case that $g(\rho, \beta) > 0$ if $\rho < (m/6\pi)$. For $\rho < (m/6\pi)$, the spin-torsion Universe would have an inflationary phase driven by the anti-particle. From Eq. (2.94) in Table 2.1, the lower bound for the density of a spin-torsion Universe is $\rho = (m/3\pi)$. Therefore, the spin-torsion solutions do not incorporate an inflationary phase at earlier times. The only inflationary phase is provided by the cosmological constant at late times.

A Table of the cosmological solutions in Spin Torsion Theories

Solution Type	Hubble Parameter, $H(t)$
Flat:	<p>(i) ($K = 0, \Lambda = 0$)</p> $H = \frac{2}{3t} . \quad (2.86)$ <p>(ii) with $\Lambda > 0$</p> $H = \frac{2\alpha}{3} \coth \alpha t . \quad (2.87)$ <p>(iii) with $\Lambda < 0$</p> $H = \frac{2\alpha}{3} \cot \alpha t , \quad (2.88)$ <p>where</p> $\alpha = \frac{3\Lambda}{2} . \quad (2.89)$
Spin Torsion Universe:	
(a) Particle	<p>General solution [region (i)]:</p> $H(t) = \frac{\alpha(\alpha \cosh 2\alpha t + m \sinh 2\alpha t)}{3 \sinh \alpha t (\alpha \cosh \alpha t + m \sinh \alpha t)} . \quad (2.90)$ <p>(i) Setting $4m^2 \gg 3\Lambda$, we obtain Eq. (2.87) for $\Lambda > 0$ and Eq. (2.88) for $\Lambda < 0$. If we set $\Lambda \rightarrow 0$, we get the solution in [35]:</p> $H(t) = \frac{1 + 2mt}{3t(1 + mt)} . \quad (2.91)$ <p>(ii) For $4m^2 = 3\Lambda$, we get</p> $\frac{2m}{3[1 - \exp(-2mt)]} . \quad (2.92)$

(b) Anti-particle	<p>General solution [region (ii)]</p> $H(t) = \frac{\alpha(\alpha \cosh 2\alpha t - m \sinh 2\alpha t)}{3 \sinh \alpha t(\alpha \cosh \alpha t - m \sinh \alpha t)}. \quad (2.93)$ <p>(i) Setting $4m^2 \gg 3\Lambda$, we obtain (2.87) for $\Lambda > 0$ and the inverse of (2.88) for $\Lambda < 0$. If we set $\Lambda \rightarrow 0$, we get the other solution in [35]:</p> $H(t) = \frac{1 - 2mt}{3t(1 - mt)}. \quad (2.94)$ <p>(ii) For $4m^2 = 3\Lambda$, we get</p> $\frac{2m}{3[\exp(2mt) - 1]}. \quad (2.95)$ <p>General solution II (Region (iii))</p> <p>(i) Setting $4m^2 \gg 3\Lambda$, we obtain</p> $H(t) = \frac{2\alpha}{3} \left[\frac{\sinh 2\alpha t}{M + \cosh 2\alpha t} \right], \quad (2.96)$ <p>where</p> $M = \frac{m}{\sqrt{m^2 - \alpha^2}}. \quad (2.97)$ <p>(ii) For the extremal case, we have</p> $H(t) = \frac{2m}{3[\exp(2mt) + 1]} \quad (2.98)$ <p>There is no analogue for this case as $\Lambda \rightarrow 0$.</p>
-------------------	---

Table 2.1: A summary of the solutions for the flat Universes and the spin-torsion Universes

Part II

Braneworld Cosmology

Chapter 3

Braneworld Cosmology I: Formalism

“I do not wish to hide the fact that I can only look with repugnance .. upon the puffed up pretentiousness of all these volumes filled with wisdom, such as are fashionable nowadays. For I am fully satisfied that .. the accepted methods must endlessly increase these follies and blunders, and that even the complete annihilation of all these fanciful achievements could not possibly be as harmful as this fictitious science with its accursed fertility.” - Immanuel Kant

In this chapter, we discuss the dynamics of linearized scalar and tensor perturbations in an almost Friedmann-Robertson-Walker braneworld cosmology of Randall-Sundrum type II using the 1+3 covariant approach based on [123] and [124]. We derive a complete set of frame-independent equations for the total matter variables, and a partial set of equations for the non-local variables which arise from the projection of the Weyl tensor in the bulk. The latter equations are incomplete since there is no propagation equation for the non-local anisotropic stress. As a first step, we derive the covariant form of the line of sight solution for the CMB temperature anisotropies in braneworld cosmologies. We discuss possible mechanisms by which braneworld effects may remain in the low-energy universe in Chapter 4.

§3.1 Introduction to Braneworld Cosmology

It is understood that Einstein’s theory of general relativity is an effective theory in the low-energy limit of a more general theory. Recent developments in theoretical physics, particularly in string theory or M-theory, have led to the idea

that gravity is a higher-dimensional theory which would become effectively four-dimensional at lower energies.

Braneworlds, which were inspired by string and M-theory, provide simple, yet plausible, models of how the extra dimensions might affect the four-dimensional world we inhabit. There is the exciting possibility that these extra dimensions might reveal themselves through specific cosmological signatures that survive the transition to the low-energy universe. It has been suggested that in the context of braneworld models the fields that govern the basic interactions in the standard model of particle physics are confined to a 3-brane, while the gravitational field can propagate in $3 + d$ dimensions (the *bulk*). It is not necessarily true that the extra dimensions are required to be small or even compact. It was shown recently by Randall and Sundrum [160] for the case $d = 1$, that gravity could be localised to a single 3-brane even when the fifth dimension was infinite. As a result, the Newtonian potential is recovered on large scales, but with a leading-order correction on small scales:

$$V(r) = -\frac{GM}{r} \left(1 + \frac{2l^2}{3r^2} \right), \quad (3.1)$$

where the 5-dimensional cosmological constant $\tilde{\Lambda} \propto -l^{-2}$. As a result, general relativity is recovered in 4 dimensions in the static weak-field limit, with a first-order correction which is believed to be constrained by sub-millimeter experiments at the TeV level [141, 160].

The aim of this chapter is to set up the evolution and constraint equations for perturbations in a cold dark matter (CDM) brane cosmology, presenting them in such a way that they can be readily compared with the standard four-dimensional results, and to provide approximate solutions in the high and low-energy universe under certain restrictions on how the bulk reacts on the brane. Our equations are clearly incomplete since they lack a propagation equation for the non-local anisotropic stress that arises from projecting the bulk Weyl tensor onto the brane, and our solutions are only valid under the neglect of this stress. However, our presentation is such that we can easily include effective four-dimensional propagation equations for the non-local stress should such equations arise from a study of the full bulk perturbations. The lack of a four-dimensional propagation equation for the non-local stress means that it is currently not possible to obtain general results for the anisotropy of the CMB in braneworld models. Such a calculation would require solving the full five-dimensional perturbation equations which is non-trivial since the equations can only be reduced to two-dimensional partial differential equations on Fourier transforming the 3-space dependence.

The theory of cosmological perturbations using the metric-based approach, or the Bardeen approach has been extensively studied in [12, 20, 44, 45, 50, 100, 101, 107, 108, 110, 111, 116, 147, 148, 149, 165, 167, 178, 186, 188] (with Z_2

symmetry) and in [162] (without Z_2 symmetry). On the other hand, it has been also explored by various authors within the 1+3 covariant methods in [21, 77, 123, 124, 135, 136]. We will further summarise some of the qualitative implications for observational cosmology of the braneworld scenarios in the literature, and explore the possible implications for the CMB anisotropies in braneworld cosmology in the next chapter.

We give a brief summary of the (1+3)-covariant approach in §3.2. In §3.3, we look at the field equations of the braneworld cosmology. Following that, we will look at the linearized perturbation equations in §3.4, where the local and nonlocal conservation equations are given in §3.4.1, and the propagation, divergence and constraint equations are given in §3.4.2. Following that, we discuss the cosmological perturbations on the brane in §3.5, distinguishing between scalar perturbations (§3.5.1), vector perturbations (§3.5.2) and tensor perturbations (§3.5.3). To conclude this chapter, we will derive a covariant expression for the temperature anisotropy in §3.6.

§3.2 (1+3)-Covariant Approach in Cosmological Perturbation Theory

The (1+3)-covariant approach, pioneered by Ehlers [57], Ellis [59] and Hawking [79] provided an alternative gauge-invariant treatment of cosmological perturbations [61, 65] other than the standard metric-based approach formulated by Bardeen[8]*. In the (1+3) treatment, based on the covariant formulation of hydrodynamics and gravito-dynamics of Ehlers and Ellis (for an extensive review of the subject, see [11, 22, 57, 59, 60, 62]), the cosmological perturbations are described by gauge-invariant variables which have simple physical interpretations in terms of inhomogeneous measures of anisotropy of the Universe.

The covariant approach has been applied in many areas of cosmology, for example, gravitational waves (see e.g. [54]), inflation [23, 53], magnetic fields [181, 182, 183] and radiative transport theory [63, 64]. This develop a strong case for its application in the study of cosmic microwave background physics. The line of sight calculation of CMB anisotropies under the instantaneous recombination based on the covariant approach was obtained by Dunsby [52] and Challinor and Lasenby [33] based on earlier work in [51, 61, 63, 64, 65, 180]. Subsequently, the covariant approach was extended to studying CMB anisotropies in the CDM

*The Bardeen approach is inherently linear. It assumes a nonlocal decomposition of the perturbations into scalar, vector and tensor modes at the outset, with each of them treated separately. Even though the Bardeen variables are gauge-invariant, they are not physically transparent, i.e. they do not characterise perturbations in a way that is amenable to simple physical interpretation.

model in [34], tensor anisotropies induced by gravitational waves in [31], polarization in [29, 32], the mode and multipole representations and their application to temperature anisotropies in [73, 74] and obtaining model-independent limits on the inhomogeneity and anisotropy of the CMB anisotropy on large scales in [139].

The covariant approach has the advantage that it does not employ the non-local decomposition into scalar, vector and tensor modes. If required, that can be adopted at later stages of the calculation in aid to solve the equations. Even if one denies that working with gauge-invariant quantities is a significant merit, a key advantage of the covariant approach is that one is able to work exclusively with physically relevant quantities, satisfying equations which make manifest their physical consequences. Another advantage of the covariant approach is that the full extension to non-linear methods [140] is straightforward.

We start by choosing a 4-velocity u^a . This must be physically defined in such a way that if the universe is exactly FRW, the velocity reduces to that of the fundamental observers to ensure gauge-invariance of the approach. From the 4-velocity u^a , we construct a projection tensor h_{ab} into the space perpendicular to u^a (the instantaneous rest space of observers whose 4-velocity is u^a):

$$h_{ab} \equiv g_{ab} + u_a u_b, \quad (3.2)$$

where g_{ab} is the metric of spacetime. The operation of projecting a tensor fully with h_{ab} , symmetrizing, and removing the trace on every index (to return the projected-symmetric-trace-free or PSTF part) is denoted by angle brackets, i.e. $T_{(ab\dots c)}$.

The symmetric tensor h_{ab} is used to define a projected (spatial) covariant derivative D^a which when acting on a tensor $T^{b\dots c}_{d\dots e}$ returns a tensor that is orthogonal to u^a on every index,

$$D^a T^{b\dots c}_{d\dots e} \equiv h^a_p h^b_r \dots h^c_s h^t_d \dots h^u_e \nabla^p T^{r\dots s}_{t\dots u}, \quad (3.3)$$

where ∇^a denotes the usual covariant derivative.

The covariant derivative of the 4-velocity can be decomposed as follows:

$$\nabla_a u_b = \omega_{ab} + \sigma_{ab} + \frac{1}{3}\Theta h_{ab} - u_a A_b, \quad (3.4)$$

where ω_{ab} is the vorticity tensor which satisfies $u^a \omega_{ab} = 0$, $\sigma_{ab} = \sigma_{(ab)}$ is the shear which is PSTF, $\Theta \equiv \nabla^a u_a = 3H$ measures the volume expansion rate (where H is the local Hubble parameter), and $A_a \equiv u^b \nabla_b u_a$ is the acceleration. In addition, we define the vorticity vector, $\omega_a = -(1/2)\text{curl}u_a$.

Gauge-invariant quantities can be constructed from scalar variables by taking their projected gradients. Such quantities vanish in the FRW limit by construction.

The comoving fractional projected gradient of the density field $\rho^{(i)}$ of a species i (for example, photons) is one important example of this construction:

$$\Delta_a^{(i)} \equiv \frac{a}{\rho^{(i)}} D_a \rho^{(i)} , \quad (3.5)$$

where a is a locally defined scale factor satisfying

$$\dot{a} \equiv u^b \nabla_b a = H a , \quad (3.6)$$

which is included to remove the effect of the expansion on the projected gradients. Another important vector variable is the comoving projected gradient of the expansion,

$$\mathcal{Z}_a \equiv a D_a \Theta , \quad (3.7)$$

which provides a measure of the inhomogeneity of the expansion.

The matter stress-energy tensor T_{ab} can be decomposed irreducibly with respect to u^a as follows:

$$T_{ab} \equiv \rho u_a u_b + 2u_{(a} q_{b)} + P h_{ab} + \pi_{ab} , \quad (3.8)$$

where $\rho \equiv T_{ab} u^a u^b$ is the energy density measured by an observer moving with 4-velocity u^a , $q_a \equiv -h^b{}_a T_{bc} u^c$ is the energy flux or momentum density (orthogonal to u^a), $P \equiv h_{ab} T^{ab}/3$ is the isotropic pressure, and the PSTF tensor $\pi_{ab} \equiv T_{\langle ab \rangle}$ is the anisotropic stress.

The remaining gauge-invariant variables are formed from the Weyl tensor C_{abcd} which vanishes in an exact FRW universe because these models are conformally flat. The ten degrees of freedom in the 4-dimensional Weyl tensor can be encoded in two PSTF tensors: the electric and magnetic parts defined respectively as

$$E_{ab} = C_{abcd} u^b u^d , \quad (3.9)$$

$$H_{ab} = \frac{1}{2} C_{acst} u^c \eta^{st}{}_{bd} u^d , \quad (3.10)$$

where η_{abcd} is the 4-dimensional covariant permutation tensor.

In the covariant approach, we defer from making the frame choice until all the relevant equations, valid for u^a are derived. There are many different frame choices and we state the two main examples[†] which we employ in this thesis: (i) the pressure-free CDM frame, where the rest frame of the CDM defines a geodesic frame i.e. the peculiar velocity of the CDM is zero, and it defines a zero-acceleration frame, $A_a = 0$; and (ii) the energy frame, which is defined by vanishing total energy flux $q_a = 0$.

[†]Other frame choices are discussed in a review paper by Gebbie, Dunsby and Ellis [74].

§3.3 Field Equations of Braneworld Cosmology

In a recent paper, Maartens [135] introduced a formalism for describing the non-linear, intrinsic dynamics of the brane in Randall-Sundrum type II braneworld models in the form of bulk corrections to the 1+3 covariant propagation and constraint equations of general relativity. This approach is well suited to identifying the geometric and physical properties which determine homogeneity and anisotropy on the brane, and serves as a basis for developing a gauge-invariant description of cosmological perturbations in these models.

An important distinction between braneworlds and general relativity is that the set of 1+3 dynamical equations does not close on the brane. This is because there is no propagation equation for the non-local effective anisotropic stress that arises from projecting the bulk Weyl tensor onto the brane. The physical implication is that the initial value problem cannot be solved by brane-bound observers. The non-local Weyl variables enter crucially into the dynamics (for example, the Raychaudhuri equation) of the intrinsic geometry of the brane. Consequently, the existence of these non-local effects leads to the violation of several important results in theoretical cosmology, such as the connection between isotropy of the CMB and the Robertson-Walker geometry.

The field equations induced on the brane are derived by Shiromizu et al [176] using the Gauss-Codazzi equations, together with the Israel junction conditions and Z_2 symmetry. We will discuss this approach in detail in the later part of this section. In their elegant geometrical approach which they employed to analyze the dynamics of the RSII model, the bulk is a 1+4-dimensional spacetime with a non-compact extra spatial dimension. What prevents gravity from ‘leaking’ into the extra dimension at low energies is the negative bulk cosmological constant $\Lambda_5 = -6/\ell^2$, where ℓ is a curvature scale of the bulk.

In the weak-field static limit, null results in tests for deviations from Newton’s law impose the limit $\ell \lesssim 1$ mm. The negative Λ_5 is offset by the positive brane tension λ , which defines the energy scale dividing low from high energies. The limit $\ell < 1$ mm implies $\lambda > (100 \text{ GeV})^4$, and the energy scales i.e. the effective cosmological constant on the brane are related by the following relations:

$$\lambda = 6 \frac{\kappa^2}{\tilde{\kappa}^4}, \quad (3.11)$$

$$\Lambda = \frac{1}{2}(\Lambda_5 + \kappa^2 \lambda), \quad (3.12)$$

where $\tilde{\kappa}^2 = 8\pi/M_5^2$, with M_5 being the fundamental 5-dimensional Planck mass, Λ_5 is the cosmological constant in the bulk and λ is the tension of the brane. The constant $\kappa^2 = 8\pi G = 8\pi/M_4^2$, and $M_4 \sim 10^{19}$ GeV is the effective Planck scale on the brane. A further intriguing feature of the braneworld scenario is that,

because of the large extra dimensions, the fundamental energy scale of gravity can be dramatically lower than the effective Planck scale on the brane – as low as $\sim \text{TeV}$ in some scenarios [141]. In generalised RSII models, the lower bound arising from current tests for deviations from Newton’s law is

$$M_5 > 10^5 \text{ TeV}, \quad \lambda > (100\text{GeV})^4 \quad (3.13)$$

and is related to M_4 via $M_5^3 = M_4^2/\ell$.

A less stringent constraint given by nucleosynthesis [18, 141] implies that $\lambda \gtrsim (1\text{MeV})^4$ which gives

$$M_5 \gtrsim \left(\frac{1 \text{ MeV}}{M_4}\right)^{\frac{2}{3}}, \quad M_5 \gtrsim 10 \text{ TeV} . \quad (3.14)$$

At energies well above the brane tension λ , gravity becomes 5-dimensional and significant corrections to general relativity occur. There are also corrections that can operate at low energies, mediated by bulk graviton or Kaluza-Klein (KK) modes.

From the above discussion, we proceed to summarise the approach in [176] to derive the effective Einstein equations induced on the brane. The induced metric on the brane on all the hypersurfaces orthogonal to the unit normal n^A (A spacelike vector), is defined to be

$$g_{AB} = \tilde{g}_{AB} - n_A n_B \quad (3.15)$$

where we use tildes to denote the 5-dimensional generalization of standard general relativity quantities. We adopt the choice of coordinates to be $x^A = (x^a, y)$, where $x^a = (t, x^i)$ are spacetime coordinates on the brane and $n_A = \delta^y_A$.

Starting from the 5-dimensional Einstein equations,

$$\tilde{G}_{AB} = \tilde{\kappa}^2[-\Lambda_5 \tilde{g}_{AB} + \delta(y)(-\lambda g_{AB} + T_{AB})], \quad (3.16)$$

where the fields are confined to the brane that make up the brane energy momentum tensor, with $T_{AB}n^B = 0$.

Applying the Gauss-Codazzi relations to (3.16),

$$R_{ABCD} = \tilde{R}_{EFGH}g_A^E g_B^F g_C^G g_D^H + 2K_{A[C}K_{D]B}, \quad (3.17)$$

$$\tilde{R}_{BC}g_A^B n^C = \nabla_B K^B_A - \nabla_A K^B_B, \quad (3.18)$$

we obtain the following equation,

$$G_{AB} = -\frac{\tilde{\kappa}^2}{2}\Lambda_5 g_{AB} + K_C^C K_{AB} - K_A^C K_{CB} + \frac{1}{2}[K^{CD}K_{CD} - (K_C^C)^2]g_{AB} - \mathcal{E}_{AB}, \quad (3.19)$$

where

$$\mathcal{E}_{AB} = \tilde{C}_{ACBD} n^C n^D, \quad (3.20)$$

is the projection of the bulk Weyl tensor orthogonal to n^A , with $\mathcal{E}_{[AB]} = 0 = \mathcal{E}_A^A$.

We evaluate (3.19) on the brane as $y \rightarrow \pm 0$ to get the standard Einstein equation on the brane. To do that, K_{AB} has to be determined at the brane. The Israel junction conditions across the brane imply that g_{AB} is continuous, while K_{AB} undergoes a jump due to the energy-momentum on the brane:

$$K_{AB}^+ - K_{AB}^- = -\tilde{\kappa}^2 \left[T_{AB} + \frac{1}{3} g_{AB} (\lambda - T_C^C) \right]. \quad (3.21)$$

We impose Z_2 symmetry[‡] which implies that

$$K_{AB}^- = -K_{AB}^+, \quad (3.22)$$

and obtain

$$K_{AB} = -\frac{\tilde{\kappa}^2}{2} \left[T_{AB} + \frac{1}{3} g_{AB} (\lambda - T_C^C) \right]. \quad (3.23)$$

where we dropped the (+) and evaluate the quantities on the brane by taking the limit $y \rightarrow +0$.

Finally, we arrive at the result in [176]. The standard Einstein equation which is modified with new terms carrying the bulk effects on the brane:

$$G_{ab} = -\Lambda g_{ab} + \kappa^2 T_{ab} + \tilde{\kappa}^4 \mathcal{S}_{ab} - \mathcal{E}_{ab}, \quad (3.24)$$

where $\kappa^2 = 8\pi/M_4^2$. The bulk corrections to the Einstein equations on the brane are made up of two parts: (i) the matter fields which contribute local quadratic energy-momentum corrections via the symmetric tensor \mathcal{S}_{ab} ; and (ii) the non-local effects from the free gravitational field in the bulk transmitted by the (symmetric) projection \mathcal{E}_{ab} of the bulk Weyl tensor. The matter corrections are given by

$$\mathcal{S}_{ab} = \frac{1}{12} T_c^c T_{ab} - \frac{1}{4} T_{ac} T^c_b + \frac{1}{24} g_{ab} [3T_{cd} T^{cd} - (T_c^c)^2]. \quad (3.25)$$

We note that the local part of the bulk gravitational field is the five dimensional Einstein tensor \tilde{G}_{AB} , which is determined by the bulk field equations. Consequently, \mathcal{E}_{ab} transmits non-local gravitational degrees of freedom from the bulk to the brane that includes both tidal (or Coulomb), gravito-magnetic, and transverse traceless (gravitational wave) effects.

[‡]The choice of Z_2 symmetry is motivated by a result in string theory by Horava and Witten in [91]. They showed that the 10-dimensional $E_8 \times E_8$ heterotic string is related to an 11 dimensional theory on the orbifold $R^{10} \times S^1/Z_2$. In that model, the standard model is confined on the 4-dimensional spacetime while the gravitons propagate in the full spacetime.

The bulk corrections can all be consolidated into an effective total energy density, pressure, anisotropic stress and energy flux. The modified Einstein equations take the standard Einstein form with a re-defined energy-momentum tensor:

$$G_{ab} = -\Lambda g_{ab} + \kappa^2 T_{ab}^{\text{tot}}, \quad (3.26)$$

where

$$T_{ab}^{\text{tot}} = T_{ab} + \frac{\tilde{\kappa}^4}{\kappa^2} \mathcal{S}_{ab} - \frac{1}{\kappa^2} \mathcal{E}_{ab}. \quad (3.27)$$

Decomposing \mathcal{E}_{ab} irreducibly with respect to u^a by analogy with Eq. (3.8), in [77, 135, 136]

$$\mathcal{E}_{ab} = - \left(\frac{\tilde{\kappa}}{\kappa} \right)^4 \left(\mathcal{U} u_a u_b + 2u_{(a} \mathcal{Q}_{b)} + \frac{\mathcal{U}}{3} h_{ab} + \mathcal{P}_{ab} \right), \quad (3.28)$$

(the prefactor is included to make e.g. \mathcal{U} have dimensions of energy density), it follows that the total density, pressure, energy flux and anisotropic pressure are given as follows:

$$\rho^{\text{tot}} = \rho + \frac{\tilde{\kappa}^4}{\kappa^6} \left[\frac{\kappa^4}{24} (2\rho^2 - 3\pi^{ab} \pi_{ab}) + \mathcal{U} \right], \quad (3.29)$$

$$P^{\text{tot}} = P + \frac{\tilde{\kappa}^4}{\kappa^6} \left[\frac{\kappa^4}{24} (2\rho^2 + 4P\rho + \pi^{ab} \pi_{ab} - 4q_a q^a) + \frac{1}{3} \mathcal{U} \right], \quad (3.30)$$

$$q_a^{\text{tot}} = q_a + \frac{\tilde{\kappa}^4}{\kappa^6} \left[\frac{\kappa^4}{24} (4\rho q_a - 6\pi_{ab} q^b) + \mathcal{Q}_a \right], \quad (3.31)$$

$$\pi_{ab}^{\text{tot}} = \pi_{ab} + \frac{\tilde{\kappa}^4}{\kappa^6} \left[\frac{\kappa^4}{12} [-(\rho + 3P)\pi_{ab} - 3\pi_{c(a} \pi_{b)}^c + 3q_{(a} q_{b)}] + \mathcal{P}_{ab} \right]. \quad (3.32)$$

Making use of eq. (3.11), the above equations can be recast into the following form which is more convenient for our purposes:

$$\rho^{\text{tot}} = \rho + \frac{1}{4\lambda} (2\rho^2 - 3\pi_{ab} \pi^{ab}) + \frac{6}{\kappa^4 \lambda} \mathcal{U}, \quad (3.33)$$

$$P^{\text{tot}} = P + \frac{1}{4\lambda} (2\rho^2 + 4\rho P + \pi_{ab} \pi^{ab} - 4q_a q^a) + \frac{2}{\kappa^4 \lambda} \mathcal{U}, \quad (3.34)$$

$$q_a^{\text{tot}} = q_a + \frac{1}{4\lambda} (4\rho q_a - \pi_{ab} q^b) + \frac{6}{\kappa^4 \lambda} \mathcal{Q}_a, \quad (3.35)$$

$$\pi_{ab}^{\text{tot}} = \pi_{ab} + \frac{1}{2\lambda} [-(\rho + 3P)\pi_{ab} + \pi_{c(a} \pi_{b)}^c + q_{(a} q_{b)}] + \frac{6}{\kappa^4 \lambda} \mathcal{P}_{ab}. \quad (3.36)$$

It is immediately obvious from the above equations that we can regain the 4-dimensional general relativity results, when $\lambda^{-1} \rightarrow 0$.

For the braneworld case, it is useful to introduce an additional dimensionless gradient which describes inhomogeneity in the non-local energy density \mathcal{U} :

$$\Upsilon_a \equiv \frac{a}{\rho} D_a \mathcal{U} . \quad (3.37)$$

The Gauss-Codazzi scalar equation for the 3-curvature defined by \mathcal{R} is given by

$$\mathcal{R} = \kappa^2 \rho \left(2 + \frac{\rho}{\lambda} \right) + \frac{12}{\kappa^2 \lambda} \mathcal{U} - \frac{2}{3} \Theta^2 + 2\Lambda , \quad (3.38)$$

where

$$\mathcal{R} \equiv {}^{(3)}R = h^{ab} {}^{(3)}R_{ab} \quad (3.39)$$

with ${}^{(3)}R_{ab}$ the intrinsic curvature of the surfaces orthogonal to u^a [§]. In braneworld models, the Gauss-Codazzi constraint reduces to the modified Friedmann equation

$$H^2 + \frac{K}{a^2} = \frac{1}{3} \kappa^2 \rho \left(1 + \frac{\rho}{2\lambda} \right) + \frac{1}{3} \Lambda + \frac{2}{\kappa^2 \lambda} \mathcal{U}, \quad (3.40)$$

where the 3-curvature scalar is $\mathcal{R} = 6K/a^2$. In non-flat models ($K \neq 0$) \mathcal{R} is not gauge-invariant since it does not vanish in the FRW limit. However, the comoving projected gradient

$$\eta_b \equiv \frac{a}{2} D_b \mathcal{R} \quad (3.41)$$

is a gauge-invariant measure of inhomogeneity in the intrinsic three curvature of the hypersurfaces orthogonal to u^a .

§3.4 Linearised perturbation equations for the total matter variables

In this section we derive the linearized perturbation equations[¶] for the study of cosmological perturbations (scalar, vector and tensor) on the brane. These linearized equations are essential for the study of CMB anisotropies and large scale structure, which provide an indirect probe of early universe cosmology.

[§]If the vorticity is non-vanishing flow-orthogonal hypersurfaces will not exist, and \mathcal{R} cannot be interpreted as the spatial curvature scalar.

[¶]The exact, non-linear local and nonlocal conservation equations, propagation and constraint equations are found in [135, 136] and these equations can be also used for both cosmological and astrophysical modelling, including strong gravity effects.

§3.4.1 Local and non-local conservation equations

Based on the form of the bulk energy-momentum tensor and Z_2 symmetry, the brane energy-momentum tensor is still covariantly conserved:

$$\nabla^b T_{ab} = 0 . \quad (3.42)$$

The contracted Bianchi identities on the brane ensure conservation of the total energy-momentum tensor, which combined with conservation of the matter tensor gives

$$\nabla^a \mathcal{E}_{ab} = \tilde{\kappa}^4 \nabla^a \mathcal{S}_{ab} = \frac{6\kappa^2}{\lambda} \nabla^a \mathcal{S}_{ab} . \quad (3.43)$$

The longitudinal part of \mathcal{E}_{ab} is sourced by quadratic energy-momentum terms including spatial gradients and time derivatives. As a result any evolution and inhomogeneity in the matter fields would generate non-local Coulomb-like gravitational effects in the bulk which back react on the brane. The conservation equation (3.42) implies evolution equations for the energy and momentum densities, and these are unchanged from their general relativistic form. To linear order in an almost-FRW brane cosmology we have

$$\dot{\rho} + \Theta(\rho + P) + D^a q_a = 0 , \quad (3.44)$$

and

$$\dot{q}_a + \frac{4}{3}\Theta q_a + (\rho + P)A_a + D_a P + D^b \pi_{ab} = 0 . \quad (3.45)$$

The linearised propagation equations for \mathcal{U} and \mathcal{Q} follow from Eq. (3.43) in [135]:

$$\dot{\mathcal{U}} + \frac{4}{3}\Theta \mathcal{U} + D^a \mathcal{Q}_a = 0 , \quad (3.46)$$

and

$$\dot{\mathcal{Q}}_a + \frac{4}{3}\Theta \mathcal{Q}_a + \frac{1}{3}D_a \mathcal{U} + D^b \mathcal{P}_{ab} + \frac{4}{3}\mathcal{U}A_a = \frac{\kappa^4}{12}(\rho + P)(-2D_a \rho + 3D^b \pi_{ab} + 2\Theta q_a) . \quad (3.47)$$

Taking the projected derivative of Eq. (3.44) we obtain the propagation equation for Δ_a at linear order:

$$\rho \dot{\Delta}_a + (\rho + P)(\mathcal{Z}_a + a\Theta A_a) + aD_a D^b q_b + a\Theta D_a P - \Theta P \Delta_a = 0 . \quad (3.48)$$

From equation (3.46), we obtain the evolution equation of the spatial gradient of the non-local energy density:

$$\dot{\Upsilon}_a = \left(\frac{P}{\rho} - \frac{1}{3} \right) \Theta \Upsilon_a - \frac{4\mathcal{U}}{3\rho} (\mathcal{Z}_a + a\Theta A_a) - \frac{a}{\rho} D_a D^b \mathcal{Q}_b . \quad (3.49)$$

From the propagation equations for \mathcal{U} and \mathcal{Q} it can be seen that the energy of the projected Weyl fluid is conserved while the momentum is not conserved; rather it is driven by the matter source terms on the right of Eq. (3.43). Note that no propagation equation for \mathcal{P}_{ab} is implied so the set of equations will not close.

§3.4.2 Propagation and constraint equations

In this section we give the general linearised gravito-electric, gravito-magnetic, shear and vorticity propagation and constraint equations on the brane, which follow from the Bianchi identities, and the equations for the kinematic variables σ_{ab} , and Θ and its gradient \mathcal{Z}_a which follow from the Ricci identity.

1. Gravito-electric propagation:

$$\begin{aligned} & \dot{E}_{ab} + \Theta E_{ab} + \frac{1}{2}\kappa^2(\rho + P)\sigma_{ab} + \frac{1}{2}\kappa^2 D_{\langle a} q_{b\rangle} + \frac{1}{6}\kappa^2 \Theta \pi_{ab} + \frac{1}{2}\kappa^2 \dot{\pi}_{ab} - \text{curl} H_{ab} \\ &= \frac{1}{12\kappa^2\lambda} [\kappa^4 \{-6\rho(\rho + P)\sigma_{ab} + 3(\dot{\rho} + 3\dot{P})\pi_{ab} + 3(\rho + 3P)\dot{\pi}_{ab} \\ & - 6\rho D_{\langle a} q_{b\rangle} + \Theta[\rho + 3P]\pi_{ab}\} - 48\mathcal{U}\sigma_{ab} - 36\dot{\mathcal{P}}_{ab} - 36D_{\langle a} \mathcal{Q}_{b\rangle} - 12\Theta\mathcal{P}_{ab}] ; \end{aligned} \quad (3.50)$$

2. Gravito-electric divergence:

$$\begin{aligned} & D^b E_{ab} + \frac{1}{2}\kappa^2 D^b \pi_{ab} - \frac{1}{3}\kappa^2 D_a \rho + \frac{1}{3}\kappa^2 \Theta q_a \\ &= \frac{1}{8\kappa^2\lambda} \left[\kappa^4 \left(-\frac{8}{3}\rho\Theta q_a + 2(\rho + 3P)D^b \pi_{ab} + \frac{8}{3}\rho D_a \rho \right) + 16D_a \mathcal{U} - 16\Theta \mathcal{Q}_a - 24D^b \mathcal{P}_{ab} \right] ; \end{aligned} \quad (3.51)$$

3. Gravito-magnetic propagation:

$$\dot{H}_{ab} + \Theta H_{ab} + \text{curl} E_{ab} - \frac{\kappa^2}{2} \text{curl} \pi_{ab} = \frac{3}{\kappa^2\lambda} \text{curl} \mathcal{P}_{ab} - \frac{\kappa^2}{4\lambda} \text{curl} [(\rho + 3P)\pi_{ab}] ; \quad (3.52)$$

4. Gravito-magnetic divergence:

$$D^b H_{ab} - \kappa^2(\rho + P)\omega_a + \frac{\kappa^2}{2} \text{curl} q_a = \frac{\kappa^2\rho}{\lambda} \omega_a + \frac{1}{\kappa^2\lambda} (8\mathcal{U}\omega_a - 3\text{curl} \mathcal{Q}_a) ; \quad (3.53)$$

5. Gravito-magnetic constraint

$$D_{\langle a} \omega_{b\rangle} + \text{curl} \sigma_{ab} - H_{ab} = 0 ; \quad (3.54)$$

6. Shear propagation:

$$\dot{\sigma}_{ab} + \frac{2}{3}\Theta\sigma_{ab} + E_{ab} - \frac{1}{2}\kappa^2 \pi_{ab} - D_{\langle a} A_{b\rangle} = \frac{1}{4\kappa^2\lambda} \{ \kappa^4 [-(\rho + 3P)\pi_{ab}] + 12\mathcal{P}_{ab} \} ; \quad (3.55)$$

7. Shear constraint:

$$D^b \sigma_{ab} - \text{curl} \omega_a - \frac{2}{3} D_a \Theta + \kappa^2 q_a = -\frac{1}{\kappa^2 \lambda} (\kappa^4 \rho q_a + 6 \mathcal{Q}_a) ; \quad (3.56)$$

8. Vorticity Propagation:

$$\dot{\omega}_{\langle a} + \frac{2}{3} \Theta \omega_a + \frac{1}{2} \text{curl} A_a = 0 ; \quad (3.57)$$

9. Vorticity Constraint:

$$D^a \omega_a - A^a \omega_a = 0 ; \quad (3.58)$$

10. Modified Raychaudhuri equation:

$$\dot{\Theta} = -\frac{1}{3} \Theta^2 - \frac{1}{2} \kappa^2 (\rho + 3P) + \Lambda - \frac{1}{2\kappa^2 \lambda} [\kappa^4 \rho (2\rho + 3P) + 12\mathcal{U}] + D^a A_a ; \quad (3.59)$$

11. Propagation equation for the comoving expansion gradient \mathcal{Z}_a which follows from Eq. (3.59):

$$\dot{\mathcal{Z}}_a + \frac{2}{3} \Theta \mathcal{Z}_a - a \dot{\Theta} A_a + \frac{\kappa^2}{2} a D_a (\rho + 3P) - a D_a D^b A_b = -\frac{1}{2\kappa^2 \lambda} \{ \kappa^4 a D_a [\rho (2\rho + 3P)] + 12a D_a \mathcal{U} \} . \quad (3.60)$$

The above propagation and constraint equations reduce to general relativity when $\lambda^{-1} \rightarrow 0$. These linearized equations together with Eqs. (3.42)–(3.47), govern the dynamics of the matter and gravitational fields on the brane, and incorporate both the quadratic energy-momentum (local) and the projected effects from the bulk (nonlocal). The local terms are proportional to ρ/λ , and they are dominant at high energies. The nonlocal terms would introduce imperfect fluid effects onto the brane, even if the matter has a perfect fluid form.

It was shown in [135, 136] that the bulk effects give rise to new driving and source terms from Eqs. (3.50)–(3.60). However, the vorticity propagation and constraint equations, together with the gravito-magnetic constraint have no direct bulk effects. The local and nonlocal energy densities act as driving terms in the expansion propagation. The spatial gradients of the local and nonlocal energy densities provide sources for the gravito-electric field. The nonlocal energy flux provides a source for the shear and gravito-magnetic field, and finally, the nonlocal anisotropic stress acts a driving term in the shear propagation and the gravito-electric and gravito-magnetic fields.

The spatial gradient of the 3-curvature scalar is an auxiliary variable. It can be related to the other gauge-invariant variables using Eqs. (3.38) and (3.41):

$$\eta_a = \kappa^2 \rho \Delta_a \left(1 + \frac{\rho}{\lambda} \right) + \frac{6}{\kappa^2 \lambda} \rho \Upsilon_a - \frac{2}{3} \Theta \mathcal{Z}_a . \quad (3.61)$$

Taking the time derivative of Eq. (3.61), commuting the spatial and temporal derivatives, and then making use of Eqs. (3.59) and (3.60), we obtain the evolution of the spatial gradient of the 3-curvature scalar:

$$\dot{\eta}_a + \frac{2}{3}\Theta\eta_a + \frac{1}{3}\mathcal{R}(\mathcal{Z}_a + a\Theta A_a) + \frac{2}{3}\Theta a D_a D^b A_b = -\kappa^2 \left(1 + \frac{\rho}{\lambda}\right) a D_a D^b q_b - \frac{6}{\kappa^2 \lambda} a D_a D^b \mathcal{Q}_b. \quad (3.62)$$

In general relativity, propagating η_a is a useful device to avoid numerical instability problems when solving for isocurvature modes in a zero acceleration frame (such as the rest-frame of the CDM) [126].

§3.5 Cosmological Perturbations on the Brane

In this section, we study the covariant, gauge-invariant splitting of linear cosmological perturbations into scalar, vector and tensor modes. In particular, we concentrate on the scalar and tensor equations on the brane, which are used for the analysis in the following chapter. The vector perturbations are placed here for completeness.

The limiting case of the background FRW brane is characterized by homogeneity and isotropy, i.e.:

$$D_a f = V_a = W_{ab} = 0, \quad (3.63)$$

where the quantities $f = \rho, P, \Theta, \mathcal{U}, V_a = A_a, \omega_a, \mathcal{Q}_a$, and $W_{ab} = \sigma_{ab}, E_{ab}, H_{ab}, \mathcal{P}_{ab}$.

The covariant and gauge-invariant splitting into scalar, vector and tensor modes is given by:

$$V_a = D_a V + \hat{V}_a, \quad (3.64)$$

and

$$W_{ab} = D_{\langle a} D_{b \rangle} W + D_{\langle a} \hat{W}_{b \rangle} + \hat{W}_{ab}, \quad (3.65)$$

where a hat denotes a transverse (divergence free) quantity (and W_{ab} is assumed trace-free). We note that V_a, W_{ab} and the other derived quantities, e.g. f and \hat{V}_a are first order.

§3.5.1 Scalar Perturbations

The scalar perturbations are covariantly characterized by

$$\hat{V}_a = \hat{W}_a = \hat{W}_{ab} = 0, \quad (3.66)$$

and consequently, we obtain

$$\text{curl} V_a = 0 = \text{curl} W_{ab}, \quad D^b W_{ab} = \frac{2}{3} D^2 (D_a W), \quad (3.67)$$

The vorticity constraint equation and gravitomagnetic constraint equation show that

$$\omega_a = 0 = H_{ab} . \quad (3.68)$$

For scalar perturbations, the magnetic part of the Weyl tensor H_{ab} and the vorticity tensor ω_{ab} vanish identically. The electric part of the Weyl tensor E_{ab} and the shear σ_{ab} need not vanish. The non-vanishing variables satisfy the propagation and constraint equations on the brane.

Scalar Harmonics

The tensor-valued, partial differential equations presented in the earlier sections can be reduced to scalar-valued, ordinary differential equations by expanding in an appropriate complete set of eigentensors. For scalar perturbations all gauge-invariant tensors can be constructed from derivatives of scalar functions. Thus it is natural to expand in STF tensors derived from the scalar eigenfunctions $Q^{(k)}$ of the projected Laplacian:

$$D^2 Q^{(k)} = -\frac{k^2}{a^2} Q^{(k)} , \quad (3.69)$$

satisfying $\dot{Q}^{(k)} = O(1)$ ^{||}. We adopt the following harmonic expansions of the gauge-invariant variables:

$$\begin{aligned} \Delta_a^{(i)} &= \sum_k k \Delta_k^{(i)} Q_a^{(k)} , & \mathcal{Z}_a &= \sum_k \frac{k^2}{a} \mathcal{Z}_k Q_a^{(k)} , \\ q_a^{(i)} &= \rho^{(i)} \sum_k q_k^{(i)} Q_a^{(k)} , & \pi_{ab}^{(i)} &= \rho^{(i)} \sum_k \pi_k^{(i)} Q_{ab}^{(k)} , \\ E_{ab} &= \sum_k \frac{k^2}{a^2} \Phi_k Q_{ab}^{(k)} , & \sigma_{ab} &= \sum_k \frac{k}{a} \sigma_k Q_{ab}^{(k)} , \\ v_a^{(i)} &= \sum_k v_k^{(i)} Q_a^{(k)} , & A_a &= \sum_k \frac{k}{a} A_k Q_a^{(k)} . \end{aligned} \quad (3.70)$$

Here $v_a^{(i)}$ is the 3-velocity of species i relative to u^a ; for the CDM model considered here we shall make use of $v_a^{(i)}$ for baryons b and CDM c . For photons γ and neutrinos ν we continue to work with the momentum densities which are related to the peculiar velocity of the energy frame for that species by e.g. $q_a^{(\gamma)} = (4/3)\rho^{(\gamma)}v_a^{(\gamma)}$ in linear theory. The scalar expansion coefficients, such as $\Delta_k^{(i)}$ are first-order gauge-invariant variables satisfying e.g. $D^a \Delta_k^{(i)} = O(2)$.

^{||}The notation $O(n)$ is short for $O(\epsilon^n)$ where ϵ is some dimensionless quantity characterising the departure from FRW symmetry. A list of identities for the scalar, vector and tensor harmonics are given in Appendix C.

We expand the non-local perturbation variables in scalar harmonics in the following manner:

$$\begin{aligned}\Upsilon_a &= \sum_k k \Upsilon_k Q_a^{(k)}, \\ \mathcal{Q}_a &= \sum_k \rho \mathcal{Q}_k Q_a^{(k)}, \\ \mathcal{P}_{ab} &= \sum_k \rho \mathcal{P}_k Q_{ab}^{(k)}.\end{aligned}\tag{3.71}$$

In addition, we can expand the projected gradient of the 3-curvature term:

$$\eta_a = \sum_k 2 \left(\frac{k^3}{a^2} \right) \left(1 - \frac{3K}{k^2} \right) \eta_k Q_a^{(k)}.\tag{3.72}$$

The form of this expansion is chosen so that if we adopt the energy frame (where $q_a = 0$) the variable η_k coincides with the curvature perturbation usually employed in gauge-invariant calculations.

Scalar equations on the brane

It is now straightforward to expand the 1+3 covariant propagation and constraint equations in scalar harmonics (see Appendix C). We shall consider the CDM model where the particle species are baryons (including electrons), which we model as an ideal fluid with pressure $p^{(b)}$ and peculiar velocity $v_a^{(b)}$, cold dark matter, which has vanishing pressure and peculiar velocity $v_a^{(c)}$, and photons and (massless) neutrinos which require a kinetic theory description. We neglect photon polarization, although this can easily be included in the 1+3 covariant framework [30]. Also, we assume that the entropy perturbations are negligible for the baryons, so that $D_a P^{(b)} = c_s^2 D_a \rho^{(b)}$ where c_s^2 is the adiabatic sound speed. A complete set of 1+3 perturbation equations for the general relativistic model can be found in [34]. We extend these equations to braneworld models here.

In the following, perturbations in the total matter variables are related to those in the individual components by

$$\rho \Delta_k = \sum_i \rho^{(i)} \Delta_k^{(i)}, \quad \rho q_k = \sum_i \rho^{(i)} q_k^{(i)}, \quad \rho \pi_k = \sum_k \rho^{(i)} \pi_k^{(i)},\tag{3.73}$$

where $q_k^{(b)} = (1 + P^{(b)}/\rho^{(b)})v_k^{(b)}$, $q_k^{(c)} = v_k^{(c)}$, and $\pi_k^{(i)}$ vanishes for baryons and CDM. Similarly, the total density and pressure are obtained by summing over components, e.g. $P = \sum_i P^{(i)}$. It is also convenient to write

$$P = (\gamma - 1)\rho,\tag{3.74}$$

but γ should not be assumed constant (in space or time).

We begin with the equation for the gravito-electric field:

$$\begin{aligned}
& \left(\frac{k}{a}\right)^2 \left(\dot{\Phi}_k + \frac{1}{3}\Theta\Phi_k \right) + \frac{1}{2}\frac{k}{a}\kappa^2\rho(\gamma\sigma_k - q_k) + \frac{1}{6}\kappa^2\rho\Theta(1 - 3\gamma)\pi_k + \frac{1}{2}\kappa^2\rho\dot{\pi}_k \\
&= \frac{1}{12\kappa^2\lambda} \left\{ -\kappa^4 \left[6\left(\frac{k}{a}\right)\rho^2(\gamma\sigma_k - q_k) - 3(\dot{\rho} + 3\dot{P})\rho\pi_k - 3(3\gamma - 2)\rho(\rho\dot{\pi}_k + \dot{\rho}\pi_k) \right. \right. \\
&\quad \left. \left. - (3\gamma - 2)\rho^2\Theta\pi_k \right] - 12\left(\frac{k}{a}\right)(4\mathcal{U}\sigma_k - 3\rho\mathcal{Q}_k) - 36(\dot{\rho}\mathcal{P}_k + \rho\dot{\mathcal{P}}_k) - 12\rho\Theta\mathcal{P}_k \right\}. \tag{3.75}
\end{aligned}$$

We have written this equation in such a form that every term is manifestly frame-independent. The shear propagation equation is

$$\frac{k}{a} \left(\dot{\sigma}_k + \frac{1}{3}\Theta\sigma_k \right) + \left(\frac{k}{a}\right)^2 (\Phi_k + A_k) - \frac{\kappa^2}{2}\rho\pi_k = \frac{1}{4\kappa^2\lambda} [-(3\gamma - 2)\kappa^4\rho^2\pi_k + 12\rho\mathcal{P}_k]. \tag{3.76}$$

The shear constraint is given by

$$\kappa^2\rho q_k - \frac{2}{3}\left(\frac{k}{a}\right)^2 \left[\mathcal{Z}_k - \left(1 - \frac{3K}{k^2}\right)\sigma_k \right] = -\frac{1}{\kappa^2\lambda}(\kappa^4\rho^2 q_k + 6\rho\mathcal{Q}_k). \tag{3.77}$$

The gravito-electric divergence is

$$\begin{aligned}
& 2\left(\frac{k}{a}\right)^3 \left(1 - \frac{3K}{k^2}\right)\Phi_k - \kappa^2\rho\left(\frac{k}{a}\right) \left[\Delta_k - \left(1 - \frac{3K}{k^2}\right)\pi_k \right] + \kappa^2\Theta\rho q_k \\
&= \frac{3}{8\kappa^2\lambda} \left\{ \kappa^4 \left[-\frac{8}{3}\rho^2\Theta q_k + \frac{4}{3}(3\gamma - 2)\rho^2 \left(1 - \frac{3K}{k^2}\right)\frac{k}{a}\pi_k + \frac{8}{3}\frac{k}{a}\rho^2\Delta_k \right] \right. \\
&\quad \left. + 16\frac{k}{a}\rho\Upsilon_k - 16\Theta\rho\mathcal{Q}_k - 16\rho\left(\frac{k}{a}\right) \left(1 - \frac{3K}{k^2}\right)\mathcal{P}_k \right\}. \tag{3.78}
\end{aligned}$$

The propagation equation for the comoving expansion gradient \mathcal{Z}_a is given by

$$\begin{aligned}
& \dot{\mathcal{Z}}_k + \frac{1}{3}\Theta\mathcal{Z}_k - \frac{a}{k}\dot{\Theta}A_k + \frac{k}{a}A_k + \frac{\kappa^2}{2}\frac{a}{k} \left[2(\rho^{(\gamma)}\Delta_k^{(\gamma)} + \rho^{(\nu)}\Delta_k^{(\nu)}) + (1 + 3c_s^2)\rho^{(b)}\Delta_k^{(b)} + \rho^{(c)}\Delta_k^{(c)} \right] \\
&= -\frac{1}{2\kappa^2\lambda}\frac{a}{k} \left\{ \kappa^4 [(2\rho + 3P)\rho\Delta_k + \rho(3\rho^{(\gamma)}\Delta_k^{(\gamma)} + 3\rho^{(\nu)}\Delta_k^{(\nu)} + (2 + 3c_s^2)\rho^{(b)}\Delta_k^{(b)} + 2\rho^{(c)}\Delta_k^{(c)})] \right. \\
&\quad \left. + 12\rho\Upsilon_k \right\}. \tag{3.79}
\end{aligned}$$

The non-local evolution equations for Υ_k and \mathcal{Q}_k are

$$\dot{\Upsilon}_k = \frac{1}{3}(3\gamma - 4)\Theta\Upsilon_k - \frac{4}{3}\Theta\frac{\mathcal{U}}{\rho}A_k - \frac{4\mathcal{U}k}{3\rho a}\mathcal{Z}_k + \frac{k}{a}\mathcal{Q}_k, \quad (3.80)$$

and

$$\begin{aligned} \dot{\mathcal{Q}}_k - \frac{1}{3}(3\gamma - 4)\Theta\mathcal{Q}_k + \frac{1}{3}\frac{k}{a}\left[\Upsilon_k + 2\left(1 - \frac{3K}{k^2}\right)\mathcal{P}_k\right] + \frac{4}{3}\frac{k\mathcal{U}}{a\rho}A_k \\ = \frac{\kappa^4}{6}\gamma\rho\left\{\Theta q_k + \frac{k}{a}\left[\left(1 - \frac{3K}{k^2}\right)\pi_k - \Delta_k\right]\right\}. \end{aligned} \quad (3.81)$$

The spatial gradient of the 3-curvature scalar is

$$\left(\frac{k}{a}\right)^2\left(1 - \frac{3K}{k^2}\right)\eta_k = \frac{\kappa^2\rho}{2}\Delta_k\left(1 + \frac{\rho}{\lambda}\right) + \frac{3}{\kappa^2\lambda}\rho\Upsilon_k - \frac{1}{3}\frac{k}{a}\Theta\mathcal{Z}_k, \quad (3.82)$$

and it evolves according to

$$\frac{k}{a}\left(1 - \frac{3K}{k^2}\right)\left(\dot{\eta}_k - \frac{1}{3}\Theta A_k\right) + \frac{K}{a^2}\mathcal{Z}_k - \frac{1}{2}\kappa^2\rho q_k = \frac{1}{2\kappa^2\lambda}(\kappa^4\rho^2 q_k + 6\rho\mathcal{Q}_k). \quad (3.83)$$

The evolution equations for the scalar harmonic components of the comoving, fractional density gradients for photons, neutrinos, baryons and cold dark matter (CDM) are

$$\dot{\Delta}_k^{(\gamma)} = -\frac{k}{a}\left(\frac{4}{3}\mathcal{Z}_k - q_k^{(\gamma)}\right) - \frac{4}{3}\Theta A_k \quad (\text{photons}), \quad (3.84)$$

$$\dot{\Delta}_k^{(\nu)} = -\frac{k}{a}\left(\frac{4}{3}\mathcal{Z}_k - q_k^{(\nu)}\right) - \frac{4}{3}\Theta A_k \quad (\text{neutrinos}), \quad (3.85)$$

$$\dot{\Delta}_k^{(b)} = \left(1 + \frac{P^{(b)}}{\rho^{(b)}}\right)\left[-\frac{k}{a}(\mathcal{Z}_k - v_k^{(b)}) - \Theta A_k\right] + \left(\frac{P^{(b)}}{\rho^{(b)}} - c_s^2\right)\Theta\Delta_k^{(b)} \quad (\text{baryons}), \quad (3.86)$$

$$\dot{\Delta}_k^{(c)} = -\frac{k}{a}(\mathcal{Z}_k - v_k^{(c)}) - \Theta A_k \quad (\text{CDM}). \quad (3.87)$$

The evolution equations for the momentum densities and peculiar velocities are

$$\dot{q}_k^{(\gamma)} = -\frac{1}{3} \frac{k}{a} \left[\Delta_k^{(\gamma)} + 4A_k + 2 \left(1 - \frac{3K}{k^2} \right) \pi_k^{(\gamma)} \right] + n_e \sigma_T \left(\frac{4}{3} v_k^{(b)} - q_k^{(\gamma)} \right), \quad (3.88)$$

$$\dot{q}_k^{(\nu)} = -\frac{1}{3} \frac{k}{a} \left[\Delta_k^{(\nu)} + 4A_k + 2 \left(1 - \frac{3K}{k^2} \right) \pi_k^{(\nu)} \right], \quad (3.89)$$

$$(\rho^{(b)} + P^{(b)}) \dot{v}_k^{(b)} = -(\rho^{(b)} + P^{(b)}) \left[\frac{1}{3} (1 - 3c_s^2) \Theta v_k^{(b)} + \frac{k}{a} A_k \right] - \frac{k}{a} (1 + c_s^2) \Delta_k^{(b)} \quad (3.90)$$

$$- n_e \sigma_T \frac{\rho^{(\gamma)}}{\rho^{(\nu)}} \left(\frac{4}{3} v_k^{(b)} - q_k^{(\gamma)} \right),$$

$$\dot{v}_k^{(c)} = -\frac{1}{3} \Theta v_k^{(c)} - \frac{k}{a} A_k, \quad (3.91)$$

where the Thomson scattering terms involving the electron density n_e and Thomson cross section σ_T arise from the interaction between photons and the tightly-coupled baryon/electron fluid. The remaining equations are the propagation equations for the anisotropic stresses of photons and neutrinos, and the higher moments of their distribution functions. These equations can be found in [34], and with polarization included in [29, 30, 32], since they are unchanged from general relativity. However, we shall not require these additional equations at the level of approximation we make in our subsequent calculations.

§3.5.2 Vector Perturbations

The vector perturbations are covariantly characterized by

$$V_a = \hat{V}_a, \quad W_{ab} = D_{\langle a} \hat{W}_{b \rangle}, \quad \text{curl} D_a f = -2 \dot{f} \omega_a, \quad (3.92)$$

and it follows that

$$D^a W_{ab} = \frac{1}{2} D^2 \hat{W}_b, \quad \text{curl} W_{ab} = \frac{1}{2} D_{\langle a} \text{curl} \hat{W}_{b \rangle}. \quad (3.93)$$

Vector equations on the brane

There are no bulk effects in the linearized vorticity propagation equation (3.57), and hence the vorticity decays away with the expansion like the general relativity, and this can be interpreted as angular momentum conservation equation on the brane. However the gravito-magnetic divergence equation becomes

$$D^b H_{ab} = \kappa^2 (\rho + P) \omega_a - \frac{\kappa^2}{2} \text{curl} q_a + \frac{1}{\kappa^2 \lambda} \{ \kappa^2 \rho (\rho + P) + 8\mathcal{U} \} \omega_a - 3 \text{curl} \mathcal{Q}_a. \quad (3.94)$$

The bulk terms provide additional sources for the gravito-magnetic field. The existence of the bulk terms made it possible to source vector perturbations even when the vorticity vanishes, since $\text{curl}\mathcal{Q}_a$ may be non-zero.

§3.5.3 Tensor Perturbations

The (1+3)-covariant description of gravitational waves in a cosmological context has been considered in detail by Challinor [31] and Dunsby et al [54] for the non-flat and flat cases respectively. In this section, we will extend to the case of braneworld cosmology.

Tensor perturbations are covariantly characterized by

$$D_a f = 0, \quad A_a = \omega_a = \mathcal{Q}_a = 0, \quad D^a W_{ab} = 0, \quad W_{ab} = \hat{W}_{ab}. \quad (3.95)$$

In this description, the linearized gravitational waves are described by the transverse degrees of freedom in the electric and magnetic parts of the Weyl tensor. $D^a W_{ab}$ indicates that the shear and anisotropic stress (both local and nonlocal) are transverse. Furthermore, the vorticity and all projected vectors vanish at linear order. The individual matter components all possess the same four-velocity which defines the fundamental velocity u^a in a pure tensor mode.

The constraint equation (Eq. (3.54)) becomes

$$H_{ab} = \text{curl}\sigma_{ab}, \quad (3.96)$$

which determines the magnetic part of the Weyl tensor from the shear.

For convenience, we define a rescaled nonlocal anisotropic stress π_{ab}^* by the following relation:

$$\kappa^2 \pi_{ab}^* = \frac{6}{\kappa^2 \lambda} \mathcal{P}_{ab}. \quad (3.97)$$

The propagation equations for the tensor perturbations from Eqs (3.50)–(3.60)

are reduced to the following set:

$$\dot{\rho} = -(\rho + P)\Theta, \quad (3.98)$$

$$\dot{\Theta} = -\frac{1}{3}\Theta^2 - \frac{1}{2}\kappa^2(\rho + 3P) + \Lambda - \frac{1}{2\kappa^2\lambda}[\kappa^4\rho(2\rho + 3P) + 12\mathcal{U}], \quad (3.99)$$

$$\dot{\sigma}_{ab} = -\frac{2}{3}\Theta\sigma_{ab} - E_{ab} + \frac{\kappa^2}{2}(\pi_{ab} + \pi_{ab}^*) - \frac{\kappa^2}{4\lambda}(\rho + 3P)\pi_{ab}, \quad (3.100)$$

$$\dot{H}_{ab} = -\Theta H_{ab} - \text{curl}E_{ab} + \frac{\kappa^2}{2}\text{curl}(\pi_{ab} + \pi_{ab}^*) - \frac{\kappa^2}{4\lambda}\text{curl}[(\rho + 3P)\pi_{ab}], \quad (3.101)$$

$$\dot{E}_{ab} = -\Theta E_{ab} + \text{curl}H_{ab} - \frac{\kappa^2}{2} \left[(\rho + P)\sigma_{ab} + \dot{\pi}_{ab} + \frac{1}{3}\Theta\pi_{ab} + \dot{\pi}_{ab}^* + \frac{1}{3}\Theta\pi_{ab}^* \right] \quad (3.102)$$

$$\begin{aligned} & + \frac{1}{12\kappa^2\lambda} \left[3\kappa^4\{(\dot{\rho} + 3\dot{P})\pi_{ab} + (\rho + 3P)\dot{\pi}_{ab}\} + \kappa^4(\rho + 3P)\Theta\pi_{ab} \right. \\ & \left. - 6\kappa^4\rho(\rho + P)\sigma_{ab} - 48\mathcal{U}\sigma_{ab} \right]. \end{aligned}$$

The inhomogeneous wave equations for the shear and the magnetic part of the Weyl tensor follow from differentiating Eqs. (3.100) and (3.101) along the flow lines of u^a , making use of Eq.(3.74) (assuming $\dot{\gamma} \neq 0$) and the identities (C.10)–(C.13) from Appendix C, we obtain:

$$\begin{aligned} & \ddot{\sigma}_{ab} + D^2\sigma_{ab} + \frac{5}{3}\theta\dot{\sigma}_{ab} + \left[\frac{1}{2}(4 - 3\gamma)\kappa^2\rho - \frac{K}{a^2} \right] \sigma_{ab} \\ & = \kappa^2 \left[\left(\dot{\pi}_{ab} + \frac{2}{3}\Theta\pi_{ab} \right) + \left(\dot{\pi}_{ab}^* + \frac{2}{3}\Theta\pi_{ab}^* \right) \right. \\ & \left. - (3\gamma - 2)\frac{\rho}{6\lambda} \left(3\dot{\pi}_{ab} - (3\gamma - 2)\Theta\pi_{ab} + \frac{9\dot{\gamma}}{3\gamma - 2}\pi_{ab} - 3\rho\sigma_{ab} \right) \right], \end{aligned} \quad (3.103)$$

and

$$\begin{aligned} & \ddot{H}_{ab} + D^2H_{ab} + \frac{7}{3}\theta\dot{H}_{ab} + 2 \left[(2 - \gamma)\kappa^2\rho - \frac{3K}{a^2} \right] H_{ab} \\ & = \kappa^2 \left[\text{curl}\dot{\pi}_{ab} + \frac{2}{3}\Theta\text{curl}\pi_{ab} \right] + \kappa^2 \left[\text{curl}\dot{\pi}_{ab}^* + \frac{2}{3}\Theta\text{curl}\pi_{ab}^* \right] \\ & \quad - \frac{\kappa^2}{12}(3\gamma - 2)\rho \left[\left(\frac{3\dot{\gamma}}{3\gamma - 2} \right) \text{curl}\pi_{ab} - \gamma\Theta\text{curl}\pi_{ab} + \text{curl}\dot{\pi}_{ab} + \frac{2}{3}\Theta\rho\text{curl}\pi_{ab} \right]. \end{aligned} \quad (3.104)$$

Tensor Harmonics

Analogous to the scalar case, the electric and magnetic parts of the Weyl tensor, the shear, and the local and non-local anisotropic stress can be expanded directly

in the electric and magnetic parity tensor harmonics defined in [31]:

$$E_{ab} = \sum_k \left(\frac{k}{a}\right)^2 \left(E_k Q_{ab}^{(k)} + \bar{E}_k \bar{Q}_{ab}^{(k)} \right), \quad (3.105)$$

$$H_{ab} = \sum_k \left(\frac{k}{a}\right)^2 \left(H_k Q_{ab}^{(k)} + \bar{H}_k \bar{Q}_{ab}^{(k)} \right), \quad (3.106)$$

$$\sigma_{ab} = \sum_k \left(\frac{k}{a}\right) \left(\sigma_k Q_{ab}^{(k)} + \bar{\sigma}_k \bar{Q}_{ab}^{(k)} \right), \quad (3.107)$$

$$\pi_{ab}^{(i)} = \sum_k \rho \left(\pi_k^{(i)} Q_{ab}^{(k)} + \bar{\pi}_k^{(i)} \bar{Q}_{ab}^{(k)} \right), \quad (3.108)$$

$$\mathcal{P}_{ab} = \sum_k \rho \left(\mathcal{P}_k^{(i)} Q_{ab}^{(k)} + \bar{\mathcal{P}}_k^{(i)} \bar{Q}_{ab}^{(k)} \right). \quad (3.109)$$

where \sum_k denotes a sum over the harmonic modes. Note that the electric and magnetic parity tensor harmonics are related by Eqs (C.14) and (C.15) in Appendix C.

Tensor Equations on the Brane

Using the gravitomagnetic constraint in Eq. (3.54) and together with tensor harmonics above, we expand the first order equations (eqs. (3.100) and (3.102)), and obtain **,

$$\left(\frac{k}{a}\right) \left(\dot{\sigma}_k + \frac{1}{3} \Theta \sigma_k \right) + \left(\frac{k}{a}\right)^2 E_k - \frac{\kappa^2}{2} \rho \pi_k = \frac{1}{4\kappa^2 \lambda} \rho [-\kappa^4 (3\gamma - 2) \rho \pi_k] + \frac{\kappa^2}{2} \rho \pi_k^*, \quad (3.111)$$

and

$$\begin{aligned} & \left(\frac{k}{a}\right)^2 \left(\dot{E}_k + \frac{1}{3} \Theta E_k \right) - \left(\frac{k}{a}\right) \left[\left(\frac{k}{a}\right)^2 + \frac{3K}{a^2} - \frac{\kappa^2}{2} \gamma \rho \right] \sigma_k + \frac{\kappa^2}{2} \rho \dot{\pi}_k - \frac{\kappa^2}{6} (3\gamma - 1) \rho \Theta \pi_k \\ &= \frac{1}{12\kappa^2 \lambda} \left\{ -\kappa^4 \left[6 \left(\frac{k}{a}\right) \gamma \rho^2 \sigma_k - 3(\dot{\rho} + 3\dot{P}) \rho \pi_k - 3(3\gamma - 2) \rho (\rho \dot{\pi}_k + \dot{\rho} \pi_k) - (3\gamma - 2) \rho^2 \Theta \pi_k \right] \right. \\ & \quad \left. - 48 \left(\frac{k}{a}\right) \mathcal{U} \sigma_k \right\} - \frac{\kappa^2}{2} \left(\dot{\rho} \pi_k^* + \rho \dot{\pi}_k^* + \frac{1}{3} \rho \Theta \pi_k^* \right). \end{aligned} \quad (3.112)$$

**Note that from eq. (3.96), we find that H_k is algebraic in $\bar{\sigma}_k$:

$$H_k = \left(1 + \frac{3K}{k^2} \right)^{\frac{1}{2}} \bar{\sigma}_k. \quad (3.110)$$

These curl terms lead to a coupling of different polarization states.

From Eq.(3.103), we get

$$\begin{aligned}
 & \ddot{\sigma}_k + \Theta \dot{\sigma}_k + \left[\frac{k^2}{a^2} + \frac{2K}{a^2} - \frac{\kappa^2 \rho}{3}(3\gamma - 2) \right] \sigma_k + \kappa^2 \rho \left(\frac{a}{k} \right) \left[\frac{1}{3}(3\gamma - 2)\Theta \pi_k - \dot{\pi}_k \right] \\
 &= \frac{a}{k} \kappa^2 \rho \left(\dot{\pi}_k^* + \left(\frac{2}{3} - \gamma \right) \Theta \pi_k^* \right) + \frac{1}{3\kappa^2 \lambda} (12\mathcal{U} + (3\gamma - 1)\kappa^4 \rho^2) \sigma_k \\
 &+ \frac{1}{6\kappa^2 \lambda} \left(\frac{a}{k} \right) \left[9(2\gamma^2 \Theta - \dot{\gamma}) \kappa^4 \rho^2 \pi_k - 3(3\gamma - 2) \kappa^4 \rho^2 \dot{\pi}_k - 2(2 - 9\gamma) \kappa^4 \rho^2 \Theta \pi_k \right].
 \end{aligned} \tag{3.113}$$

This equation is equivalent to the form found by Maartens in [135, 136] for the transverse traceless modes on the brane. From the above equation, the nonlocal bulk effects would provide driving terms which would act like the anisotropic stress in general relativity. For the local anisotropic stress, the evolution is determined by the Boltzmann equation. However, the evolution equation of the non-local anisotropic stress is not known. We will make an local approximation to the evolution equation of the non-local anisotropic stress in the subsequent chapter to see its effects on the CMB tensor power spectra.

§3.6 A covariant expression for the temperature anisotropy

In this final section, we discuss the line of sight solution to the Boltzmann equation for the scalar contribution to the gauge-invariant temperature anisotropy $\delta_T(e)$ of the CMB in braneworld models. We employ the 1+3 covariant approach, and show that our result is equivalent to that given recently by Langlois et al [118] using the Bardeen formalism.

Over the epoch of interest the individual matter constituents of the universe interact with each other under gravity only, except for the photons and baryons (including the electrons), which are also coupled through Thomson scattering. The variation of the gauge-invariant temperature perturbation $\delta_T(e)$, where e^a is the (projected) photon propagation direction, along the line of sight is given by the (linearized) covariant Boltzmann equation (valid for scalar, vector, and tensor modes) [33]:

$$\begin{aligned}
 \delta_T(e)' + \sigma_T n_e \delta_T(e) &= -\sigma_{ab} e^a e^b - A_a e^a - \frac{e^a D_a \rho^{(\gamma)}}{4\rho^{(\gamma)}} - \frac{D^a q_a^{(\gamma)}}{4\rho^{(\gamma)}} \\
 &+ \sigma_T n_e \left(v_a^{(b)} e^a + \frac{3}{16} \rho^{(\gamma)} \pi_{ab}^{(\gamma)} e^a e^b \right),
 \end{aligned} \tag{3.114}$$

where the prime denotes the derivative with respect to a parameter λ defined along the line of sight by $d\lambda = -u_a dx^a$.

Following the steps in [33], we expand the right-hand side of Eq. (3.114) in scalar harmonics and integrate along the line of sight from the early universe to the observation point R . Neglecting effects due to the finite thickness of the last scattering surface, on integrating by parts we find that the temperature anisotropy involves the quantity

$$\left(\frac{a}{k}\sigma'_k\right)' + \frac{1}{3}\frac{k}{a}(\sigma_k - \mathcal{Z}_k) + A'_k - HA_k = -2\dot{\Phi}_k + \left(\frac{a}{k}\right)^2 I \quad (3.115)$$

integrated along the line of sight (after multiplying with $Q^{(k)}$). In simplifying Eq. (3.115) we have made use of the derivative of the shear propagation equation (3.76), substituted for q_k and \mathcal{Z}_k from Eqs. (3.75) and (3.77), and finally used Eqs. (3.40) and (3.59). The quantity I is the total sum of all the braneworld corrections:

$$I = \left(\frac{a}{k}\right)^2 \left[\dot{I}_1 + \frac{1}{3}\Theta I_1 + I_2 + \frac{1}{3}\left(\frac{k}{a}\sigma_k\right) I_3 + \frac{1}{2}\left(\frac{k}{a}\right) I_4 \right], \quad (3.116)$$

where

$$\begin{aligned} I_1 &= \frac{1}{4\kappa^2\lambda} [-(3\gamma - 2)\kappa^4\rho^2\pi_k + 12\rho\mathcal{P}_k], \\ I_2 &= \frac{1}{12\kappa^2\lambda} \left\{ -\kappa^4 \left[6\left(\frac{k}{a}\right)\gamma\rho^2\sigma_k - 3(\dot{\rho} + 3\dot{P})\rho\pi_k - 3(3\gamma - 2)\rho(\rho\dot{\pi}_k + \dot{\rho}\pi_k) - 6\left(\frac{k}{a}\right)\rho^2q_k \right. \right. \\ &\quad \left. \left. - (3\gamma - 2)\rho^2\Theta\pi_k \right] - 48\left(\frac{k}{a}\right)\mathcal{U}\sigma_k - 36(\dot{\rho}\mathcal{P}_k + \rho\dot{\mathcal{P}}_k) + 36\left(\frac{k}{a}\right)\rho\mathcal{Q}_k - 12\rho\Theta\mathcal{P}_k \right\}, \\ I_3 &= \frac{1}{2\kappa^2\lambda} [(3\gamma - 1)\kappa^4\rho^2 + 12\mathcal{U}], \\ I_4 &= \frac{\kappa^2\rho^2}{3\lambda}\sigma_k + \frac{4}{\kappa^2\lambda}\mathcal{U}\sigma_k - \frac{1}{4\kappa^2\lambda}(4\kappa^4\rho^2q_k + 24\rho\mathcal{Q}_k). \end{aligned} \quad (3.117)$$

A lengthy calculation making use of the propagation and constraint equations shows that $I = 0$. The final result for the temperature anisotropies is then

$$\begin{aligned} [\delta_T(e)]_R &= -\sum_k \left[\left(\frac{1}{4}\Delta_k^{(\gamma)} + \frac{a}{k}\dot{\sigma}_k + A_k \right) Q^{(k)} \right]_A + \sum_k [(v_k^{(b)} - \sigma_k)e^a Q_a^{(k)}]_A \\ &\quad + \frac{3}{16} \sum_k (\pi_k^{(\gamma)} e^a e^b Q_{ab}^{(k)})_A + 2 \sum_k \int_{\lambda_A}^{\lambda_R} \dot{\Phi}_k Q^{(k)} d\lambda, \end{aligned} \quad (3.118)$$

where the event A is the intersection of the null geodesic with the last scattering surface.

In retrospect, one could re-derive the result for the temperature anisotropy in braneworld models much more simply by retaining the effective stress-energy variables ρ^{tot} , P^{tot} , q_a^{tot} and π_{ab}^{tot} in the propagation and constraint equations used in the manipulation of the left-hand side of Eq. (3.115), rather than isolating the braneworld contributions.

If we adopt the longitudinal gauge, defined by $\sigma_{ab} = 0$, we find that the electric part of the Weyl tensor and the acceleration are related by $\Phi_k = -A_k$ if the total anisotropic stress π_{ab}^{tot} vanishes. It follows that in this zero shear frame we recover the result found by Langlois et al [118].

Chapter 4

Braneworld Cosmology II: Initial Conditions and CMB Anisotropies

“Order and simplification are the first steps toward the mastery of a subject - the actual enemy is the unknown.”

- **Thomas Mann**

In this chapter, we discuss the possible implications of braneworld cosmology for the CMB, based on work described in [123] and [124]. For the scalar perturbations, we supplement the equations for the total matter variables with equations for the independent matter components in a cold dark matter cosmology, and provide solutions in the high and low-energy radiation-dominated phase under the assumption that the non-local anisotropic stress vanishes. These solutions reveal the existence of new modes arising from the two additional non-local degrees of freedom. Our solutions should prove useful in setting up initial conditions for numerical codes aimed at exploring the effect of braneworld corrections on the cosmic microwave background (CMB) power spectrum. We show that the 3-curvature is only constant in the high energy limit for the modes which correspond similarly to the growing and decaying mode in general relativity. The CMB temperature anisotropies are insensitive to the brane tension λ if the dark energy contribution is ignored. For the tensor perturbations, we set out the framework of a program to compute the tensor anisotropies in the CMB that are generated in braneworld models. In the simplest approximation, we show the braneworld imprint as a correction to the power spectra for standard temperature and polarization anisotropies and similarly show that the tensor anisotropies are also insensitive to high energy effects.

§4.1 From Perturbation Theory to CMB Anisotropies in Braneworlds

The cosmic microwave background (CMB) currently occupies a central role in modern cosmology. It is the cleanest cosmological observable, providing us with a unique record of conditions along our past light cone back to the epoch of decoupling when the mean free path to Thomson scattering rose suddenly due to hydrogen recombination. Present (e.g. BOOMERANG [115], MAXIMA [14], and VSA [164]) and future (e.g. MAP and PLANCK) data on the CMB anisotropies, combined with large-scale structure data, provide extensive information on the amplitude and evolution of cosmological perturbations. Potentially this allows us to infer the spectrum of initial perturbations in the early universe and to determine the standard cosmological parameters to high accuracy. An obvious question to ask is whether there are any signatures of extra dimensions which could be imprinted on the cosmic microwave sky.

There has been an explosion of interest in the theory of cosmological perturbations in braneworlds and their implications for observational cosmology. We will briefly summarize * most of the work which has explored these issues.

The relation between braneworld cosmology, the AdS/CFT correspondence and quantum cosmology has been discussed in [4]. Binetruy et al [12] have studied the background cosmological dynamics of a Friedmann brane in a Schwarzschild-Anti-de Sitter bulk. The modifications to inflation are also explored by various authors in [41, 71, 75, 128], in [95] (for quintessence) and in [76, 116, 166] (for gravitational waves). The large scale perturbations generated from quantum fluctuations during de Sitter inflation on the brane have been computed and studied in [20, 71, 80, 117, 141]. High-energy inflation on the brane generates a zero-mode (4D graviton mode) of tensor perturbations, and stretches it to super-Hubble scales. This zero-mode has the same qualitative features as in general relativity, remaining frozen at constant amplitude while beyond the Hubble horizon, but the overall amplitude is higher [119]. The massive KK modes (5D graviton modes) remain in the vacuum state during slow-roll inflation. The evolution of the super-Hubble zero mode is the same as in general relativity, so that high-energy braneworld effects in the early universe serve only to re-scale the amplitude. However, when the zero mode re-enters the Hubble horizon, massive KK modes can be excited. Qualitative arguments [76, 80] indicate that this is a very small effect, but it remains to be properly quantified, so that the signature on the CMB may be calculated, and constraints may be imposed on the braneworld parameters.

Other authors [19, 50, 100, 101, 107, 108, 110, 111, 165, 166, 178, 187] have considered the cosmological consequences of interactions between the brane and

*We apologize in advance if we have missed some of the literature in this thesis.

the bulk. These authors constructed approximations from the bulk equations and explored the implications for observational cosmology on the brane. Their methods are based mainly on the Bardeen approach.

For the study of cosmological perturbations and its relation to the cosmic microwave background (CMB) and large scale structure (LSS), the covariant formalism has been well described in the previous chapter. We will summarize some of the main results for the scalar and tensor perturbations based on earlier work by various authors.

For scalar perturbations, the bulk effects introduce a non-adiabatic mode on large scales. The additional non-adiabatic has been found in [21, 77, 118, 123, 135]. In addition, another growing mode was found in [123] in Λ CDM cosmology. The density perturbations on large scales can be solved on the brane without solving for the bulk perturbations [77], but the Sachs-Wolfe effect cannot be found on the brane because of the non-local anisotropic stress (see also [118]), which is underdetermined. There are possible changes on the scalar modes for both large and small scales.

For tensor perturbations, we recall earlier that the bulk effects generate a massless mode during inflation and a continuum of KK modes [71, 117]. The massive modes stay in the vacuum state, and on large scales, there is a constant mode with enhanced amplitude in [117]. In this case, there is no qualitative change on large scales in the low energy regime (4D general relativity), but significant change in small scales.

We have learned from the previous chapter that there are two types of corrections which will arise from braneworld cosmology. The first type of correction occurs at energies well above the brane tension λ , where gravity becomes 5-dimensional. This will introduce significant corrections to general relativity. On the other hand, there are also corrections that can operate at low energies, mediated by bulk graviton or Kaluza-Klein (KK) modes. Both types of correction play an important role in both scalar and tensor perturbations.

In §4.2, we work out the perturbative dynamics and initial conditions for the scalar perturbations in both the CDM (§4.2.1) and energy frames (§4.2.2). We first show that there are two additional non-local isocurvature modes present in braneworld cosmology and subsequently examine whether they will contribute significantly to the CMB anisotropy in §4.2.3.

We develop the formalism to compute the tensor anisotropies in the CMB in §4.3, which incorporates the early-universe high-energy braneworld effects, and we carefully delineate what is known on the brane from what is required from bulk equations. Once the 5D solutions are provided, our formalism, with its modified CMB code (based on CAMB [125, 126]), is able to compute these anisotropies. We illustrate this by using a simple approximation in §4.3.1 to the 5D effects (refer

to the analysis of the braneworld scalar Sachs-Wolfe effect in [9]). We plot the braneworld correction to the CMB power spectra for temperature and polarization anisotropies and discuss their implications in §4.3.2.

§4.2 Perturbation dynamics and Initial Conditions of Scalar Modes

§4.2.1 The CDM Frame

In this section we specialize our equations to FRW backgrounds that are spatially flat[†] and we ignore the effects of the cosmological constant in the early radiation-dominated universe. To solve the equations it is essential to make a choice of frame u^a . We adopted a frame comoving with the CDM similar to [34]. Since the CDM is pressure free, this u^a is geodesic ($A_a = 0$) which simplifies the equations considerably. We shall adopt this frame choice here also, though we note it may be preferable to use a frame more closely tied to the dominant matter component over the epoch of interest. This can be easily accomplished by adopting the energy frame ($q_a = 0$). For completeness, we give equations in the energy frame in the following section.

We neglect baryon pressure ($c_s^2 \rightarrow 0$ and $P^{(b)} \rightarrow 0$) and work to lowest order in the tight-coupling approximation ($n_e \sigma_T \rightarrow \infty$; see e.g. [133]). At this order the energy frame of the photons coincides with the rest frame of the baryons, so that $v_a^{(b)} = 3q_a^{(\gamma)}/(4\rho^{(\gamma)})$, and all moments of the photon distribution are vanishingly small beyond the dipole.

With these approximations and frame choice we obtain the following equations for the density perturbations of each component:

$$\dot{\Delta}_k^{(\gamma)} = -\frac{k}{a} \left(\frac{4}{3} \mathcal{Z}_k - q_k^{(\gamma)} \right) \quad (\text{photons}), \quad (4.1)$$

$$\dot{\Delta}_k^{(\nu)} = -\frac{k}{a} \left(\frac{4}{3} \mathcal{Z}_k - q_k^{(\nu)} \right) \quad (\text{neutrinos}), \quad (4.2)$$

$$\dot{\Delta}_k^{(b)} = -\frac{k}{a} (\mathcal{Z}_k - v_k^{(b)}) \quad (\text{baryons}), \quad (4.3)$$

$$\dot{\Delta}_k^{(c)} = -\frac{k}{a} \mathcal{Z}_k \quad (\text{CDM}). \quad (4.4)$$

[†]More generally, curvature effects can be ignored for modes with wavelength much shorter than the curvature scale, $k \gg \sqrt{|K|}$, provided the curvature does not dominate the background dynamics.

The equations for the peculiar velocities and momentum densities are

$$(4\rho^{(\gamma)} + 3\rho^{(b)})\dot{q}_k^{(\gamma)} = -\frac{4k}{3a}\rho^{(\gamma)}\Delta_k^{(\gamma)} - \rho^{(b)}\Theta q_k^{(\gamma)}, \quad (4.5)$$

$$\dot{q}_k^{(\nu)} = -\frac{1k}{3a}\left(\Delta_k^{(\nu)} + 2\pi_k^{(\nu)}\right), \quad (4.6)$$

along with $v_k^{(c)} = 0$ and $v_k^{(b)} = 3q_k^{(\gamma)}/4$. The latter equation, together with Eqs. (4.1) and (4.3), implies that $\dot{\Delta}_k^{(b)} = 3\dot{\Delta}_k^{(\gamma)}/4$ so that any entropy perturbation between the photons and baryons is conserved while tight coupling holds. The effects of baryon inertia appear in Eq. (4.5) because of the tight coupling between the baryons and photons.

The constraint equations are found to be:

$$\kappa^2\rho q_k - \frac{2}{3}\left(\frac{k}{a}\right)^2(\mathcal{Z}_k - \sigma_k) - \frac{1}{6}\left(\frac{\tilde{\kappa}}{\kappa}\right)^4(\kappa^4\rho^2 q_k + 6\rho\mathcal{Q}_k) = 0, \quad (4.7)$$

and

$$\begin{aligned} & 2\left(\frac{k}{a}\right)^3\Phi_k - \kappa^2\rho\left(\frac{k}{a}\right)(\Delta_k - \pi_k) + \kappa^2\Theta\rho q_k \\ &= \frac{1}{16}\left(\frac{\tilde{\kappa}}{\kappa}\right)^4\left[\kappa^4\left(-\frac{8}{3}\Theta\rho^2 q_k + \frac{4k}{3a}\rho^2[(3\gamma - 2)\pi_k + 2\Delta_k]\right)\right. \\ & \left.+ 16\left(\frac{k}{a}\right)\rho(\Upsilon_k - \mathcal{P}_k) - 16\Theta\rho\mathcal{Q}_k\right]. \end{aligned} \quad (4.8)$$

The propagation equation for the comoving expansion gradient in the CDM frame is

$$\begin{aligned} & \dot{\mathcal{Z}}_k + \frac{1}{3}\Theta\mathcal{Z}_k + \frac{\kappa^2 a}{2k}\left[2(\rho^{(\gamma)}\Delta_k^{(\gamma)} + \rho^{(\nu)}\Delta_k^{(\nu)}) + \rho^{(b)}\Delta_k^{(b)} + \rho^{(c)}\Delta_k^{(c)}\right] \\ &= -\frac{1}{12}\left(\frac{\tilde{\kappa}}{\kappa}\right)^4\frac{a}{k}\left\{\kappa^4[(2\rho + 3P)\rho\Delta_k + \rho(3\rho^{(\gamma)}\Delta_k^{(\gamma)} + 3\rho^{(\nu)}\Delta_k^{(\nu)} + (2 + 3c_s^2)\rho^{(b)}\Delta_k^{(b)} + 2\rho^{(c)}\Delta_k^{(c)})]\right. \\ & \left.+ 12\rho\Upsilon_k\right\}. \end{aligned} \quad (4.9)$$

The variables Φ_k and σ_k can be determined from the constraint equations so their propagation equations are not independent of the above set. The propagation equation for Φ_k is unchanged from Eq. (3.75) since that equation was already written in frame-invariant form. The propagation equation for the shear in the

CDM frame is

$$\frac{k}{a} \left(\dot{\sigma}_k + \frac{1}{3} \Theta \sigma_k \right) + \left(\frac{k}{a} \right)^2 \Phi_k - \frac{\kappa^2}{2} \rho \pi_k = \frac{1}{24} \left(\frac{\tilde{\kappa}}{\kappa} \right)^4 [-(3\gamma - 2) \kappa^4 \rho^2 \pi_k + 12 \rho \mathcal{P}_k]. \quad (4.10)$$

Finally we have the non-local evolution equations for Υ_k and \mathcal{Q}_k which in the CDM frame become

$$\dot{\Upsilon}_k = \frac{1}{3} (3\gamma - 4) \Theta \Upsilon_k - \frac{4\mathcal{U}k}{3\rho a} \mathcal{Z}_k + \frac{k}{a} \mathcal{Q}_k, \quad (4.11)$$

and

$$\dot{\mathcal{Q}}_k - \frac{1}{3} (3\gamma - 4) \Theta \mathcal{Q}_k + \frac{1}{3} \frac{k}{a} (\Upsilon_k + 2\mathcal{P}_k) = \frac{\kappa^4}{6} \gamma \rho \left[\Theta q_k + \frac{k}{a} (\pi_k - \Delta_k) \right]. \quad (4.12)$$

Solutions for the CDM Frame in the radiation-dominated era

We now use the above equations to extract the solutions of the scalar perturbation equations in the radiation-dominated era, $\gamma = 4/3$. To simplify matters, as well as neglecting the contribution of the baryons and CDM to the background dynamics, we shall only consider those modes for which $D_a \rho^{(b)}$ and $D_a \rho^{(c)}$ make a negligible contribution to the total matter perturbation $D_a \rho$. This approximation allows us to write the total matter perturbations in the form

$$(\rho^{(\gamma)} + \rho^{(\nu)}) \Delta_k = \rho^{(\gamma)} \Delta_k^{(\gamma)} + \rho^{(\nu)} \Delta_k^{(\nu)}, \quad (\rho^{(\gamma)} + \rho^{(\nu)}) q_k = \rho^{(\gamma)} q_k^{(\gamma)} + \rho^{(\nu)} q_k^{(\nu)}, \quad (4.13)$$

and effectively removes the back-reaction of the baryon and CDM perturbations on the perturbations of the spacetime geometry. We note that in making this approximation we lose two modes corresponding to the baryon and CDM isocurvature (density) modes of general relativity, in which the sub-dominant matter components make significant contributions to the total fractional density perturbation (which vanishes as $t \rightarrow 0$). However, for our purposes the loss of generality is not that important, while the simplifications resulting from decoupling the baryon and photon perturbations are considerable. We also neglect moments of the neutrino distribution function above the dipole (so there is no matter anisotropic stress). This approximation is good for super-Hubble modes, but fails due to neutrino free streaming on sub-Hubble scales.

We shall also assume that the non-local energy density \mathcal{U} vanishes in the background for all energy regimes [77]. Physically, vanishing \mathcal{U} corresponds to the background bulk being conformally flat and strictly anti-de Sitter. Note that $\mathcal{U} = 0$ in the background need not imply that the fluctuations in the non-local energy density are zero, i.e. $\Upsilon_a \neq 0$.

With the above conditions the following set of equations are obtained:

$$\left(\frac{k}{a}\right)^2 (\dot{\Phi}_k + H\Phi_k) + \frac{\kappa^2 \rho}{2} \left(\frac{k}{a}\right) \left(\frac{4}{3}\sigma_k - q_k\right) \left(1 + \frac{\rho}{\lambda}\right) = \frac{3}{\kappa^2 \lambda} \rho \left[\left(\frac{k}{a}\right) \mathcal{Q}_k + 3H\mathcal{P}_k - \dot{\mathcal{P}}_k \right], \quad (4.14)$$

$$\left(\frac{k}{a}\right) (\dot{\mathcal{Z}}_k + H\mathcal{Z}_k) + \kappa^2 \rho \left(1 + \frac{3\rho}{\lambda}\right) \Delta_k = -\frac{6}{\kappa^2 \lambda} \rho \Upsilon_k \quad (4.15)$$

$$\left(\frac{k}{a}\right) (\dot{\sigma}_k + H\sigma_k) + \left(\frac{k}{a}\right)^2 \Phi_k = \frac{3}{\kappa^2 \lambda} \rho \mathcal{P}_k, \quad (4.16)$$

$$\dot{q}_k^{(\gamma)} + \frac{1}{3} \frac{k}{a} \Delta_k^{(\gamma)} = 0, \quad (4.17)$$

$$\dot{q}_k^{(\nu)} + \frac{1}{3} \frac{k}{a} \Delta_k^{(\nu)} = 0, \quad (4.18)$$

$$\dot{\Delta}_k^{(\gamma)} + \frac{k}{a} \left(\frac{4}{3}\mathcal{Z}_k - q_k^{(\gamma)}\right) = 0, \quad (4.19)$$

$$\dot{\Delta}_k^{(\nu)} + \frac{k}{a} \left(\frac{4}{3}\mathcal{Z}_k - q_k^{(\nu)}\right) = 0, \quad (4.20)$$

where recall $H = \Theta/3$. For the constraint equations we find

$$3\kappa^2 \left(1 + \frac{\rho}{\lambda}\right) \rho q_k - 2 \left(\frac{k}{a}\right)^2 (\mathcal{Z}_k - \sigma_k) = -\frac{18}{\kappa^2 \lambda} \rho \mathcal{Q}_k, \quad (4.21)$$

$$2 \left(\frac{k}{a}\right)^3 \Phi_k + \kappa^2 \rho \left(1 + \frac{\rho}{\lambda}\right) \left[3Hq_k - \left(\frac{k}{a}\right) \Delta_k\right] = \frac{6}{\kappa^2 \lambda} \rho \left[\left(\frac{k}{a}\right) (\Upsilon_k - \mathcal{P}_k) - 3H\mathcal{Q}_k \right]. \quad (4.22)$$

Finally the non-local evolution equations are found to be :

$$\dot{\Upsilon}_k = \frac{k}{a} \mathcal{Q}_k, \quad (4.23)$$

$$9\dot{\mathcal{Q}}_k + 3 \left(\frac{k}{a}\right) (\Upsilon_k + 2\mathcal{P}_k) = -2\kappa^4 \rho \left(\frac{k}{a} \Delta_k - 3Hq_k\right). \quad (4.24)$$

It is easy to show by propagating the constraint equations that the above set of equations are consistent.

By inspection, there is a solution of these equations with

$$\Phi_k = 0, \quad (4.25)$$

$$\mathcal{Z}_k = \left[3\dot{H} \left(\frac{a}{k} \right)^2 - 1 \right] \frac{A}{a}, \quad (4.26)$$

$$\sigma_k = -\frac{A}{a}, \quad (4.27)$$

$$q_k^{(\gamma)} = -\frac{4}{3} \frac{A}{a}, \quad (4.28)$$

$$q_k^{(\nu)} = -\frac{4}{3} \frac{A}{a}, \quad (4.29)$$

$$\Delta_k^{(\gamma)} = -4H \frac{A}{k}, \quad (4.30)$$

$$\Delta_k^{(\nu)} = -4H \frac{A}{k}, \quad (4.31)$$

$$\Upsilon_k = 0, \quad (4.32)$$

$$\mathcal{Q}_k = 0, \quad (4.33)$$

$$\mathcal{P}_k = 0, \quad (4.34)$$

where A is a constant. This solution describes a radiation-dominated universe that is exactly FRW except that the CDM has a peculiar velocity $\bar{v}_a^{(c)} = (A/a)Q_a^{(k)}$ relative to the velocity of the FRW fundamental observers. [This form for $\bar{v}_a^{(c)}$ clearly satisfies Eq. (3.91) with $A_a = 0$.] Such a solution is possible since we have neglected the gravitational effect of the CDM (and baryon) perturbations in making the approximations in Eq. (4.13). The same solution arises in general relativity [34]. Including the back-reaction of the CDM perturbations, we would find additional small peculiar velocities in the dominant matter components which compensate the CDM flux. We shall not consider this irregular CDM isocurvature velocity mode any further here.

Another pair of solutions are easily found by decoupling the photon/neutrino entropy perturbations. Introducing the photon/neutrino entropy perturbation (up to a constant) Δ_2 and relative flux q_2 :

$$\begin{aligned} \Delta_2 &= \Delta_k^{(\gamma)} - \Delta_k^{(\nu)}, \\ q_2 &= q_k^{(\gamma)} - q_k^{(\nu)}, \end{aligned} \quad (4.35)$$

the equations for Δ_2 and q_2 decouple to give

$$\dot{\Delta}_2 - \frac{k}{a} q_2 = 0, \quad (4.36)$$

$$\dot{q}_2 + \frac{1}{3} \frac{k}{a} \Delta_2 = 0. \quad (4.37)$$

Switching to conformal time ($d\tau = dt/a$) we can solve for Δ_2 and q_2 to find

$$q_2(\tau) = B \cos\left(\frac{k\tau}{3}\right) + C \sin\left(\frac{k\tau}{3}\right), \quad (4.38)$$

$$\Delta_2(\tau) = B \sin\left(\frac{k\tau}{3}\right) - C \cos\left(\frac{k\tau}{3}\right). \quad (4.39)$$

The constants B and C label the neutrino velocity and density isocurvature modes respectively [24, 34], in which the neutrinos and photons initially have mutually compensating peculiar velocities and density perturbations. The perfect decoupling of these isocurvature modes is a consequence of our neglecting anisotropic stresses (and higher moments of the distribution functions) and baryon inertia.

Having decoupled the entropy perturbations, we write the remaining equations in terms of the total variables Δ_k and q_k . The propagation equations for the non-local variables Υ_k and \mathcal{Q}_k are redundant since these variables are determined by the constraint equations (4.21) and (4.22):

$$\frac{6}{\kappa^2 \lambda} \rho \Upsilon_k = 2 \left(\frac{k}{a}\right)^2 \Phi_k + 2H \left(\frac{k}{a}\right) (\mathcal{Z}_k - \sigma_k) - \kappa^2 \rho \left(1 + \frac{\rho}{\lambda}\right) \Delta_k + \frac{6}{\kappa^2 \lambda} \rho \mathcal{P}_k, \quad (4.40)$$

$$\frac{3}{\kappa^2 \lambda} \rho \mathcal{Q}_k = \frac{1}{3} \left(\frac{k}{a}\right)^2 (\mathcal{Z}_k - \sigma_k) - \frac{\kappa^2 \rho}{2} \left(1 + \frac{\rho}{\lambda}\right) q_k. \quad (4.41)$$

Substituting these expressions in the right-hand sides of Eqs. (4.14) and (4.15) we find

$$\left(\frac{k}{a}\right)^2 (\dot{\Phi}_k + H\Phi_k) + \frac{2\kappa^2 \rho}{3} \left(\frac{k}{a}\right) \left(1 + \frac{\rho}{\lambda}\right) \sigma_k - \frac{1}{3} \left(\frac{k}{a}\right)^3 (\mathcal{Z}_k - \sigma_k) = \frac{3}{\kappa^2 \lambda} \rho (3H\mathcal{P}_k - \dot{\mathcal{P}}_k), \quad (4.42)$$

$$\left(\frac{k}{a}\right) (\dot{\mathcal{Z}}_k + H\mathcal{Z}_k) + \kappa^2 \rho \left(\frac{2\rho}{\lambda}\right) \Delta_k + 2 \left(\frac{k}{a}\right)^2 \Phi_k + 2H \left(\frac{k}{a}\right) (\mathcal{Z}_k - \sigma_k) = -\frac{6\rho}{\kappa^2 \lambda} \mathcal{P}_k, \quad (4.43)$$

$$\left(\frac{k}{a}\right) (\dot{\sigma}_k + H\sigma_k) + \left(\frac{k}{a}\right)^2 \Phi_k = \frac{3}{\kappa^2 \lambda} \rho \mathcal{P}_k, \quad (4.44)$$

$$\dot{\Delta}_k + \frac{k}{a} \left(\frac{4}{3} \mathcal{Z}_k - q_k\right) = 0, \quad (4.45)$$

$$\dot{q}_k + \frac{1}{3} \frac{k}{a} \Delta_k = 0. \quad (4.46)$$

These equations describe the evolution of the intrinsic perturbations to the brane. The usual general relativistic constraint equations are now replaced by the constraints (4.40) and (4.41) which determine two of the non-local variables. The lack of a propagation equation for \mathcal{P}_k reflects the incompleteness of the 1+3 dimensional description of braneworld dynamics.

In the following it will prove convenient to adopt the dimensionless independent variable

$$x = \frac{k}{Ha}, \quad (4.47)$$

which is (to within a factor of 2π) the ratio of the Hubble length to the wavelength of the perturbations. Using the (modified) Friedmann equations for the background in radiation domination, and with $\mathcal{U} = 0$, we find that

$$\frac{dx}{dt} = \frac{k}{a} \left(\frac{2 + 3\rho/\lambda}{2 + \rho/\lambda} \right). \quad (4.48)$$

The relative importance of the local (quadratic) braneworld corrections to the Einstein equation depends on the dimensionless ratio ρ/λ . In the low-energy limit, $\rho \ll \lambda$, the quadratic local corrections can be neglected although the non-local corrections \mathcal{E}_{ab} may still be important. In the opposite (high-energy) limit the quadratic corrections dominate over the terms that are linear in the energy-momentum tensor. We now consider these two limits separately.

Low-energy regime

In the low-energy regime we have $dx/dt \approx k/a$ and $x \approx k\tau$. The total energy density ρ is proportional to x^{-4} . Denoting derivatives with respect to x with a prime, using $\rho \ll \lambda$, and assuming that we can neglect the term involving $(\rho/\lambda)\Delta_k$ in Eq. (4.43) compared to the other terms, we find

$$3x^2\Phi'_k + 3x\Phi_k + (6 + x^2)\sigma_k - x^2\mathcal{Z}_k = \frac{27}{\kappa^4\lambda}(3\mathcal{P}_k - x\mathcal{P}'_k) \quad (4.49)$$

$$x^2\mathcal{Z}'_k + 3x\mathcal{Z}_k + 2x^2\Phi_k - 2x\sigma_k = -\frac{18}{\kappa^4\lambda}\mathcal{P}_k \quad (4.50)$$

$$x^2\sigma'_k + x\sigma_k + x^2\Phi_k = \frac{9}{\kappa^4\lambda}\mathcal{P}_k \quad (4.51)$$

$$\Delta'_k + \frac{4}{3}\mathcal{Z}_k - q_k = 0 \quad (4.52)$$

$$q'_k + \frac{1}{3}\Delta_k = 0 \quad (4.53)$$

Combining these equations we find an inhomogeneous, second-order equation for Φ_k :

$$3x\Phi''_k + 12\Phi'_k + x\Phi_k = F_k(x), \quad (4.54)$$

where

$$F_k(x) \equiv -\frac{27}{\kappa^4 \lambda} \left[\mathcal{P}_k'' - \frac{\mathcal{P}_k'}{x} + \left(\frac{2}{x^3} - \frac{3}{x^2} + \frac{1}{x} \right) \mathcal{P}_k \right]. \quad (4.55)$$

In general relativity the same second-order equation holds for Φ_k but with $F_k(x) = 0$.

The presence of terms involving the non-local anisotropic stress on the right-hand side of Eq. (4.54) ensure that Φ_k cannot be evolved on the brane alone. The resolution of this problem will require careful analysis of the bulk dynamics in five dimensions. In this thesis, our aims are less ambitious; we shall solve Eq. (4.54) with $\mathcal{P}_k = 0$. Although we certainly do not expect $\mathcal{P}_{ab} = 0^\ddagger$, the solutions of the homogeneous equation may still prove a useful starting point for a more complete analysis. For example, they allow one to construct Green's functions for Eq. (4.54) which could be used to assess the impact of specific ansatze for \mathcal{P}_{ab} [9].

With $\mathcal{P}_k = 0$ we can solve Eqs. (4.49)–(4.53) analytically to find

$$\Phi_k = \frac{c_1}{x^3} \left[3 \sin \left(\frac{x}{\sqrt{3}} \right) - x\sqrt{3} \cos \left(\frac{x}{\sqrt{3}} \right) \right] + \frac{c_2}{x^3} \left[3 \cos \left(\frac{x}{\sqrt{3}} \right) + x\sqrt{3} \sin \left(\frac{x}{\sqrt{3}} \right) \right], \quad (4.56)$$

$$\sigma_k = \frac{3}{x^2} \left[c_2 \cos \left(\frac{x}{\sqrt{3}} \right) + c_1 \sin \left(\frac{x}{\sqrt{3}} \right) \right] + \frac{c_3}{x}, \quad (4.57)$$

$$\mathcal{Z}_k = \frac{c_3(6+x^2)}{x^3} + \frac{6\sqrt{3}}{x^3} \left[c_1 \cos \left(\frac{x}{\sqrt{3}} \right) - c_2 \sin \left(\frac{x}{\sqrt{3}} \right) \right] + \frac{6}{x^2} \left[c_2 \cos \left(\frac{x}{\sqrt{3}} \right) + c_1 \sin \left(\frac{x}{\sqrt{3}} \right) \right], \quad (4.58)$$

$$\begin{aligned} \Delta_k &= c_4 \cos \left(\frac{x}{\sqrt{3}} \right) + c_5 \sin \left(\frac{x}{\sqrt{3}} \right) + \frac{4c_3}{x^2} + \frac{4}{x} \left[c_2 \cos \left(\frac{x}{\sqrt{3}} \right) + c_1 \sin \left(\frac{x}{\sqrt{3}} \right) \right] \\ &\quad + \left(\frac{4\sqrt{3}}{x^2} - \frac{2}{\sqrt{3}} \right) \left[c_1 \cos \left(\frac{x}{\sqrt{3}} \right) - c_2 \sin \left(\frac{x}{\sqrt{3}} \right) \right], \end{aligned} \quad (4.59)$$

$$\begin{aligned} q_k &= \frac{c_5}{\sqrt{3}} \cos \left(\frac{x}{\sqrt{3}} \right) - \frac{c_4}{\sqrt{3}} \sin \left(\frac{x}{\sqrt{3}} \right) + \frac{4c_3}{3x} + \frac{4x}{\sqrt{3}} \left[c_1 \cos \left(\frac{x}{\sqrt{3}} \right) - c_2 \sin \left(\frac{x}{\sqrt{3}} \right) \right] \\ &\quad + \frac{2}{3} \left[c_2 \cos \left(\frac{x}{\sqrt{3}} \right) + c_1 \sin \left(\frac{x}{\sqrt{3}} \right) \right]. \end{aligned} \quad (4.60)$$

The mode labelled by c_3 is the CDM velocity isocurvature mode discussed earlier. The modes labelled by c_1 and c_2 are the same as in general relativity; they describe the adiabatic growing and decaying solutions respectively. However, in the low-energy limit we also find two additional isocurvature modes (c_4 and c_5) that are

[‡]We have not investigated the consistency of the condition $\mathcal{P}_{ab} = 0$ with the five-dimensional bulk dynamics in the presence of a perturbed brane.

not present in general relativity. These arise from the two additional degrees of freedom Υ_k and \mathcal{Q}_k present in the braneworld model (with $P_k = 0$). The mode c_4 initially has non-zero but compensating gradients in the total matter and non-local densities, and c_5 initially has compensated energy fluxes. Formally these isocurvature solutions violate the assumption that the term involving $(\rho/\lambda)\Delta_k$ be negligible compared to the other terms in Eq. (4.43) since all other terms vanish. In practice, there will be some gravitational back-reaction onto the other gauge-invariant variables controlled by the dimensionless quantity ρ/λ , but the general character of these isocurvature modes will be preserved for $\rho/\lambda \ll 1$.

High-energy regime

We now turn to the high-energy regime, where the quadratic terms in the stress-energy tensor dominate the (local) linear terms. In this limit the scale factor $a \propto t^{1/4}$. The modification to the expansion rate leads to an increase in the amplitude of scalar and tensor fluctuations produced during high-energy inflation [9]. With $\mathcal{U} = 0$ in the background, and $\rho \gg \lambda$, the Hubble parameter is approximately

$$H^2 \approx \frac{1}{36} \tilde{\kappa}^4 \rho^2 = \frac{\kappa^2 \rho^2}{6\lambda}, \quad (4.61)$$

and $dx/dt \approx 3k/a$. In terms of conformal time τ , $x \approx 3k\tau$. The total energy density, ρ is proportional to $x^{(-4/3)}$.

Power series solutions for the high-energy regime

It is convenient to rescale the non-local variables by the dimensionless quantity $\kappa^4 \rho$. Thus we define

$$\bar{\Upsilon}_k \equiv \frac{\Upsilon_k}{\kappa^4 \rho}, \quad (4.62)$$

$$\bar{\mathcal{Q}}_k \equiv \frac{\mathcal{Q}_k}{\kappa^4 \rho}, \quad (4.63)$$

$$\bar{\mathcal{P}}_k \equiv \frac{\mathcal{P}_k}{\kappa^4 \rho}. \quad (4.64)$$

The fractional total (effective) density perturbation and energy flux can be written in terms of the barred variables [e.g. $\bar{\Upsilon}_a \equiv \Upsilon_a/(\kappa^4\rho)$][§] in the high-energy limit as

$$\frac{aD_a\rho^{\text{tot}}}{\rho^{\text{tot}}} \approx 2(\Delta_a + 6\bar{\Upsilon}_a), \quad (4.65)$$

$$q_a^{\text{tot}} \approx \frac{2\rho^{\text{tot}}}{\rho}(q_a + 6\bar{\mathcal{Q}}_a). \quad (4.66)$$

Making the high-energy approximation $\rho \gg \lambda$ in Eqs. (4.42)–(4.46), we obtain

$$9x^2\Phi'_k + 3x\Phi_k + (12 + x^2)\sigma_k - x^2\mathcal{Z}_k = 54 \left[\frac{7\bar{\mathcal{P}}_k}{x} - 3\bar{\mathcal{P}}'_k \right], \quad (4.67)$$

$$3x^2\mathcal{Z}'_k + 3x\mathcal{Z}_k - 2x\sigma_k + 2x^2\Phi_k + 12\Delta_k = -36\bar{\mathcal{P}}_k, \quad (4.68)$$

$$3x\sigma'_k + \sigma_k + x\Phi_k = 18\frac{\bar{\mathcal{P}}_k}{x}, \quad (4.69)$$

$$\Delta'_k - \frac{1}{3}q_k + \frac{4}{9}\mathcal{Z}_k = 0, \quad (4.70)$$

$$q'_k + \frac{1}{9}\Delta_k = 0. \quad (4.71)$$

The non-local quantities $\bar{\Upsilon}_k$ and $\bar{\mathcal{Q}}_k$ are determined by the constraints

$$\bar{\Upsilon}_k = \frac{1}{18}x^2\Phi_k + \frac{1}{18}x(\mathcal{Z}_k - \sigma_k) - \frac{1}{6}\Delta_k + \bar{\mathcal{P}}_k, \quad (4.72)$$

$$\bar{\mathcal{Q}}_k = \frac{1}{54}x^2(\mathcal{Z}_k - \sigma_k) - \frac{1}{6}q_k. \quad (4.73)$$

We can manipulate Eqs. (4.67)–(4.71) to obtain a fourth-order equation for the gravitational potential Φ_k :

$$729x^2\frac{\partial^4\Phi_k}{\partial x^4} + 3888x\frac{\partial^3\Phi_k}{\partial x^3} + (1782 + 54x^2)\frac{\partial^2\Phi_k}{\partial x^2} + 144x\frac{\partial\Phi_k}{\partial x} + (90 + x^2)\Phi_k = F_k(x), \quad (4.74)$$

where

$$F_k(x) = -\frac{54}{x^4} \left(243x^4\frac{\partial^4\bar{\mathcal{P}}_k}{\partial x^4} - 810x^3\frac{\partial^3\bar{\mathcal{P}}_k}{\partial x^3} + 18x^2(135 + 2x^2)\frac{\partial^2\bar{\mathcal{P}}_k}{\partial x^2} - 30x(162 + x^2)\frac{\partial\bar{\mathcal{P}}_k}{\partial x} + [x^4 + 30(162 + x^2)]\bar{\mathcal{P}}_k \right). \quad (4.75)$$

[§]A general and useful identity for these variables is employed in deriving the equations for the high energy regime:

$$\frac{\dot{\Upsilon}_k}{\kappa^4\rho} = \dot{\Upsilon}_k - 3\gamma H\bar{\Upsilon}_k$$

Since we do not have an evolution equation for $\bar{\mathcal{P}}_k$ we adopt the strategy taken in the low-energy limit and look for solutions of the homogeneous equations ($\bar{\mathcal{P}}_k = 0$). In principle one can use these solutions to construct formal solutions of the inhomogeneous equations with Green's method.

To solve Eq. (4.74) with $\bar{\mathcal{P}}_k = 0$ we construct a Frobenius (or power) series solution for $\Phi_k(x)$:

$$\Phi_k(x) = x^m \sum_{n=0}^{\infty} a_n x^n, \quad (4.76)$$

where $a_0 \neq 0$. The indicial equation for m is

$$m(m-1)(3m+5)(3m-4) = 0. \quad (4.77)$$

For each value of m we substitute into Eq. (4.74) and solve the resulting recursion relations for the $\{a_n\}$. We then obtain the other gauge-invariant variables by direct integration. The original set of equations (4.67)–(4.71) has five degrees of freedom, so we expect one additional solution with $\Phi_k = 0$. This solution is the CDM isocurvature solution discussed earlier, and has a finite series expansion:

$$\Phi_k = 0, \quad (4.78)$$

$$\sigma_k = Dx^{-\frac{1}{3}}, \quad (4.79)$$

$$\mathcal{Z}_k = Dx^{-\frac{7}{3}}(12 + x^2), \quad (4.80)$$

$$\Delta_k = 4Dx^{-\frac{4}{3}}, \quad (4.81)$$

$$q_k = \frac{4}{3}Dx^{-\frac{1}{3}}, \quad (4.82)$$

where D is a constant. The non-local variables vanish.

The first two terms of the mode with $m = 0$ are

$$\Phi_k = a_1 \left(1 - \frac{5}{198}x^2 \right), \quad (4.83)$$

$$\sigma_k = a_1 \left(-\frac{1}{4}x + \frac{1}{396}x^3 \right), \quad (4.84)$$

$$\mathcal{Z}_k = a_1 \left(-\frac{3}{4}x + \frac{5}{864}x^3 \right), \quad (4.85)$$

$$\Delta_k = a_1 \left(\frac{1}{6}x^2 - \frac{1}{864}x^4 \right), \quad (4.86)$$

$$q_k = a_1 \left(-\frac{1}{162}x^3 + \frac{1}{38880}x^5 \right), \quad (4.87)$$

$$\bar{\Upsilon}_k = a_1 \left(-\frac{1}{972}x^4 + \frac{1}{249480}x^6 \right) = \frac{a_1}{972} \left(-x^4 + \frac{3}{770}x^6 \right), \quad (4.88)$$

$$\bar{\mathcal{Q}}_k = a_1 \left(-\frac{2}{243}x^3 + \frac{1}{17820}x^5 \right) = \frac{2a_1}{243} \left(-x^3 + \frac{3}{440}x^5 \right), \quad (4.89)$$

where a_1 is a constant. The form of this solution is similar to the adiabatic growing mode of general relativity.

The mode corresponding to $m = 1$ is

$$\Phi_k = a_2 \left(x - \frac{13}{1890}x^3 \right), \quad (4.90)$$

$$\sigma_k = a_2 \left(-\frac{1}{7}x^2 + \frac{1}{1890}x^4 \right), \quad (4.91)$$

$$\mathcal{Z}_k = a_2 \left(\frac{72}{7} - \frac{12}{35}x^2 \right), \quad (4.92)$$

$$\Delta_k = a_2 \left(-\frac{18}{7}x + \frac{1}{15}x^3 \right), \quad (4.93)$$

$$q_k = a_2 \left(6 + \frac{1}{7}x^2 \right), \quad (4.94)$$

$$\bar{\Upsilon}_k = a_2 \left(x + \frac{1}{30}x^3 \right), \quad (4.95)$$

$$\bar{\mathcal{Q}}_k = a_2 \left(-1 + \frac{1}{6}x^2 \right), \quad (4.96)$$

with a_2 a constant. This mode has no analogue in general relativity, except that Φ_k is a growing mode. As $t \rightarrow 0$ there are non-zero but compensating contributions to the effective peculiar velocity $q_a^{\text{tot}}/\rho^{\text{tot}}$ from the matter and the non-local en-

ergy fluxes. The contributions of these components to the fractional total density perturbation $aD_a\rho^{\text{tot}}/\rho^{\text{tot}}$ vanish as $t \rightarrow 0$.

The mode corresponding to $m = -\frac{5}{3}$ is singular as $t \rightarrow 0$ (it is a decaying mode with a_3 a constant):

$$\Phi_k = a_3 x^{-\frac{5}{3}} \left(1 - \frac{5}{18} x^2 \right), \quad (4.97)$$

$$\sigma_k = a_3 x^{-\frac{2}{3}} \left(1 + \frac{1}{18} x^2 \right), \quad (4.98)$$

$$\mathcal{Z}_k = a_3 \left(\frac{14}{99} x^{\frac{4}{3}} - \frac{1217}{1590435} x^{\frac{10}{3}} \right), \quad (4.99)$$

$$\Delta_k = a_3 \left(-\frac{8}{297} x^{\frac{7}{3}} + \frac{64}{433755} x^{\frac{13}{3}} \right), \quad (4.100)$$

$$q_k = a_3 \left(\frac{4}{4455} x^{\frac{10}{3}} - \frac{4}{1301265} x^{\frac{16}{3}} \right), \quad (4.101)$$

$$\bar{\Upsilon}_k = a_3 \left(-\frac{1}{162} x^{\frac{7}{3}} + \frac{7}{43740} x^{\frac{13}{3}} \right) = \frac{a_3}{162} x^{\frac{7}{3}} \left(-x + \frac{7}{270} x^2 \right), \quad (4.102)$$

$$\bar{\mathcal{Q}}_k = a_3 \left(-\frac{1}{54} x^{\frac{4}{3}} + \frac{7}{4860} x^{\frac{10}{3}} \right) = \frac{a_3}{54} x^{\frac{4}{3}} \left(-1 + \frac{7}{90} x^2 \right). \quad (4.103)$$

A similar mode is found in general relativity but there the decay of Φ_k is more rapid ($\Phi_k \propto x^{-3}$) on large scales. The solution (4.103) describes an isocurvature velocity mode [¶] where the early time matter and non-local (Weyl) components have equal but opposite peculiar velocities in the CDM frame. The existence of such isocurvature modes was predicted in [77] and [118] for large-scale density perturbations.

[¶]We note that we have identified this mode incorrectly in [123] since the variable \mathcal{Q} is rescaled by $x^{4/3}$.

Finally, for $m = \frac{4}{3}$, with a_4 a constant, we have

$$\Phi_k = a_4 x^{\frac{4}{3}} \left(1 - \frac{17}{3150} x^2 \right), \quad (4.104)$$

$$\sigma_k = a_4 x^{\frac{4}{3}} \left(-\frac{1}{8} x + \frac{17}{44100} x^3 \right), \quad (4.105)$$

$$\mathcal{Z}_k = a_4 x^{\frac{1}{3}} \left(\frac{27}{2} - \frac{117}{392} x^2 \right), \quad (4.106)$$

$$\Delta_k = a_4 x^{\frac{4}{3}} \left(-\frac{9}{2} + \frac{3}{49} x^2 \right), \quad (4.107)$$

$$q_k = a_4 x^{\frac{4}{3}} \left(\frac{3}{14} x - \frac{1}{637} x^3 \right), \quad (4.108)$$

$$\tilde{\Upsilon}(x) = a_4 x^{\frac{4}{3}} \left(\frac{3}{2} + \frac{1}{28} x^2 \right) = \frac{3a_4}{2} x^{\frac{4}{3}} \left(1 + \frac{1}{42} x^2 \right), \quad (4.109)$$

$$\bar{\mathcal{Q}}(x) = a_4 x^{\frac{4}{3}} \left(\frac{3}{14} x - \frac{29}{9828} x^3 \right) = \frac{3a_4}{14} x^{\frac{4}{3}} \left(x - \frac{29}{2106} x^3 \right). \quad (4.110)$$

In this mode the universe asymptotes to an FRW (brane) model in the past as $t \rightarrow 0$. Note that this requires careful cancellation between $aD_a\rho^{\text{tot}}/\rho^{\text{tot}}$ and q_a^{tot} to avoid a singularity in the gravitational potential Φ_k (which would diverge as $x^{-2/3}$ without such cancellation). Like the velocity isocurvature mode ($m = 1$) discussed above, this mode has no analogue in general relativity. We identify the solution (4.109) to be the non-local isocurvature density mode. The pair of non-local velocity and density isocurvature modes (4.103) and (4.109) is analogous to the neutrino density and velocity isocurvature modes (see Eqs. (4.38) and (4.39)).

§4.2.2 The Energy Frame

In this section, we present a complete set of evolution equations for the total matter variables in the matter energy frame, $q_a = 0$. Note that the four-velocity of the energy frame is not necessarily a timelike eigenvector of the Einstein tensor in the presence of the non-local braneworld corrections to the effective stress-energy tensor. We assume that the matter is radiation dominated, the non-local energy density vanishes in the background, and we ignore local anisotropic stresses. We also assume that the baryons and CDM make a negligible contribution to the fractional gradient in the total matter energy density and to the energy flux, thus excluding the CDM and baryon isocurvature modes. We also give the evolution equations for the non-local density gradient and energy flux in the matter energy frame.

Denoting the variables in the energy frame by a tilde on the quantity, for example, $\tilde{\Delta}_a$, the relevant equations for scalar perturbations are

$$\dot{\tilde{\Delta}}_a = \frac{1}{3}\Theta\tilde{\Delta}_a - \frac{4}{3}\tilde{\mathcal{Z}}_a, \quad (4.111)$$

$$\dot{\tilde{\mathcal{Z}}}_a = -\frac{2}{3}\Theta\tilde{\mathcal{Z}}_a - \frac{1}{4}D^2\tilde{\Delta}_a - \frac{6\rho}{\kappa^2\lambda}\tilde{\Upsilon}_a - \frac{1}{2}\kappa^2\rho\tilde{\Delta}_a \left(1 + \frac{5\rho}{\lambda}\right), \quad (4.112)$$

$$\dot{\tilde{\Upsilon}}_a = -\frac{a}{\rho}D^2\tilde{\mathcal{Q}}_a, \quad (4.113)$$

$$\dot{\tilde{\mathcal{Q}}}_a = -\frac{4}{3}\Theta\tilde{\mathcal{Q}}_a - \frac{\rho}{3a}\tilde{\Upsilon}_a - \frac{2\kappa^4\rho^2}{9a}\tilde{\Delta}_a - D^b\tilde{\mathcal{P}}_{ab}. \quad (4.114)$$

Solutions of these equations are related to those in the CDM frame (§4.2.1) by linearising the frame transformations given in [140]. If the CDM projected velocity is $\tilde{v}_a^{(c)}$ in the energy frame, the variables in the CDM frame are given by

$$\Delta_a = \tilde{\Delta}_a - \frac{4}{3}a\Theta\tilde{v}_a^{(c)}, \quad (4.115)$$

$$\mathcal{Z}_a = \tilde{\mathcal{Z}}_a + \frac{1}{a}D_a D^b \tilde{v}_b^{(c)} - \frac{2\kappa^2\rho}{a} \left(1 + \frac{\rho}{\lambda}\right) \tilde{v}_a^{(c)}, \quad (4.116)$$

$$\Upsilon_a = \tilde{\Upsilon}_a, \quad (4.117)$$

$$\mathcal{Q}_a = \tilde{\mathcal{Q}}_a, \quad (4.118)$$

$$q_a = -\frac{4}{3}\rho\tilde{v}_a^{(c)}, \quad (4.119)$$

where we have used $\mathcal{U} = 0$ in the background. Note that the quantities Υ_a and \mathcal{Q}_a are frame-invariant, hence we can assume the same form for these quantities for the subsequent calculations in the energy frame like the CDM frame.

The CDM peculiar velocity evolves in the energy frame according to

$$\dot{\tilde{v}}_a^{(c)} = -\frac{1}{3}\Theta\tilde{v}_a^{(c)} + \frac{1}{4a}\tilde{\Delta}_a. \quad (4.120)$$

Energy frame solutions in the High-energy Regime

In the high energy limit, $\rho/\lambda \gg 1$, using the variable x defined in Eq. (4.47), we obtain the following four equations:

$$9x\tilde{\Delta}'_k = 3\tilde{\Delta}_k - 4x\tilde{\mathcal{Z}}_k, \quad (4.121)$$

$$3x^2\tilde{\mathcal{Z}}'_k = -x\tilde{\mathcal{Z}}_k + \left(\frac{x^2}{4} - 15\right)\tilde{\Delta}_k - 36\tilde{\Upsilon}_k, \quad (4.122)$$

$$3x\tilde{\Upsilon}'_k = 4\tilde{\Upsilon}_k + x\tilde{\mathcal{Q}}_k, \quad (4.123)$$

$$3x\tilde{\mathcal{Q}}'_k = 4\tilde{\mathcal{Q}}_k - \frac{1}{3}\left(\tilde{\Upsilon}_k + \frac{2}{3}\tilde{\Delta}_k - 2\tilde{\mathcal{P}}_k\right). \quad (4.124)$$

Setting $\bar{\mathcal{P}}_k = 0$, we decouple the above equations to find a 4th order differential equation,

$$\begin{aligned} \frac{9}{16}x^4 \frac{\partial^4 \tilde{\Delta}_k}{\partial x^4} + \frac{3}{4}x^3 \frac{\partial^3 \tilde{\Delta}_k}{\partial x^3} + \left(\frac{x^4}{24} - \frac{5x^2}{4}\right) \frac{\partial^2 \tilde{\Delta}_k}{\partial x^2} + \left(3x + \frac{x^3}{36}\right) \frac{\partial \tilde{\Delta}_k}{\partial x} \\ + \left(-\frac{7}{2} + \frac{x^2}{36} + \frac{x}{1296}\right) \tilde{\Delta}_k = 0. \end{aligned} \quad (4.125)$$

Using eq. (4.76), we obtain the indicial equation:

$$(m-2)(3m-4)(3m-7)(1+m) = 0. \quad (4.126)$$

We proceed to substitute each value of m back in (4.125) and solve the recurrence relations for $\{b_n\}$. The original set of equations (4.121)–(4.124) has four degrees of freedom, and we note that the peculiar CDM isocurvature mode vanishes in the energy frame. In addition, we compute the spatial gradient of the 3-curvature, η_k from eq. (3.82).

The mode corresponding to $m = 2$ are

$$\tilde{\Delta}_k = b_1 \left(x^2 - \frac{1}{150}x^4\right), \quad (4.127)$$

$$\tilde{\mathcal{Z}}_k = b_1 \left(-\frac{15}{4}x + \frac{11}{200}x^3\right), \quad (4.128)$$

$$\bar{\Upsilon}_k = \frac{b_1}{180} \left(-x^4 + \frac{3}{770}x^6\right), \quad (4.129)$$

$$\bar{\mathcal{Q}}_k = \frac{2b_1}{45} \left(-x^3 + \frac{3}{440}x^5\right), \quad (4.130)$$

$$\eta_k = b_1 \left(\frac{27}{4} - \frac{7}{40}x^2\right). \quad (4.131)$$

The mode corresponding to $m = \frac{4}{3}$ are

$$\tilde{\Delta}_k = b_2 x^{\frac{4}{3}} \left(1 - \frac{1}{78}x^2\right), \quad (4.132)$$

$$\tilde{\mathcal{Z}}_k = b_2 \left(-\frac{9}{4}x^{\frac{1}{3}} + \frac{9}{104}x^{\frac{7}{3}}\right), \quad (4.133)$$

$$\bar{\Upsilon}_k = -\frac{7b_2}{24}x^{\frac{4}{3}} \left(1 + \frac{1}{42}x^2\right), \quad (4.134)$$

$$\bar{\mathcal{Q}}_k = -\frac{b_2}{24}x^{\frac{4}{3}} \left(x - \frac{29}{2106}x^3\right) \quad (4.135)$$

$$\eta_k = b_2 x^{\frac{4}{3}} \left(-\frac{1}{4} + \frac{19}{14040}x^2\right). \quad (4.136)$$

The mode corresponding to $m = \frac{7}{3}$ are

$$\tilde{\Delta}_k = b_3 x^{\frac{7}{3}} \left(1 - \frac{1}{189} x^2 \right), \quad (4.137)$$

$$\tilde{\mathcal{Z}}_k = b_3 \left(-\frac{9}{2} x^{\frac{4}{3}} + \frac{1}{21} x^{\frac{10}{3}} \right), \quad (4.138)$$

$$\bar{\Upsilon}_k = -\frac{5b_3}{24} \left(-x^{\frac{7}{3}} + \frac{7}{270} x^{\frac{13}{3}} \right), \quad (4.139)$$

$$\bar{\mathcal{Q}}_k = -\frac{5b_3}{8} \left(-x^{\frac{4}{3}} + \frac{7}{90} x^{\frac{10}{3}} \right), \quad (4.140)$$

$$\eta_k = b_3 x^{\frac{1}{3}} \left(\frac{45}{4} - \frac{9}{56} x^2 \right). \quad (4.141)$$

The mode corresponding to $m = -1$ are

$$\tilde{\Delta}_k = b_4 x^{-1} \left(1 + \frac{1}{6} x^2 \right), \quad (4.142)$$

$$\tilde{\mathcal{Z}}_k = b_4 \left(\frac{3}{x^2} - \frac{1}{4} \right), \quad (4.143)$$

$$\bar{\Upsilon}_k = -\frac{b_4}{18} \left(x + \frac{1}{30} x^3 \right), \quad (4.144)$$

$$\bar{\mathcal{Q}}_k = -\frac{b_4}{18} \left(-1 + \frac{1}{6} x^2 \right), \quad (4.145)$$

$$\eta_k = b_4 \left(-\frac{1}{4x} - \frac{5}{72} x^2 \right). \quad (4.146)$$

with b_1, b_2, b_3 and b_4 being constants.

From the solutions (Eqs. (4.127)–(4.145)) in the high energy frame, we observe that powers and coefficients of the solutions for $\tilde{\Upsilon}$ and $\bar{\mathcal{Q}}$ match the ones in the CDM frame with constants of integration (up to some pre-factor). The solutions are checked by transforming them to the CDM using Eqs. (4.115)–(4.119). Eqs. (4.134) and (4.140) correspond to the pair of non-local isocurvature density and velocity modes found earlier in the CDM frame. From Eq. (4.131), we find that the spatial gradient of the 3-curvature for the adiabatic mode is a constant on large scales as $x \rightarrow 0$. We have arrived at the same result found in [21, 77]. With a more detailed analysis, we can characterize the $m = 2$ and $m = -1$ modes as the growing and decaying modes that are similar to the case in general relativity. We found that the curvature is conserved for the GR-like modes for $\mathcal{U} = 0$, but not for the other two additional braneworld modes.

§4.2.3 Discussion on the Scalar Modes

Regarding the imprint of braneworld effects on the CMB, we note several possible sources. Once the universe enters the low-energy regime the dynamics of the perturbations are essentially general relativistic in the absence of non-local anisotropic stress (see §4.2.1). If \mathcal{P}_{ab} really were zero, the only imprints of the braneworld on the CMB could arise from modifications to the power spectrum (and cross correlations) between the various low-energy modes. Since there are two additional isocurvature modes in the low-energy universe due to braneworld effects, it need not be the case that adiabatic fluctuations produced during high-energy (single-field) inflation give rise to a low-energy universe dominated by the growing, adiabatic, general-relativistic mode (See 4.1 for a history of the scalar modes from the high to low energy regime). Hence there exist the possibility of exciting the low-energy isocurvature (brane) modes from plausible fluctuations in the high-energy regime.

However, if we consider linear scales at last scattering which project onto angular scales corresponding to $l \sim 200$ and $h = 0.75$ in a $K = 0$ and $\Lambda = 0$ universe, assuming the standard nucleosynthesis constraint [refer to eq.(3.14) in the previous chapter] and ignoring the contributions of the dark radiation term, we find these modes enter the Hubble radius at approximately 10^4 . This large redshift would indicate that the modes are outside the Hubble radius. If this is the case, the matching from the high energy regime (brane-world) to the low energy regime (general relativity) would render the modes to be super-Hubble. An immediate consequence is that the CMB anisotropies would be insensitive to the brane tension, λ , i.e. the high energy effects.

Similarly in practice, we do not expect $\mathcal{P}_{ab} = 0$. In this case the non-local anisotropic stress provides additional driving terms to the dynamics of the fluctuations, and we can expect a significant manifestation of five-dimensional Kaluza-Klein effects on the CMB scalar anisotropies. Barrow and Maartens have shown in [9] that the 5-dimensional KK graviton stresses can slow down the decay of the shear anisotropy on the brane to observable levels. They found that with a suitable approximation for \mathcal{P}_{ab} that the initial shear to the Hubble distortion of $\sim 10^3 \Omega_0 H_0^2$ at 5D Planck time would allow the large-angle CMB signal to be a relic of purely KK effects. These possibilities may reveal new braneworld imprints that would be more realistic for observational testing.

§4.3 Braneworld Tensor Anisotropies in the CMB

In this section, we investigate the dynamics of tensor perturbations in braneworlds. Recalling Eqs. (3.111) and (3.112) from Chapter 3, we rewrite these equations in

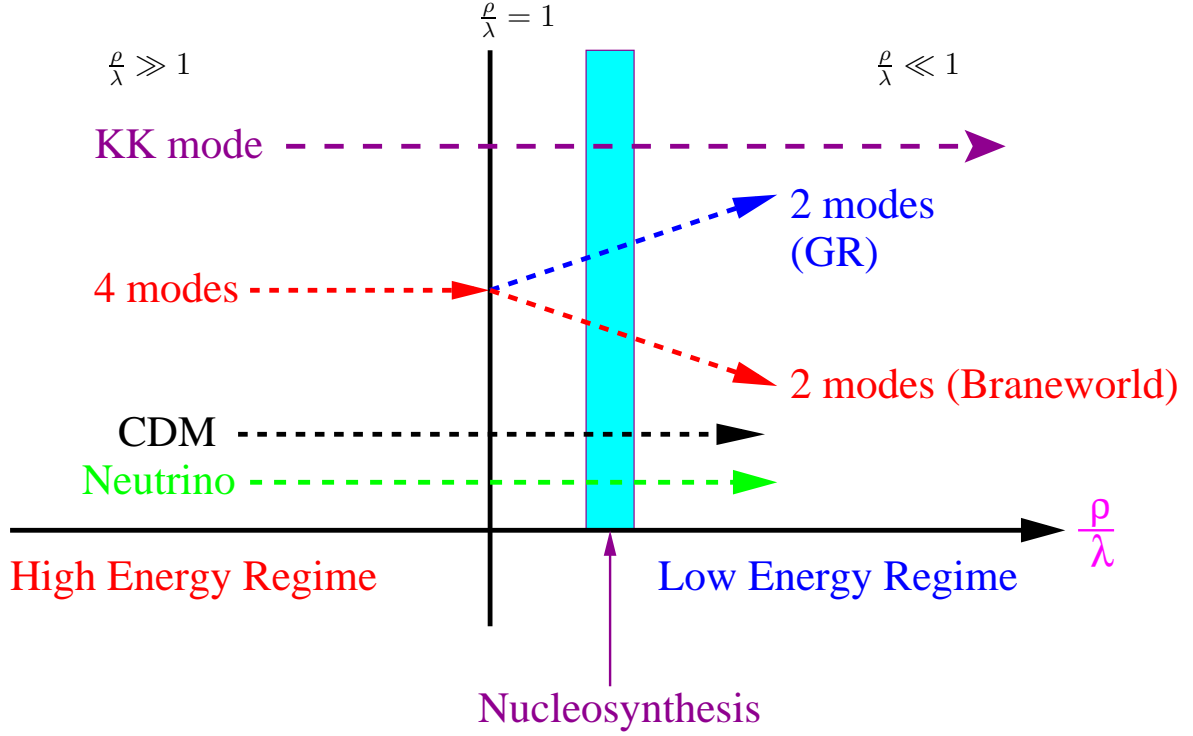


Figure 4.1: A figure which depicts the history of the different modes for the braneworlds. The KK mode, the CDM and the neutrino isocurvature modes will trail from the high energy to the low energy regime, after inflation. In the high energy regime, where $\rho/\lambda \gg 1$, there are 4 degenerate modes in the case of the braneworld. When the instantaneous transition from high to low energy regime ($\rho/\lambda \ll 1$) at $\rho/\lambda = 1$, the modes will be split up from four modes to two modes which correspond to the case in general relativity and the other remaining two modes which are the non-local isocurvature modes. The two remaining non-local isocurvature modes from the high energies are redshifted by approximately 10^4 if there is no dark energy term. Hence the only effect on the CMBR anisotropies is induced only by the KK mode.

conformal time:

$$\frac{k}{a^2} (\sigma'_k + \mathcal{H}\sigma_k) + \frac{k^2}{a^2} E_k - \frac{\kappa^2}{2} \rho \pi_k = \kappa^2 (2 - 3\gamma) \frac{\rho^2}{4\lambda} \pi_k + \frac{\kappa^2}{2} \rho \pi_k^*, \quad (4.147)$$

$$\begin{aligned}
 & \frac{k^2}{a^2} (E'_k + \mathcal{H}E_k) - k \left(\frac{k^2}{a^2} + \frac{3K}{a^2} - \frac{\kappa^2}{2} \gamma \rho \right) \sigma_k + \frac{\kappa^2}{2} \rho \pi'_k - \frac{\kappa^2}{2} (3\gamma - 1) \mathcal{H} \rho \pi_k \\
 &= -\frac{\kappa^2}{4\lambda} \{ 2k\gamma \rho^2 \sigma_k - (3\gamma - 2) \rho^2 \pi'_k - [3\gamma' - (3\gamma - 2)(6\gamma - 1) \mathcal{H}] \rho^2 \pi_k \} \\
 & \quad - \frac{2}{3} k \kappa^2 \rho^* \sigma_k - \frac{\kappa^2}{2} \left[\rho \pi_k^{*'} + (1 - 3\gamma) \mathcal{H} \rho \pi_k^* \right], \tag{4.148}
 \end{aligned}$$

where the non-local energy density is defined as in [9]:

$$\rho^* = \frac{6}{\kappa^4 \lambda} \mathcal{U}. \tag{4.149}$$

A prime denotes $d/d\tau$, $\mathcal{H} = a'/a$, and the (non-constant) parameter γ is defined in Eq. (3.74). Equations (4.147) and (4.148), which have all the braneworld terms on the right-hand sides, determine the tensor anisotropies in the CMB, once π_k and π_k^* are given.

§4.3.1 A Local Approximation to the Nonlocal Anisotropic Stress

The general solution for the non-local anisotropic stress will be of the form

$$\pi_k^*(\tau) \propto \int d\tilde{\tau} \mathcal{G}(\tau, \tilde{\tau}) F[\pi_k, \sigma_k] \Big|_{\tilde{\tau}}, \tag{4.150}$$

where \mathcal{G} is a retarded Green's function evaluated on the brane. The functional F is known in the case of a Minkowski background [167], but not in the cosmological case. (An equivalent integro-differential formulation of the problem is given in [148]; see also [178].) Once \mathcal{G} and F are determined, Eq. (4.150) can in principle be incorporated into a modified version of Boltzmann codes such as CAMB [126] or CMBFAST [175]. It remains a major task of braneworld cosmological perturbation theory to find this solution, or its equivalent forms in other formalisms. In the meanwhile, in order to make progress towards understanding braneworld signatures on tensor CMB anisotropies, we can consider approximations to the solution.

The non-local nature of π_k^* , as reflected in Eq. (4.150), is fundamental, but is also the source of the great complexity of the problem. The lowest level approximation to π_k^* is local. Despite removing the key aspect of the KK anisotropic stress, we can get a feel for its influence on the CMB if we capture at least part of its qualitative properties. The key qualitative feature is that inhomogeneity and

anisotropy on the brane are a source for KK modes in the bulk which “backreact” [135] or “feed back” [147], onto the brane. The transverse traceless part of inhomogeneity and anisotropy on the brane is given by the transverse traceless anisotropic stresses in the geometry, i.e. by the matter anisotropic stress π_{ab} and the shear anisotropy σ_{ab} . The radiation and neutrino anisotropic stresses are in turn sourced by the shear to lowest order (neglecting the role of the octupole and higher Legendre moments).

Thus the simplest local approximation which reflects the essential qualitative feature of the spin-2 KK modes is

$$\kappa^2 \pi_{ab}^* = -\zeta H \sigma_{ab}, \quad \zeta' = 0, \quad (4.151)$$

where ζ is a dimensionless KK parameter, with $\zeta = 0$ corresponding to no KK effects on the brane, and $\zeta = 0 = \lambda^{-1}$ giving the general relativity limit. [Note that for tensor perturbations, where there is no freedom over the choice of frame (i.e. u^a), there is no gauge ambiguity in Eq. (4.151). However, for scalar or vector perturbations, this relation could only hold in one frame, since π_{ab}^* is frame-invariant in linear theory while σ_{ab} is not.]

The approximation in Eq. (4.151) has the qualitative form of a shear viscosity, which suggests that KK effects lead to a damping of tensor anisotropies. This is indeed consistent with the conversion of part of the zero-mode at Hubble re-entry into massive KK modes [117, 76]. The conversion may be understood equivalently as the emission of KK gravitons into the bulk, and leads to a loss of energy in the 4D graviton modes on the brane, i.e. to an effective damping. The approximation in Eq. (4.151) therefore also incorporates this key feature qualitatively.

With this first approximation, we can close the system of equations on the brane by adding the equation

$$\kappa^2 \rho \pi_k^* = -\zeta \mathcal{H} \frac{k}{a^2} \sigma_k. \quad (4.152)$$

We will also assume $K = 0 = \rho^*$ in the background. The parameter ζ (together with the brane tension λ) then controls braneworld effects on the tensor CMB anisotropies in this simplest approximation.

Initial Conditions

Ignoring the photon anisotropic stress (i.e. $\pi_{ab} = 0$), we differentiate Eq. (4.147) and decouple it with Eq. (4.148) and the modified Raychaudhuri equation [see Eq. (3.59) of Chapter 3]. Using the variable $u_k \equiv a^{1+\zeta/2}$, the shear satisfies the following equation of motion

$$u_k'' + \left[k^2 + 2K - \frac{(a^{-1-\zeta/2})''}{a^{-1-\zeta/2}} \right] u_k = 0, \quad (4.153)$$

where we have used Eq. (4.152). In flat models ($K = 0$) on large scales there is a decaying solution $\sigma_k \propto a^{-(2+\zeta)}$. Since Eq. (4.153) contains no first derivative term the Wronskian is conserved. On large scales we can use the solution $\sigma_k \propto a^{-(2+\zeta)}$ to write the conserved Wronskian as $W = \sigma'_k + (2 + \zeta)\mathcal{H}\sigma_k$. (The Wronskian vanishes in the decaying mode.) Integrating gives the following two independent solutions on large scales in flat models:

$$\sigma_k = \begin{cases} A_k a^{-(2+\zeta)}, \\ B_k a^{-(2+\zeta)} \int^\tau d\tilde{\tau} a(\tilde{\tau})^{2+\zeta}, \end{cases} \quad (4.154)$$

where A_k and B_k are constants of integration. If we let $\zeta \rightarrow 0$, we recover the results in [125] for the general relativity case.

The conserved Wronskian is proportional to the metric perturbation variable, H_T , characterising the amplitude of 4D gravitational waves. In flat models H_T is related to the covariant variables quite generally by

$$H_{Tk} = \frac{\sigma'_k}{k} + 2E_k. \quad (4.155)$$

Ignoring photon anisotropic stress, we can eliminate the electric part of the Weyl tensor via the shear propagation equation (4.147) to find $kH_{Tk} = -\sigma'_k - (\zeta + 2)\mathcal{H}\sigma_k = -W$. The fact that H_T is conserved on large scales in flat models in the absence of photon anisotropic stress can also be seen directly from its propagation equation,

$$H''_{Tk} + (2 + \zeta)\mathcal{H}H'_{Tk} + k^2 H_{Tk} = 0. \quad (4.156)$$

We can solve Eq. (4.153) on all scales in the high-energy ($\rho \gg \lambda$ and $a \propto \tau^{1/3}$) and low-energy ($\rho \ll \lambda$ and $a \propto \tau$) radiation-dominated regimes, and during matter-domination ($a \propto \tau^2$). The solutions are

$$u_k(\tau) = \sqrt{k\tau} \left[d_1 J_{\frac{1}{6}(5+\zeta)}(k\tau) + d_2 Y_{\frac{1}{6}(5+\zeta)}(k\tau) \right] \quad (\text{high energy radiation}),$$

(4.157)

$$u_k(\tau) = \sqrt{k\tau} \left[d_3 J_{\frac{1}{2}(3+\zeta)}(k\tau) + d_4 Y_{\frac{1}{2}(3+\zeta)}(k\tau) \right] \quad (\text{low energy radiation}), \quad (4.158)$$

$$u_k(\tau) = \sqrt{k\tau} \left[d_5 J_{\frac{5}{2}+\zeta}(k\tau) + d_6 Y_{\frac{5}{2}+\zeta}(k\tau) \right] \quad (\text{matter domination}), \quad (4.159)$$

where d_i are integration constants. The solutions for the electric part of the Weyl tensor can be found from Eq. (4.147). For modes of cosmological interest the wavelength is well outside the Hubble radius at the transition from the high-energy regime to the low-energy. It follows that the regular solution (labelled by

d_1) in the high-energy regime will only excite the regular solution (d_3) in the low-energy, radiation-dominated era. Performing a series expansion, we arrive at the appropriate initial conditions for large-scale modes in the low-energy radiation era:

$$H_{Tk} = 1 - \frac{(k\tau)^2}{2(3+\zeta)} + \frac{(k\tau)^4}{8(3+\zeta)(5+\zeta)} + O[(k\tau)^6], \quad (4.160)$$

$$\sigma_k = -\frac{k\tau}{3+\zeta} + \frac{k^3\tau^3}{2(3+\zeta)(5+\zeta)} + O[(k\tau)^5], \quad (4.161)$$

$$E_k = \frac{(4+\zeta)}{2(3+\zeta)} - \frac{(k\tau)^2(8+\zeta)}{4(3+\zeta)(5+\zeta)} + O[(k\tau)^4]. \quad (4.162)$$

In the limit $\zeta \rightarrow 0$, we recover the general relativity results [31].

For modes that are super-Hubble at matter-radiation equality (i.e. $k\tau_{\text{eq}} \ll 1$), the above solution joins smoothly onto the regular solution labelled by d_5 in Eq. (4.159). For $k\tau_{\text{eq}} \gg 1$, the shear during matter domination takes the form

$$\sigma_k = -2^{\frac{3}{2}+\zeta} \Gamma(\frac{5}{2} + \zeta) (k\tau)^{-(\frac{3}{2}+\zeta)} J_{\frac{5}{2}+\zeta}(k\tau). \quad (4.163)$$

In the opposite limit, the wavelength is well inside the Hubble radius at matter-radiation equality. The asymptotic form of the shear in matter domination is then

$$\sigma_k \sim \frac{\Gamma[\frac{1}{2}(3+\zeta)]}{\sqrt{\pi}} \left(\frac{2\tau_{\text{eq}}}{\tau}\right)^{1+\zeta/2} (k\tau)^{-(1+\zeta/2)} \sin(k\tau - \pi\zeta/4). \quad (4.164)$$

We use the initial conditions, Eqs. (4.160)–(4.162), in a modified version of the CAMB code to obtain the tensor temperature and polarization power spectra. The temperature and electric polarization spectra are shown in Figs. 4.2 and 4.3 for a scale-invariant initial power spectrum. The normalisation is set by the initial power in the gravity wave background. Figs. 4.2 and 4.3, together with Eqs. (4.157)–(4.162), are the main result of this work, and we now discuss the physical conclusions following from these results.

§4.3.2 Discussion on the Tensor Power Spectra

As expected, we find that the power spectra are insensitive to high-energy effects, i.e. effectively independent of the brane tension λ : the $\zeta = 0$ curve in Fig. 1 is indistinguishable from that of the general relativity model (both power spectra are identical at the resolution of the plot). For the computations, we have used the lowest value of the brane tension $\lambda = (100 \text{ GeV})^4$, consistent with the tests of Newton's law.

There are three notable effects visible in Figs. 1 and 2, from our approximate model of the KK stress: (i) the power on large scales reduces with increasing KK parameter ζ ; (ii) features in the spectrum shift to smaller angular scales with increasing ζ ; and (iii) the power falls off more rapidly on small scales as ζ increases. Neglecting scattering effects, the shear is the only source of linear tensor anisotropies (see e.g. [31]). For $1 \ll l < 60$ the dominant modes to contribute to the temperature C_l s are those whose wavelengths subtend an angle $\sim 1/l$ when the shear first peaks (around the time of Hubble crossing). The small suppression in the C_l s on large scales with increasing ζ arises from the reduction in the peak amplitude of the shear at Hubble entry [see Eq. (4.163)], qualitatively interpreted as the loss of energy in the 4D graviton modes to 5D KK modes.

Increasing ζ also has the effect of adding a small positive phase shift to the oscillations in the shear on sub-Hubble scales, as shown e.g. by Eq. (4.164). The delay in the time at which the shear first peaks leads to a small increase in the maximum l for which $l(l+1)C_l$ is approximately constant, as is apparent in Fig. 4.2. The phase shift of the subsequent peaks in the shear has the effect of shifting the peaks in the tensor C_l s to the right. For $l > 60$ the main contribution to the tensor anisotropies at a given scale is localized near last scattering and comes from modes with wavenumber $k \sim l/\tau_0$, where τ_0 is the present conformal time. On these scales the gravity waves have already entered the Hubble radius at last scattering. Such modes are undergoing adiabatic damping by the expansion and this results in the sharp decrease in the anisotropies on small scales. Increasing the KK parameter ζ effectively produces more adiabatic damping and hence a sharper fall off of power. The transition to a slower fall off in the C_l s at $l \sim 200$ is due to the weaker dependence of the amplitude of the shear on wavenumber at last scattering for modes that have entered the Hubble radius during radiation domination [179]. [The asymptotic expansion of Eq. (4.163) gives the shear amplitude $\propto k^{-(2+\zeta)}$ at fixed τ , whereas for modes that were sub-Hubble at matter-radiation equality Eq. (4.164) gives the amplitude $\propto k^{-(1+\zeta/2)}$.]

Similar comments apply to the tensor electric polarization C_l^E , shown in Fig. 4.3. As with the temperature anisotropies, we see the same shifting of features to the right and increase in damping on small scales. Since polarization is only generated at last scattering (except for the feature at very low l that arises from scattering at reionization, with an assumed optical depth $\tau_C = 0.03$), the large-scale polarization is suppressed, since the shear (and hence the temperature quadrupole at last scattering) is small for super-Hubble modes. In matter domination the large-scale shear is $\sigma_k = -k\tau/(5 + 2\zeta)$; the reduction in the magnitude of the shear with increasing KK parameter ζ is clearly visible in the large-angle polarization. The braneworld modification to the tensor magnetic polarization C_l^B has the same qualitative features as in the electric case (see Fig. 4.4).

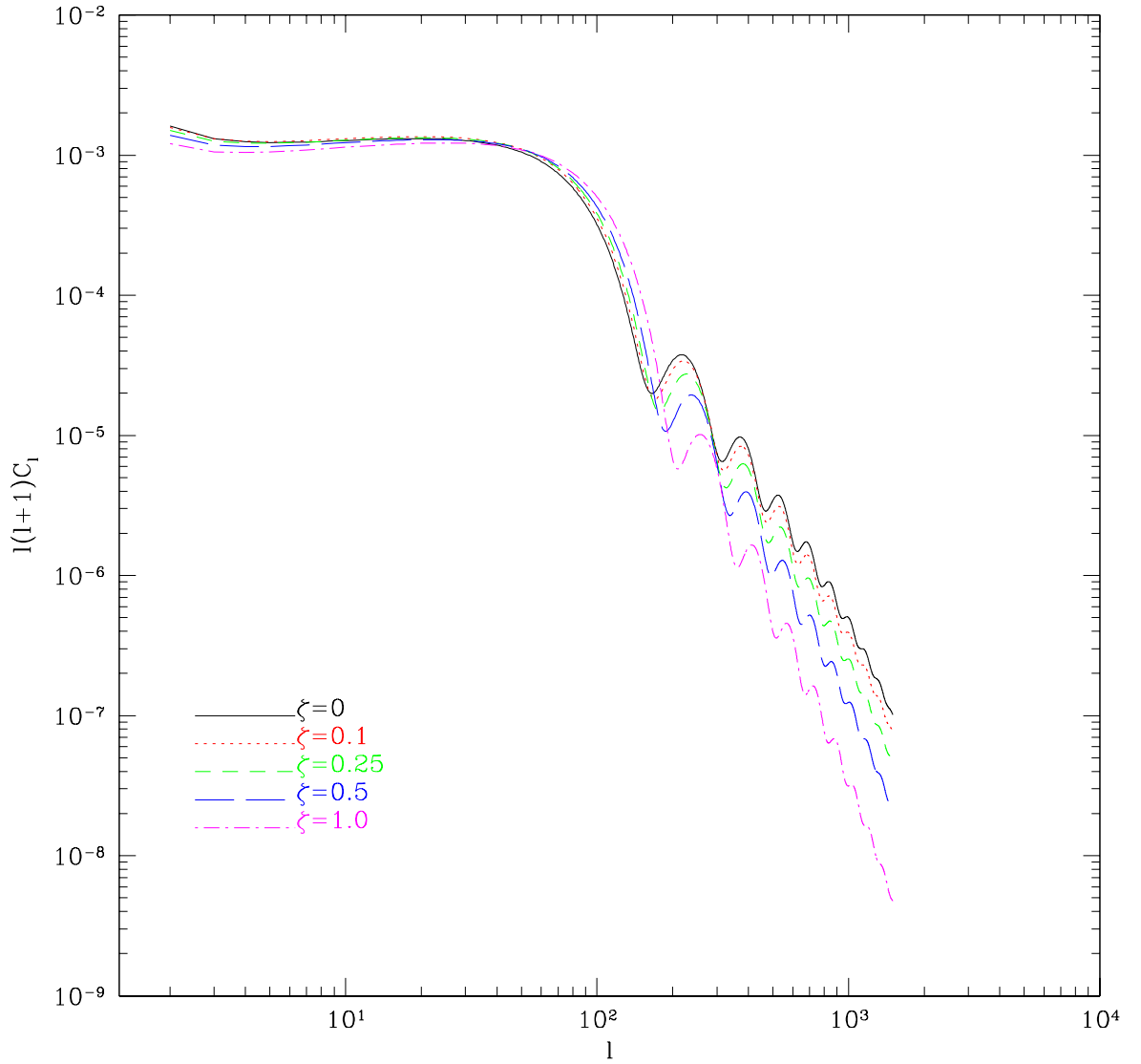


Figure 4.2: The temperature power spectrum for tensor perturbations in braneworld models using the approximation in Eq. (4.151), with ζ the dimensionless KK parameter. Models are shown with $\zeta = 0.0, 0.1, 0.25, 0.5$ and 1.0 . The initial tensor power spectrum is scale invariant and we have adopted an absolute normalisation to the power in the primordial gravity wave background. The background cosmology is the spatially flat Λ CDM (concordance) model with density parameters $\Omega_b = 0.035$, $\Omega_c = 0.315$, $\Omega_\Lambda = 0.65$, no massive neutrinos, and the Hubble constant $H_0 = 65 \text{ km s}^{-1} \text{ Mpc}^{-1}$.

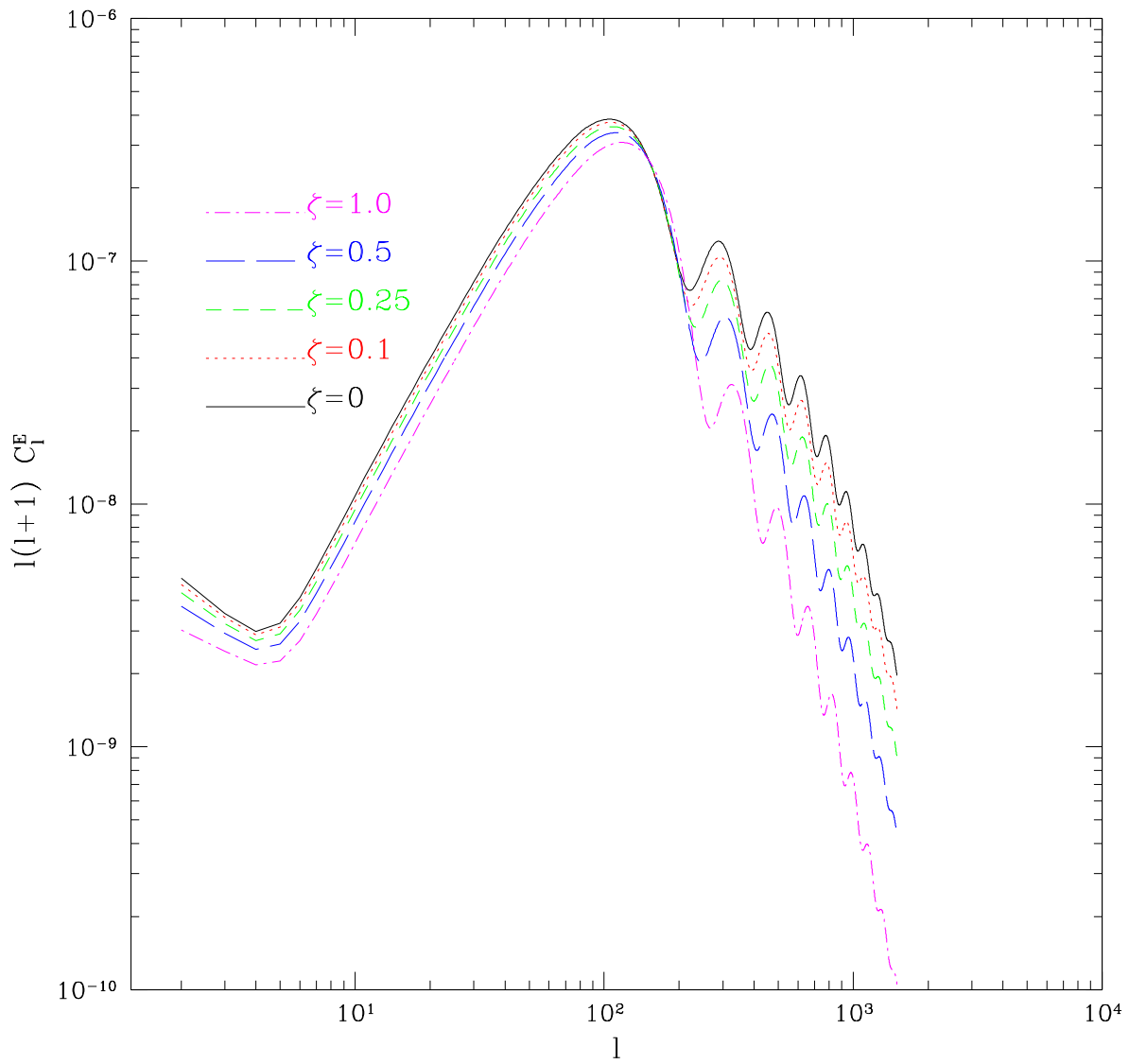


Figure 4.3: The electric polarization power spectrum for tensor perturbations for the same braneworld models as in Fig. 4.2.

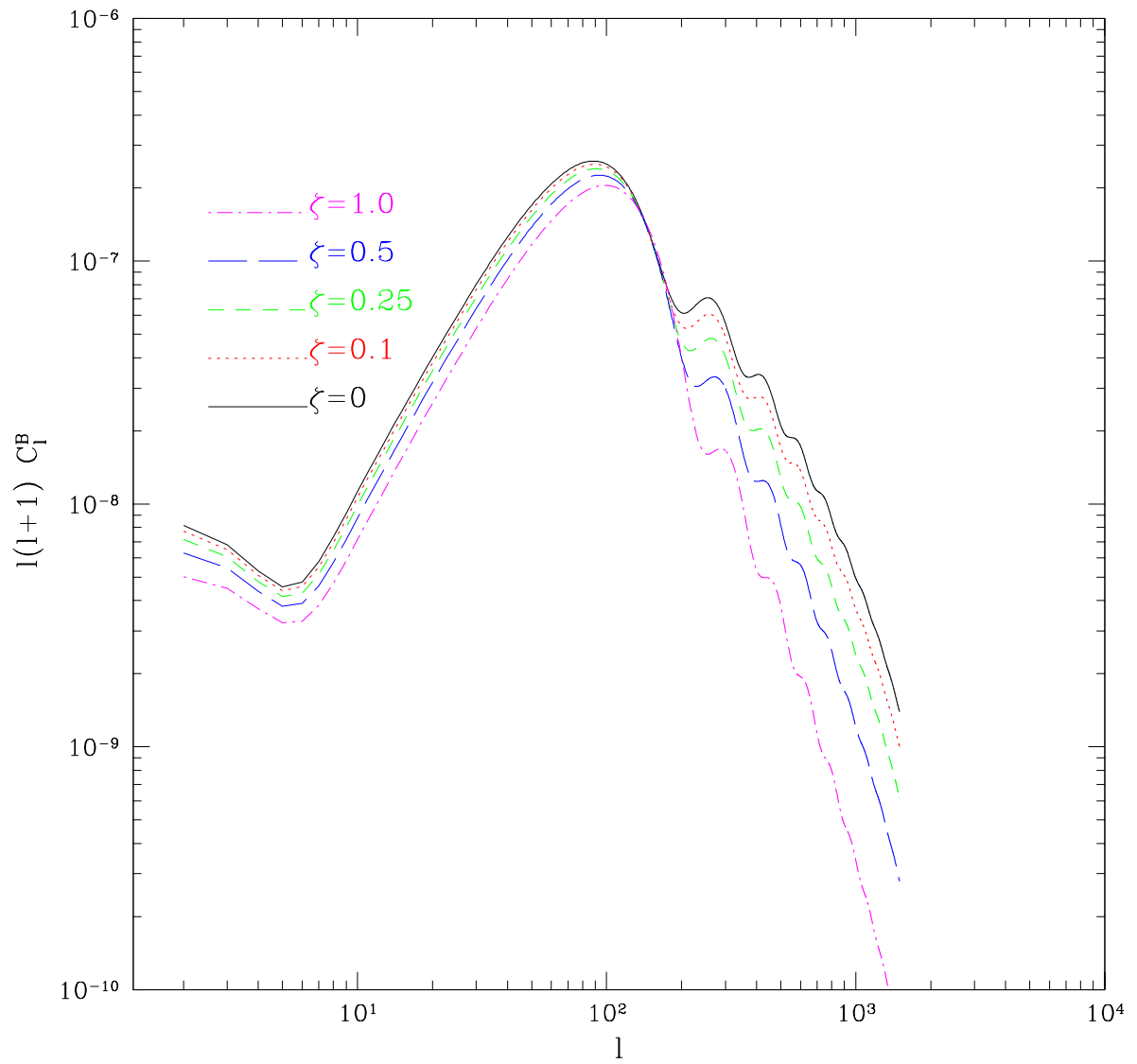


Figure 4.4: The magnetic polarization power spectrum for tensor perturbations for the same braneworld models as in Fig. 4.2.

Part III

Changing Global Symmetry

Chapter 5

Changing Global Symmetry

*Some say the world will end in fire
some say in ice.
From what I've tasted of desire
I hold with those who favor fire.
- Robert Frost*

*This is the way the world ends,
Not with a bang but a whimper.
- T.S. Eliot*

In this chapter, we examine the changing global symmetry of the Einstein-de Sitter Universe and see how it could lead to a possible phase transition in the future as in reference [10]. The largest galaxy cluster in a flat Einstein-de Sitter universe may grow indefinitely to encompass most of space after an extremely long time. We derive a general relativistic metric for a very large, bounded nearly isothermal cluster of galaxies which is embedded in such a universe. The embedding is done by means of a "Schwarzschild membrane". Pressure is important, unlike previous Tolman-Bondi models of inhomogeneities. The cluster's expansion, represented by a sequence of models, alters the average global symmetry of an increasing volume of space-time. Initially the metric is homogeneous and isotropic, having translational and rotational symmetry around every point. As the metric evolves, it eventually loses its translational symmetry throughout larger regions and retains rotational symmetry around only one point: the centre of the cluster becomes the centre of the universe. Our sequence of hybrid models transforms between the Einstein-de Sitter and the isothermal cluster limits and illustrates how a changing equation of state of matter can alter the global symmetry of space-time.

§5.1 Introduction

It is well known in standard texts [40, 156, 189] that one can have a changing equation of state in a single metric. For example, one can study the behaviour of the FRW metric in the radiation-dominated and the matter-dominated era which correspond to different equations of state. In these situations, the equation of state does not influence the global symmetry of the metric, and there is a smooth transition from the radiation-dominated to the matter-dominated era. In other previous inhomogeneous models, the equation of state has zero pressure [15, 58, 112, 113, 122]. Therefore, it remains an interesting fundamental question to ask whether such a dynamical symmetry breaking process can be modelled in general relativity. To paraphrase this question in a more concrete form, can one find a metric to describe a changing global symmetry, with a changing equation of state that will alter the form of the metric? Here, the basic effect of the pressure on the metric arises not from its contribution to the energy density or to the expansion, but from its support of growing inhomogeneity.

At first sight, it may not seem possible to solve the Einstein field equations directly for a changing equation of state which induces symmetry changes in the metric. Even the form of such an equation of state has not been examined previously. Hence, to answer the above question, we need to adopt a different approach to find a more general solution. Our method is to find a continuous hybrid metric which is consistent with the known limit-solutions. The hybrid solution is parameterised by two constants and applies only to the quasi-static phases of the universe when it is dominated by one gigantic isothermal cluster. As a second cluster of comparable size enters the horizon the hybrid description breaks down. The clusters merge and eventually form a new, larger isothermal sphere. After relaxation of this larger system the hybrid solution is valid again with changed values of its characteristic constants.

This allows us to separate the problem into two parts. First, we find the parameterised hybrid solution which describes those periods in the evolution of the universe, which are dominated by a large isothermal core. We then describe the temporal evolution as a discrete sequence of such stages i.e. as a sequence of hybrid solutions with changed parameterisation.

Due to the different equations of state, it is not possible to find direct matching conditions for the generalised isothermal metric and the FRW metric. The reason can be understood physically. Clustering induces a change from a universe with zero pressure to a universe with non-zero cosmologically significant pressure. There is a symmetry change from the spherical, homogeneous FRW models, which have no centre to the isothermal model, which singles out the point with highest density as its centre.

§5.2 The Isothermal Universe

§5.2.1 The Isothermal Metric

We begin with a brief summary of the isothermal universe found by Saslaw et al[172]. The starting point is to consider an asymptotically static universe that satisfies the general static, spherically symmetric line element:

$$ds^2 = -e^{\nu(r)} dt^2 + e^{\lambda(r)} dr^2 + r^2(d\theta^2 + \sin^2 \theta d\phi^2). \quad (5.1)$$

The Einstein field equations are given by

$$G_{ab} = R_{ab} - \frac{1}{2}Rg_{ab} = 8\pi T_{ab}, \quad (5.2)$$

where the energy-momentum tensor of a perfect fluid is

$$T_{ab} = (\rho + P)u_a u_b + P g_{ab}. \quad (5.3)$$

To derive the solution for the isothermal universe, an equation of state is required to determine the metric. The isothermal equation of state is characterized by a pressure gradient which balances the mutual self-gravity of its constituent particles i.e. idealized point galaxies. The dispersion of the particles' peculiar velocities is independent of position. Therefore the equation of state is:

$$P = \alpha \rho, \quad (5.4)$$

where α is a constant for the whole spacetime and $0 \leq \alpha \leq 2/3$.

There are two assumptions in obtaining the solution of the isothermal sphere. Firstly, we assume $e^{\lambda(r)}$ to be independent of time. This has the geometrical interpretation that the radial coordinate of the metric scales radially as a constant. Secondly, we assume the density distribution of a finite isothermal sphere (which realistically would be bounded by an external pressure or tidal disruption) is described by the relation $\rho \propto r^{-2}$ at large radii, as was first shown by Emden [67] for the Newtonian case and subsequently extended to the relativistic case by Chandrasekhar [36]. To obtain the cosmological metric describing an infinite isothermal universe one has to make the simplifying approximation that $\rho \propto r^{-2}$ throughout the entire sphere. Solving the Einstein field equations (5.2) using the line element (5.1) together with Eqs. (5.3) and (5.4) and the density distribution given above, gives the following relations:

$$e^{\nu} = Ar^{\frac{4\alpha}{1+\alpha}}, \quad (5.5)$$

$$e^{\lambda} = 1 + \frac{4\alpha}{(1+\alpha)^2}, \quad (5.6)$$

$$8\pi\rho = \frac{4\alpha}{4\alpha + (1+\alpha)^2} \frac{1}{r^2}. \quad (5.7)$$

The line element for the isothermal universe is therefore stated as follows:

$$ds^2 = -Ar^{\frac{4\alpha}{1+\alpha}} dt^2 + \left(1 + \frac{4\alpha}{(1+\alpha)^2}\right) dr^2 + r^2(d\theta^2 + \sin^2\theta d\phi^2), \quad (5.8)$$

where A is an arbitrary constant.

Here we find that the transformation $\bar{r} = r^U$ casts the metric in Eq. (5.8) into its isotropic form

$$ds^2 = -A\bar{r}^V dt^2 + \bar{r}^{2W} [d\bar{r}^2 + \bar{r}^2 d\Omega^2], \quad (5.9)$$

where the functions U , V and W are defined as

$$U = \left(1 + \frac{4\alpha}{(1+\alpha)^2}\right)^{\frac{1}{2}}, \quad (5.10)$$

$$V = \frac{4\alpha}{U(1+\alpha)}, \quad (5.11)$$

$$W = \frac{1}{U} - 1. \quad (5.12)$$

For completeness, we also state the conformal form of Eq. (5.8), which relates to minimally curved spaces, as found by Dadhich [42]:

$$ds^2 = r^{\frac{-2m}{1+m}} [-dt^2 + k_1^2 dr^2 + r^2(d\theta^2 + \sin^2\theta d\phi^2)]. \quad (5.13)$$

where $e^\lambda = k_1^2$ and $e^\nu = r^{-2m}$. Note that k_1^2 and m are constants relating to α .

§5.2.2 Properties and Implications of the Isothermal solution with a Global Phase Transition of the Universe

Before we proceed further, we note a few interesting features with the isothermal solution, (5.8), found by Saslaw et al in [172]. First of all, the isothermal universe in their case, is a infinite isothermal sphere without a boundary. The solution is not a realistic one which we could use to model the ultimate phase transition of the universe. However, even with that limitation, from examining the physical interpretation of the unbounded isothermal sphere, we could infer why a global phase transition would eventually happen.

From an extensive study in the dynamics of galaxy clustering (which was well discussed in the references [169, 170, 171]), there is a discussion on whether the many-body clustering of galaxies in our expanding Universe would be represented as a phase transition. The conclusion is reached in [170] that galaxy clustering lacks the near simultaneity of the transition over all scales, even though it has some basic features of such a phase transition. In Einstein-Friedmann cosmologies with

$\Omega_0 < 1$, and in related cosmologies with $\Omega_\Lambda > 0$, the universe would eventually expand so rapidly relative to the gravitational clustering timescales such that the pattern of galaxies would freeze out on large scales, and correlations cease to grow, and the attempt at a second order phase transition would die away before it could ever happen.

However, in the case of the flat $\Omega_0 = 1$, $\Omega_\Lambda = 0$, Einstein-de Sitter cosmology, there is a possibility for this phase transition to occur. In present day observational cosmology, in the viewpoint of the data from the observed fluctuations in the cosmic microwave background anisotropies [14, 115], it seems very likely that our Universe is nearly flat. However, whether there is a cosmological constant, is still being debated, but if there is, the consequence of a phase transition would have been different.

One would ponder how the phase transition would enter in the unbounded isothermal sphere scenario. The first thing is to recognise that there is a change of fundamental symmetry between the Einstein-de Sitter model and the isothermal model. We recall the form of the Friedmann-Robertson-Walker metric (Eq.(1.1) in Chapter 1).

To match Eqs.(1.1) and (5.8), we need to show that the pressure must be discontinuous at the junction across the hypersurface where r is a constant. Comparison of the two metrics would show that for $\alpha > 0$, there is no such hypersurface where this match occurs. Therefore this change must be continuous. Since there is a time dependence in the global expansion $a(t)$, and the isothermal metric has no time dependence, it suggests that in the limit that $t \rightarrow \infty$, the transition would take place everywhere. Such an event would correspond to a phase transition. Of course, a more complicated metric that allows growing inhomogeneities would be required to follow this transition.

This has set the scene and motivation for this chapter on the theme of changing global symmetry in our thesis on alternative cosmologies. In [10], we have found and studied a hybrid model which corresponds to the global symmetry change mentioned above. In the next section, we will subsequently derive a generalized form of their metric to include a *bounded* isothermal sphere using an approach by Tolman [184]. We review and discuss the properties of the bounded isothermal sphere. This is followed by a discussion of the approximations involved in the general solution (§5.3) and the thermodynamic consequences implied by the modified equation of state (§5.4). In §5.5, we first match the bounded isothermal sphere to a Schwarzschild background, and then embed the combined metric into the expanding Einstein-de Sitter universe, adapting earlier techniques (McVittie [145, 146] and Hogan [89]). In §5.6, we describe the evolution of the universe as a sequence of static stages. Each stage is described by a hybrid metric with characteristic parameterisation. Finally, in §5.7, we discuss the implications of such

a cosmological solution, linking the dynamical breaking of symmetry to a phase transition. In the same light, we mention an additional role for the cosmological constant which counteracts the formation of the isothermal sphere.

§5.2.3 Generalization of the Isothermal Metric to Finite Spheres

The basic problem in the search for a solution by direct matching of the isothermal metric and the FRW metric, lies in the finite pressure-mismatch between the FRW models, which are based on the assumption of zero pressure, whereas our FRW fitting uses zero pressure, but the isothermal sphere could have a nonzero uniform pressure. To circumvent this difficulty, one has to generalise the infinite isothermal sphere in [172] to a finite sphere, where the pressure drops to zero at the boundary. Then it is possible to match this finite sphere solution to the expanding space surrounding it.

To generalise the isothermal solution we employed the technique used by Tolman [184]. By starting with the general static, spherically symmetric line element described by Eq. (5.1) one arrives at the following field equations for the perfect fluid case:

$$\frac{d}{dr} \left(\frac{e^{-\lambda} - 1}{r^2} \right) + \frac{d}{dr} \left(\frac{e^{-\lambda} \nu'}{2r} \right) + e^{-\lambda-\nu} \frac{d}{dr} \left(\frac{e^{\nu} \nu'}{2r} \right) = 0, \quad (5.14)$$

$$8\pi\rho = e^{-\lambda} \left(\frac{\nu'}{r} + \frac{1}{r^2} \right) - \frac{1}{r^2}, \quad (5.15)$$

$$8\pi P = e^{-\lambda} \left(\frac{\lambda'}{r} - \frac{1}{r^2} \right) + \frac{1}{r^2}. \quad (5.16)$$

We assume $e^{-\lambda} = \text{constant}$ in order to obtain a simple generalization of the isothermal equation of state, so that a very large central cluster can have a finite boundary. This allows us to integrate Eq. (5.14), and leads to the corresponding solution:

$$e^{\nu} = (Cr^{1-n} - Dr^{1+n})^2, \quad (5.17)$$

$$e^{\lambda} = 2 - n^2, \quad (5.18)$$

$$8\pi\rho = \frac{1 - n^2}{2 - n^2} \frac{1}{r^2}, \quad (5.19)$$

$$8\pi P = \frac{1}{2 - n^2} \frac{1}{r^2} \frac{(1 - n)^2 C - (1 + n)^2 D r^{2n}}{C - D r^{2n}}, \quad (5.20)$$

where n , C and D are arbitrary constants of integration.

To relate Tolman's solution to the isothermal metric, one makes the following identification

$$e^\lambda \equiv 1 + \frac{4\alpha}{(1 + \alpha)^2} = 2 - n^2, \quad (5.21)$$

where

$$n = \pm \frac{1 - \alpha}{1 + \alpha}. \quad (5.22)$$

By taking the positive root* of the above relation the isothermal metric is generalised to the form

$$e^\nu = \left(Cr^{\frac{2\alpha}{1+\alpha}} - Dr^{\frac{2}{1+\alpha}} \right)^2, \quad (5.23)$$

$$e^\lambda = 1 + \frac{4\alpha}{(1 + \alpha)^2}, \quad (5.24)$$

$$8\pi\rho = \frac{4\alpha}{4\alpha + (1 + \alpha)^2} \frac{1}{r^2}, \quad (5.25)$$

$$8\pi P = \frac{4\alpha^2}{4\alpha + (1 + \alpha)^2} \frac{1}{r^2} \frac{C - \frac{1}{\alpha^2} Dr^{\frac{2(1-\alpha)}{1+\alpha}}}{C - Dr^{\frac{2(1-\alpha)}{1+\alpha}}}. \quad (5.26)$$

D is interpreted as a deviation term for the isothermal sphere. The original isothermal metric without a boundary is included in this form in the limit $D \rightarrow 0$.

The specific case for $n = 1/2$ was discussed by Tolman [184]. In the limit $D/C \rightarrow 0$, the ratio of pressure to density (α) approaches one-third throughout and the sphere grows without limit. Physically, it represents the blackbody radiation solution in the Oppenheimer-Volkoff analysis. In the limit of large ρ , the equation of state for the sphere goes over to the approximate form, $\rho - 3P \propto \rho^{1/2}$, as for a highly compressed Fermi gas.

In the generalised form of the bounded isothermal metric, we still require the fixed density distribution $\rho \propto r^{-2}$, but allow the pressure-density relation to deviate from the perfect isothermal equation of state. Hence, we deduce the following generalised isothermal equation of state:

$$\frac{P}{\rho} = \alpha \frac{C - \frac{1}{\alpha^2} Dr^{\frac{2(1-\alpha)}{1+\alpha}}}{C - Dr^{\frac{2(1-\alpha)}{1+\alpha}}}, \quad (5.27)$$

where α is defined as the constant of proportionality between pressure and density *at the centre* of the sphere. Note that the above equation of state allows the pressure to drop to zero at a finite radial distance, r_b . Hence, our metric incorporates the feature of describing a finite sphere, each shell of which is approximately

*Choosing the negative root gives the same solutions with C and D interchanged. This reflects an implicit symmetry of the Tolman solution.

isothermal. It is the requirement that the isothermal solution has a boundary, which introduces deviations from the perfect isothermal equation of state. A related class of spherically symmetric solutions of Einstein's equation which consist of a perfect fluid with uniform density but non-uniform pressure, was found by Wesson and Ponce de Leon [190, 191]. In their solution, the equation of state is similar to Eq. (5.27) except that their equation of state for the metric is both dependent on time, t and radial position, r . These solutions are recognised to be scale free and self-similar and were discussed in detail by Carr [25, 26]. The nature of equation (5.27) is that at any given radius and for any given value of α , the pressure P is proportional to ρ , but the constant of proportionality varies with position (see §5.4 for a discussion). We denote this as a generalised isothermal sphere. Formally, this is a result of the finite boundary. Physically, this could result from incomplete dynamical relaxation in the outer regions of the cluster where the densities are lower and the relaxation timescales longer, but a detailed model of these dynamics is beyond the scope of this chapter. The pressure decreases to zero at the boundary and it remains zero for larger radii. This means that infall or expansion around the cluster is radial, moving mainly with the Hubble flow, and has negligible random velocity.

The boundary of the generalised isothermal sphere is physically defined by $P(r = r_b) = 0$:

$$r_b = \left(\frac{\alpha^2 C}{D} \right)^{\frac{1+\alpha}{2(1-\alpha)}}. \quad (5.28)$$

The pressure parameter at the centre, α , is directly related to the scale of the generalised isothermal sphere. For vanishing α , Eq. (5.28) agrees with the fact that in this limit there is no isothermal sphere. Larger values of the constant α correspond to a sequence of static solutions for larger spheres which have grown through the merger of clusters at later stages. We find that C and D can be used to normalise the scale of the generalised isothermal sphere. We will also discover that C and D are not independent, since the matching to the Schwarzschild exterior provides a relation between them.

The mass of the generalised isothermal sphere can be determined by integrating its density up to the boundary:

$$M_{iso} = \int_0^{r_b} \rho(r) 4\pi r^2 dr = \frac{2\alpha}{4\alpha + (1 + \alpha)^2} r_b. \quad (5.29)$$

Given the functional form of the isothermal boundary, r_b , in terms of C , D and α we can rewrite the generalised isothermal metric in the following form which closely resembles the original isothermal metric, but with a radially dependent

deviation term.

$$e^\nu = Ar^{\frac{4\alpha}{1+\alpha}} \left[1 - \alpha^2 \left(\frac{r}{r_b} \right)^{\frac{2(1-\alpha)}{1+\alpha}} \right]^2, \quad (5.30)$$

$$e^\lambda = 1 + \frac{4\alpha}{(1+\alpha)^2}, \quad (5.31)$$

$$8\pi\rho = \frac{4\alpha}{4\alpha + (1+\alpha)^2} \frac{1}{r^2}, \quad (5.32)$$

$$P = \alpha\rho \frac{1 - \left(\frac{r}{r_b} \right)^{\frac{2(1-\alpha)}{1+\alpha}}}{1 - \alpha^2 \left(\frac{r}{r_b} \right)^{\frac{2(1-\alpha)}{1+\alpha}}}, \quad (5.33)$$

where we have set $C^2 \equiv A$.

Hence we have found the interior metric for a generalised isothermal sphere of finite radius:

$$ds^2 = -Ar^{\frac{4\alpha}{1+\alpha}} \left[1 - \alpha^2 \left(\frac{r}{r_b} \right)^{\frac{2(1-\alpha)}{1+\alpha}} \right]^2 dt^2 + \left(1 + \frac{4\alpha}{(1+\alpha)^2} \right) dr^2 + r^2(d\theta^2 + \sin^2\theta d\phi^2) \quad (5.34)$$

for $r < r_b$.

§5.3 The Isothermal Approximation

Our generalization of the isothermal universe involves two approximations which we now want to consider in turn. First we review the approximation of the generalised metric to the ideal isothermal counterpart. For the generalised isothermal metric to be a good approximation to Eq. (5.8), Eq. (5.30) requires the condition

$$j \equiv \alpha^2 \left(\frac{r}{r_b} \right)^{\frac{2(1-\alpha)}{1+\alpha}} \ll 1, \quad (5.35)$$

where $0 \leq \alpha \leq \frac{2}{3}$. This condition on α incorporates the possibilities of relativistic pressure ($\alpha = 1/3$) and of a perfect monatomic gas ($\alpha = 2/3$).

A contour plot of $j(r/r_b, \alpha)$ is given in Fig. 5.1. It shows that $j < 1$ for all α and (r/r_b) -ratios. The generalised metric therefore resembles the perfect isothermal metric very closely. Deviations from the perfect isothermal metric express the feedback of the finite boundary of the isothermal sphere on the metric.

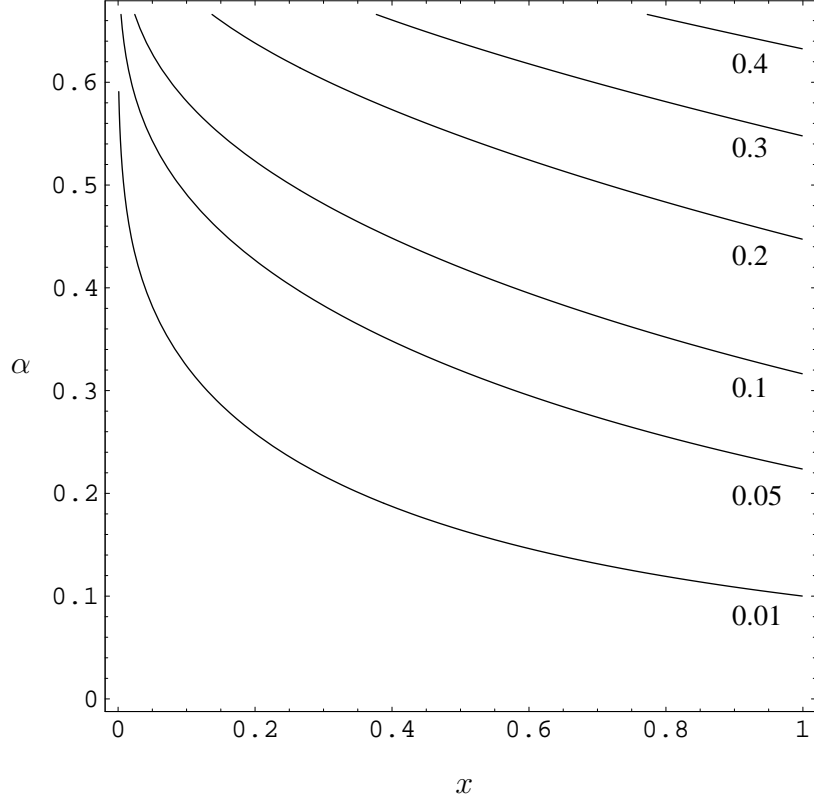


Figure 5.1: Contour plot of j . Here $x \equiv (r/r_b)$. For $j \ll 1$, which characterizes almost all combinations of α and x , the deviation of the generalised metric from the ideal isothermal form is negligible.

The generalised equation of state can be rewritten in the form $P = \alpha\rho[1 - \Delta]$ where we define the deviation term

$$\Delta \equiv \frac{(1 - \alpha^2) \left(\frac{r}{r_b}\right)^{\frac{2(1-\alpha)}{1+\alpha}}}{1 - \alpha^2 \left(\frac{r}{r_b}\right)^{\frac{2(1-\alpha)}{1+\alpha}}}. \quad (5.36)$$

Next we define the transformation $x \equiv (r/r_b)$ to obtain the normalised radial gradient of the deviation:

$$\frac{\partial \Delta}{\partial x} = \frac{2(1 - \alpha)^2 x}{\left(x^{\frac{2\alpha}{1+\alpha}} - \alpha^2 x^{\frac{2}{1+\alpha}}\right)^2}. \quad (5.37)$$

For a good approximation to the isothermal equation of state $p = \alpha\rho$, we suggest two necessary limits: (a) $\Delta \rightarrow 0$ which scales the pressure-density dependence and

(b) $|d\Delta/dx| \ll 1$, which expresses the fact that in an ideal isothermal sphere, the form of the equation of state is independent of position.

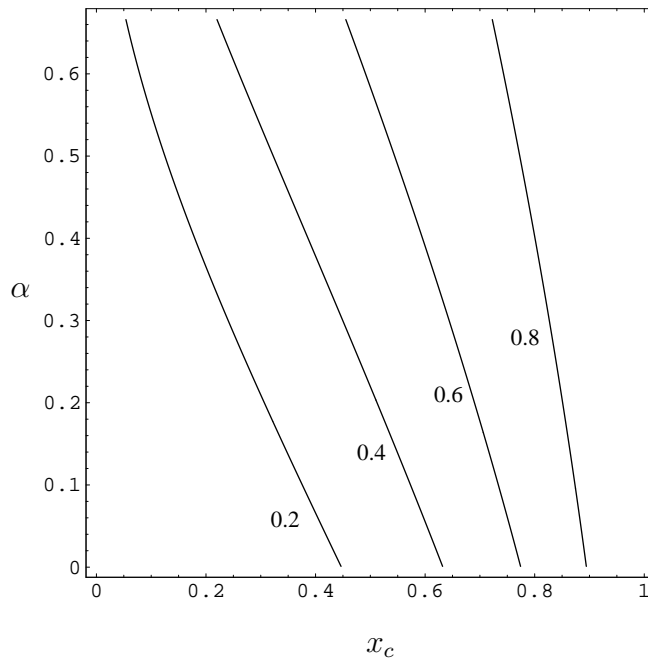


Figure 5.2: Contour plot of the deviation term Δ . The plot gives the characteristic core region where the deviation from the perfect isothermal equation of state is less than a particular contour value. Note that although the ratio of the core radius to the boundary radius $x_c = (r_c/r_b)$ decreases with increasing α (and hence with step number), both r_c and r_b are monotonically increasing with each step. The decreasing x_c merely reflects their relative rates of increase.

Fig. 5.2 shows a contour plot of the deviation term Δ . We see that for a particular value of the constant α the approximation gets worse with increasing distance from the center, as the radius-dependent perturbation becomes more significant. The plot gives a characteristic core region where the deviation from the perfect isothermal equation of state is less than a particular contour value. Note that although the ratio of the core radius to the boundary radius $x_c = (r_c/r_b)$ decreases with increasing α , at later evolutionary steps, both r_c and r_b are monotonically increasing with each step. The decreasing x_c merely reflects their relative rates of increase.

Fig. 5.3 shows diagrams of the radial derivative of the deviation term $d\Delta/dx$. This derivative becomes very small for both small α and small r/r_b . For large α and r/r_b there is a significant variation of the equation of state with position. The derivative $d\Delta/dx$ shows the complex functional form expected for a finite sphere.

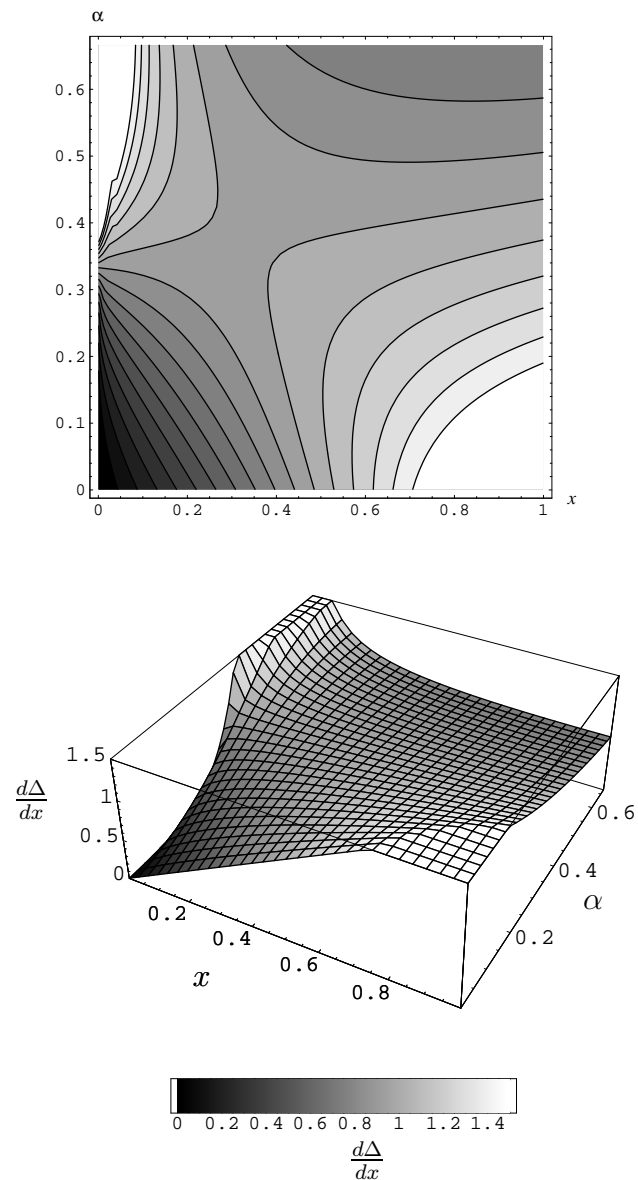


Figure 5.3: Contour plot of the derivative of the deviation term ($d\Delta/dx$). The plots gives the core region (small α , $r \ll r_b$) where the derivative is less than a particular value and the ratio of pressure to density is therefore nearly independent of position.

The contour plots of Figs. 5.1 - 5.3 indicate that there exists a core region within our generalised sphere for which the metric and the equation of state are close to the ideal isothermal limit. There are several alternative ways of defining

this core region. All of these arbitrary definitions, however, have in common that they describe the same qualitative picture. In that picture our metric describes a sphere which tends to the perfect isothermal limit at the centre, has a core region where it is close to the isothermal state and then a transition region approaching the boundary where the isothermal approximation breaks down.

For small α , a good approximation to the ideal isothermal equation of state requires

$$\Delta \equiv k = \left(\frac{r}{r_b} \right)^{\frac{2(1-\alpha)}{1+\alpha}} \ll 1. \quad (5.38)$$

We may ask for the range of $r < r_c$ (relative to r_b) that satisfies a fixed constraint, for example, $k_c \equiv \text{const} = (1/3)$. This gives a core sphere, r_c , within the isothermal sphere for which the approximation does not deviate by more than the set limit. This critical core radius is given by

$$r_c = k_c^{\frac{1+\alpha}{2(1-\alpha)}} r_b. \quad (5.39)$$

As $r \rightarrow 0$, Eq. (5.38) implies that $\Delta \rightarrow 0$, and the approximation to the isothermal equation of state goes to its ideal limit. For larger r the approximation gets continuously worse at a rate described by Eq. (5.38). Both the outer radius r_b and the core radius r_c grow with each step as α and A change. Moreover, from equation (5.39), we see that r_b expands faster than r_c and the ‘wobble’ region between the isothermal core and the boundary radius grows.

§5.4 Thermodynamic Consequences implied by the Generalised Equation of State

Although an isothermal equation of state is well-known to be a reasonable zeroth-order approximation for rich clusters of galaxies (like the Coma cluster) it is also known not to be realistic, especially in the outer regions, for clusters with finite boundaries. From a physical point of view, this is because the longer dynamical relaxation timescales at the lower densities in the outer regions do not allow sufficient energy exchange for thermalization. From a mathematical point of view, the departure from isothermality is forced by the outer boundary at a finite radius.

The generalised equation of state can be written as

$$P = \alpha_{\text{eff}}(r) \cdot \rho \quad (5.40)$$

where

$$\alpha_{\text{eff}}(\alpha, r) \equiv \alpha \cdot \frac{1 - \left(\frac{r}{r_b}\right)^{\frac{2(1-\alpha)}{1+\alpha}}}{1 - \alpha^2 \left(\frac{r}{r_b}\right)^{\frac{2(1-\alpha)}{1+\alpha}}} \quad (5.41)$$

We determine the limits: (i) $r = 0$, $\alpha_{\text{eff}} \rightarrow \alpha$, (ii) $(r/r_b) \ll 1$, $\alpha_{\text{eff}} \approx \alpha$, and (iii) $(r/r_b) \rightarrow 1$, $\alpha_{\text{eff}} \rightarrow 0$. Note that we have implicitly introduced a new definition of α :

$$\alpha \equiv \frac{P(r=0)}{\rho(r=0)} \quad (5.42)$$

i.e. α characterizes the constant of proportionality between pressure and density at the centre of the sphere.

Eq. (5.40) can be regarded as an isothermal equation of state with a temperature that depends on r according to the fractional term in (5.41). This type of temperature behavior is quite common in problems involving boundary conditions. In our case, the pressure is zero at the boundary since the temperature is zero there for a good physical reason, namely the galaxies there have not relaxed and randomised their peculiar velocities significantly since the density of galaxies is low and there are fewer gravitational scatterings. The peculiar motions of galaxies near the boundary are mainly streaming motions, probably mostly infall into the approximately isothermal cluster.

Note that for any constant r (or given temperature), Eq. (5.40) shows that $dP/d\rho$ is positive so this equation of state has a positive isothermal compressibility, as needed for mechanical stability. Because Eq. (5.40) is close to an isothermal equation of state, and equivalent to it at any fixed radius, it should have reasonable thermodynamic properties as long as the number density of galaxies is large enough that one can define the thermodynamic properties in a volume smaller than that of the range of radii one is considering. This is similar (though not exactly the same) as defining the local temperature in a gas which has a temperature gradient.

All that the equation of state is saying is that the temperature is a function of position. This is similar to the case of polytropes in stars, where it is sometimes generalised to include inhomogeneous polytropes [36]. In real stars the temperature dependence of the equation of state on position occurs because of the nuclear reactions and energy transport processes. In our largest cluster it occurs because the relaxation timescales are dependent on the local density. Calculating this is a separate problem. For the equation of state to be physically acceptable, it must satisfy the first and second laws of thermodynamics locally. An isothermal equation of state does this, although our case is complicated by the long range nature of gravity in the cluster. We can regard the isothermal case with variable temperature as an approximation, just as it is in stellar structure.

§5.5 A Solution of an Expanding, Centrally Isothermal Universe

In this section, we derive a hybrid metric which encompasses the behavior of both an expanding universe and a static nearly isothermal core. Physically, we consider the evolution of such a hybrid metric to occur through three stages. First, the universe follows the usual globally homogeneous Einstein-de Sitter expansion, which tends asymptotically to stationarity, i.e. the expansion timescale, a/\dot{a} , of the universe tends to infinity at late times. Second, the condensation stage (which is attributed to galaxy clustering) gradually produces a significant cosmological pressure which alters the initial global homogeneity and supports a radially inhomogeneous global distribution of matter. Consequently, the equation of state changes with time, resulting in a dynamical feedback on the metric. Third, the postulated asymptotic final state is the generalised isothermal sphere with a boundary characterized by the equation of state in Eq. (5.27). Our solution only applies to stages one and three. It only describes the relaxed states of the universe with a static approximately isothermal core. The temporal evolution will be a sequence of such relaxed, static stages. We do not have a continuous description in time, but only discrete steps between quasi-static periods with constant α . Our solution breaks down in between. We note that the sequence of hybrid metrics (with different values of the constants α and A) is constrained by various boundary conditions in both space and time, namely, (a) at early times (for $t = 0$) the metric is FRW for all r , and (b) at late times (for $t \rightarrow \infty$) the universe would have a bounded approximately isothermal metric with a horizon expanding proportional to t , and be FRW on large scales ($r \rightarrow \infty$) which increase at $t^{(2/3)}$.

A possible counter argument to this proposal would be the following: the horizon of the Einstein-de Sitter can expand rapidly enough that the matter inside is not consolidated into a single bound system, no matter how long one waits. The only loophole is if the primordial perturbation spectrum tilts towards long wavelengths. However it would seem at first sight that the scenario we propose is not valid.

However, the key point against the skeptic's argument is that we are considering the very non-linear case of structure formation after very long times when the clustering parameter $b \rightarrow 1$ and nearly all the matter is in a few dominant massive clusters. The metric still expands at the Einstein-de Sitter rate which is proportional to $t^{(2/3)}$ since this is determined to a first approximation by an average over all horizons, so the approximate expansion timescale, $t_{expansion}$, is given by the usual

$$t_{expansion} = \frac{2a}{3\dot{a}} = \frac{1}{\sqrt{6\pi G\bar{\rho}_{crit}}} . \quad (5.43)$$

We wish to compare this expansion with the timescale, t_{merge} , for the clusters to merge. We are interested in the **non-linear** merging of smaller galaxy clusters with a larger cluster in the expanding Einstein-de Sitter Universe. In the simplest approximation, as an example to estimate the basic merging timescale, t_{merge} , for collapse into a single cluster, consider a massive cluster surrounded by a roughly spherical distribution of less massive clusters, where the whole configuration has an average large initial overdensity, $\bar{\rho}_i$, compared to the initial critical average density $\bar{\rho}_{ci}$ in that volume. For simplicity, suppose the clusters have negligible initial comoving velocity. We know that this region which has gradually become overdense will subsequently expand more slowly than the universe, turn around and collapse leading to a merger of the cluster.

To estimate the collapse (merger) timescale, we use the illustrative example in [168] (See Eqs. (37.10)–(37.19) in the reference). For $\bar{\rho}_i \gg \bar{\rho}_{ci}$ (and thus $E \approx 1$ where $E = a_{\max}^{-1}$), the time scale to maximum expansion is

$$\frac{\pi}{2} = t_{max} \sqrt{\frac{8\pi G \bar{\rho}_i}{3}} \quad (5.44)$$

where $\bar{\rho}_i$ is the initial average density in a volume containing the clusters, and

$$t_{max}^2 = \frac{\pi^2}{4} \frac{3}{8\pi G \bar{\rho}_i} = \frac{3\pi}{32G \bar{\rho}_i} . \quad (5.45)$$

Thus

$$\frac{t_{max}^2}{t_{expansion}^2} \approx \frac{3\pi}{32G \bar{\rho}_i} \times (6\pi G \rho_{crit}) = \frac{9\pi^2 \bar{\rho}_{crit}}{16 \bar{\rho}_i} \approx 5.65 \frac{\bar{\rho}_{crit}}{\bar{\rho}_i} \quad (5.46)$$

and we obtain

$$t_{max} \approx 2.36 \left(\sqrt{\frac{\bar{\rho}_{crit}}{\bar{\rho}_i}} \right) t_{expansion} . \quad (5.47)$$

If the clusters are a factor of ~ 2 closer than the average separation, $\bar{\rho}_i \approx 8\rho_{crit}$ and $t_{max} \approx 0.8t_{expansion}$. The timescale for the clusters to merge is less than about $2t_{max}$. If the clusters have initial velocities (which they will probably acquire while they form) that are mainly toward the most massive cluster, then this merging timescale is shorter. Therefore, any clusters that have less than about half of the average separation of clusters (i.e. where $\bar{\rho}_i \gtrsim 8\rho_{crit}$) are likely to merge within one expansion timescale. Clusters with larger initial separations will merge after longer times. On these longer timescales, the horizon scale will double on a timescale equal to $t_{expansion}$, which becomes infinite. This may or may not be the timescale to introduce new clusters into a particular horizon, depending on where they are located in the adjacent horizons. In the asymptotic limit, $t \rightarrow \infty$, which we are interested for this chapter, an arbitrary large horizon can contain an

arbitrary large dominant cluster, separated from such clusters in other horizons by arbitrarily large distances.

What is the effect of the matter that enters the horizons? At any given time within a horizon centred on a dominant supercluster, the galaxies not in the supercluster will be accreted by it on a timescale less than the expansion timescale. If the accretion is nonlinear, e.g. if the supercluster dominates the local gravitational field, this accretion timescale is shorter than the average expansion timescale by a factor of about $\sqrt{2}$. At any finite time, the infinite E-deS universe will contain an infinite number of these expanding horizons. The positions of their central superclusters throughout the whole universe may have a Poisson distribution since they have not had time to influence each other. However, they could, have long wavelength primordial perturbations which would speed up their clustering. Some of the horizons at any given time will be dominated by one supercluster, others may contain more, or may contain merging superclusters. Outside any of these horizons, the other clusters may be averaged over an increasingly large scale to give the effective average density of the E-deS universe.

In the limit of infinite future time (which is what we consider), for a Poisson distribution of superclusters initially outside each other's horizons, they come within each other's horizons and can merge into our isothermal sphere solution which grows to ultimately incorporate all the matter of the universe in the limit of infinite time. If long wavelength initial perturbations are important, this could happen sooner. In either case, the average separation of superclusters increases more slowly than the horizon expands, which is what our model requires.

§5.5.1 The derivation of the hybrid metric

Bounded isothermal universes with non-zero pressure (but with zero-pressure and non-zero density at the boundary at $r = r_b$) cannot be matched directly to the Einstein-de Sitter model across a specific $r = \text{constant}$ hypersurface. However, one can achieve a hybrid solution by first matching the isothermal metric to a Schwarzschild exterior. This is physically justified by Birkhoff's theorem. A formal mathematical treatment is given by Fayos et al [68] for the general matching of two spherically symmetric metrics for various pressure and density conditions. One can perceive the Schwarzschild metric as a kind of membrane (equivalent to the requirement of a closed trapped surface discussed by Fayos et al [68] for the spherically symmetric solution, such as the Vaidya metric, to match onto the FRW metric) which facilitates the matching between the *bounded static isothermal sphere* and the *expanding Einstein-de Sitter universe*. Such a procedure would be analogous to the astrophysical case for an isothermal star whose external Schwarzschild metric can be embedded in its small region of the universe.

The continuity condition of the metric coefficients, requires the following rela-

tions to be satisfied:

$$e^{\nu(r=r_b)} = \left(Cr_b^{\frac{2\alpha}{1+\alpha}} - Dr_b^{\frac{2}{1+\alpha}} \right)^2 = 1 - \frac{2m}{r_b}, \quad (5.48)$$

$$e^{\lambda(r=r_b)} = 1 + \frac{4\alpha}{(1+\alpha)^2} = \left(1 - \frac{2m}{r_b} \right)^{-1}. \quad (5.49)$$

where r_b is defined by Eq. (5.28). These provide the matching relation between C and D :

$$D(\alpha) = E(\alpha)C^{\frac{1}{\alpha}}, \quad (5.50)$$

where

$$E(\alpha) \equiv \left[1 + \frac{4\alpha}{(1+\alpha)^2} \right]^{\frac{1-\alpha}{2\alpha}} \alpha^2 [1 - \alpha^2]^{\frac{1-\alpha}{\alpha}}. \quad (5.51)$$

Substituting the matching condition into Eq. (5.28) we find

$$r_b(\alpha) = F(\alpha)A^{-\frac{1+\alpha}{4\alpha}} \quad (5.52)$$

where $A \equiv C^2$ and

$$F(\alpha) \equiv \left(\frac{\alpha^2}{E(\alpha)} \right)^{\frac{1+\alpha}{2(1-\alpha)}} \quad (5.53)$$

with $E(\alpha)$ defined in Eq. (5.51). The matching eliminates the constant D and therefore shows that the boundary radius r_b is only dependent on the parameters α and A . Hence, we also deduce immediately that the generalised isothermal metric (5.34) is parameterised by the two constants α and A .

This procedure also determines a Schwarzschild mass from the matching condition:

$$m(\alpha) = \left(\frac{2\alpha}{4\alpha + (1+\alpha)^2} \right) r_b = M_{iso} \quad (5.54)$$

Hence, the Schwarzschild mass $m(\alpha)$ is equal to the mass of the bounded generalised isothermal sphere, M_{iso} , as found independently by direct integration of the density. The equality of the results indicates consistency in our approach. The corresponding Schwarzschild radius is

$$r_s = 2m = \left(\frac{4\alpha}{4\alpha + (1+\alpha)^2} \right) r_b, \quad (5.55)$$

which indicates that $r_s < r_b$, i.e. the Schwarzschild radius is always inside the bounded isothermal sphere (as is the case for a star).

To complete the picture, we adapted the method in McVittie [145] to enable us to embed the finite generalised isothermal sphere with given properties in the

Einstein-de Sitter model. A sequence of embeddings with different properties is later used to describe the time evolution of the universe. McVittie's solution applies to a mass particle in an expanding universe and has been applied by Noerdlinger and Petrosian in [150] to investigate the motion of galaxies in galaxy clusters under the influence of cosmic expansion. In [145], he found a way of embedding a Schwarzschild geometry in a FRW spacetime. Having matched the generalised isothermal metric to a Schwarzschild exterior, we use McVittie's approach to embed this exterior spacetime in an expanding Einstein-de Sitter cosmological background. The most general form of the McVittie metric was summarised in a later paper by McVittie in [146] which incorporates a larger class of such solutions.

Hence, we find

$$ds^2 = - \left(\frac{1 - \frac{m(\alpha)}{2a\bar{r}}}{1 + \frac{m(\alpha)}{2a\bar{r}}} \right)^2 dt^2 + \left(1 + \frac{m(\alpha)}{2a\bar{r}} \right)^4 a^2(t) [d\bar{r}^2 + \bar{r}^2(d\theta^2 + \sin^2\theta d\phi^2)] \quad (5.56)$$

for the exterior ($r > r_b$) matched solution of a generalised isothermal sphere of mass $m(\alpha)$ in an expanding FRW universe. Note that the solution is stated in isotropic coordinates. Here $a(t)$ is the scale factor of the standard cosmological solution and $m(\alpha)$ is defined by Eq. (5.54).

If one makes the substitution $\bar{r}_1 = a \cdot \bar{r}$, the line element in Eq. (5.56), at any particular instant t_1 , reduces to the Schwarzschild line element for small \bar{r} (isotropic coordinate). McVittie also showed that the transformation of the time-dependent metric in Eq. (5.56) into the static Schwarzschild field is independent of the moment in time at which the transformation is made in [161]. This proves that the embedding is valid for all times t .

To relate the interior generalised isothermal metric and the exterior metric, we give the transformation between the spherical polar radial coordinate r used in Eq. (5.34) and the isotropic coordinate \bar{r}_1 in Eq. (5.56):

$$r \equiv \bar{r}_1 \left(1 + \frac{m}{2\bar{r}_1} \right)^2, \quad (5.57)$$

$$\bar{r}_1 \equiv \frac{1}{2} \left[\sqrt{r^2 - 2mr} + (r - m) \right]. \quad (5.58)$$

It can then be shown that the interior and exterior metrics match at $r = r_b$, for a particular instant t_1 and that the matching is valid for all t in [151]. For a given value of $\alpha = \text{constant}$, the derivatives of the metric coefficients also match according to the junction conditions described by Bonnor and Vickers [16]. In the next section, we will discuss the matching of the metrics in a more rigorous manner.

At the beginning of this section we discussed the limits in space and time that the sequence of hybrid solutions has to satisfy. We now compare these constraints

to the corresponding limits of Eqs. (5.34) and (5.56). For vanishing α , the mass and the boundary radius of the isothermal sphere tend to zero and the metric is FRW on all scales. For small α (i.e. early evolutionary steps) the applicable hybrid metric has the generalised isothermal form for small r and is FRW for large r . For relatively large α (i.e. late evolutionary steps) the metric tends to the isothermal form on much larger scales. We therefore see that all limits of our hybrid solution in both time (discrete steps between static periods) and space agree with the limits required by physical arguments.

§5.5.2 The validity of the matching of the metric

We may ask more generally whether using the generalised isothermal sphere parameters in the Schwarzschild interior metric could lead to a problem in matching the FRW exterior. Mars[143] has shown that *the only static, spatially compact, vacuum region in a Friedman-Lemaitre spacetime must be a 2-sphere comoving with the cosmological flow and with the Schwarzschild-exterior geometry*. In our model, at the boundary between the Schwarzschild metric and the bounded isothermal sphere, there are no problems that arise from the energy momentum tensor. This is because at that boundary between the bounded isothermal sphere and the Schwarzschild exterior, the pressure P is zero. Therefore, there is no problem embedding the matched system of a bounded isothermal sphere and the Schwarzschild metric into the FRW metric, if the solution of the combined system is expanding.

Since the energy momentum tensor is not an issue in the matching, we can work out the intrinsic and extrinsic curvatures of the metric by matching on a hypersurface Σ , at a constant comoving radius, r . The smooth matching of the 2 spacetimes across a hypersurface Σ is guaranteed if the Darmois junction conditions are satisfied, i.e. if the first fundamental (intrinsic metrics) forms and second fundamental (extrinsic metrics) forms are calculated in terms of the coordinates on the hypersurface, and they are identical on both sides of the hypersurface. If both the first and second fundamental forms are continuous on Σ , then the matching is not piecewise i.e. it will match for all times rather than just at single instants. The Darmois junction conditions allow us to use different coordinate systems on both sides of the hypersurface. We adopt the procedure in [55] and have calculated explicitly the interior and the exterior metrics and they match on a 3-dimensional timelike tube and exhibit no curvature discontinuity for all times. In the process, we applied the procedure in [55] to check the conditions for matching the Schwarzschild-Tolman system and the FRW metric on a hypersurface Σ , where $r = r_0$ for the radial constant comoving coordinate in the FRW metric.

We recall the Schwarzschild-Tolman metric (bounded isothermal sphere interior

with a Schwarzschild exterior), which is written in coordinates (T, ρ, θ, ϕ) ,

$$ds^2 = - \left(1 - \frac{2M(\alpha)}{\rho}\right) dT^2 + \left(1 - \frac{2M(\alpha)}{\rho}\right)^{-1} d\rho^2 + \rho^2 d\theta^2 + \rho^2 \sin^2 \theta d\phi^2, \quad (5.59)$$

where

$$M(\alpha) = \frac{2\alpha}{4\alpha + (1 + \alpha)^2} r_b, \quad (5.60)$$

and r_b is a constant. The general FRW metric is given in Eq. (1.1).

The first fundamental form is the metric which the hypersurface Σ inherits from its spacetime in which it is imbedded:

$$\gamma_{ij} = g_{\mu\nu} \frac{\partial x^\mu}{\partial u^i} \frac{\partial x^\nu}{\partial u^j}, \quad (5.61)$$

where $u^i = (u^1, u^2, u^3) = (u, v, w)$ is the coordinate system defined on the hypersurface. Note that i, j denotes only the coordinates of the hypersurface of 3-dimensions while μ, ν denotes the coordinates of the 4-dimensional spacetime. The second fundamental form is defined by

$$\Omega_{ij} = (\Gamma_{\nu\lambda}^\mu n_\mu - \partial_\lambda n_\nu) \frac{\partial x^\nu}{\partial u^i} \frac{\partial x^\lambda}{\partial u^j}, \quad (5.62)$$

where n_μ is the unit normal to the hypersurface, Σ . Finally if Σ is given by the function $f[x^\mu(u^i)] = 0$, then n_μ can be calculated by:

$$n_\mu = - \frac{\partial_\mu f}{\sqrt{g^{\alpha\beta} \partial_\alpha f \partial_\beta f}} \quad (5.63)$$

We will denote the FRW and Schwarzschild-Tolman (ST) frames by the subscripts or brackets with F and S in our quantities.

We consider a spherical hypersurface Σ given by the function $f_F(x_F^\mu) = r - r_0 = 0$, where r_0 is constant.

For the FRW frame

$$x_F^t = t = u, \quad x_F^r = r = r_0, \quad x_F^\theta = \theta = v, \quad x_F^\phi = \phi = w, \quad (5.64)$$

and similarly for the ST frame,

$$x_S^t = T = T(u), \quad x_S^\rho = \rho = \rho(u), \quad x_S^\theta = \theta = v, \quad x_S^\phi = \phi = w. \quad (5.65)$$

The first matching condition $\gamma_{ij}(F) = \gamma_{ij}(S)$ gives

$$\left(1 - \frac{2M(\alpha)}{\rho}\right) \left(\frac{dT}{du}\right)^2 - \left(1 - \frac{2M(\alpha)}{\rho}\right)^{-1} \left(\frac{d\rho}{du}\right)^2 = 1, \quad (5.66)$$

$$a(t)^2 r_0^2 = \rho^2. \quad (5.67)$$

Next we calculate the second fundamental forms. The (outward pointing) unit normal in the FRW frame follows from (5.63), and since $f_F(x_F^\mu) = r - r_0 = 0$, we get $n_\mu(F) = \delta^r_\mu n_r(F)$.

For the unit normal in the Schwarzschild case, we cannot derive the result directly from Eq. (5.63), but we use the result that $n_\mu(S)$ must satisfy the following conditions:

$$n^\mu(F)n_\mu(F) = n^\mu(S)n_\mu(S) = 1, \quad (5.68)$$

$$n_\mu(S)\frac{\partial x_S^\mu}{\partial u^i} = 0, \quad (5.69)$$

where the second condition comes from the fact that partial differentiation of $f_S[x_S^i(u^i)] = 0$ with respect to u^i . With these conditions we get the following equations in component form:

$$n_\theta(S) = n_\phi(S) = 0, \quad (5.70)$$

$$n_T(S)\frac{dT}{du} + n_\rho(S)\frac{d\rho}{du} = 0 \quad (5.71)$$

$$\left(1 - \frac{2M(\alpha)}{\rho}\right)^{-1} n_T^2(S) - \left(1 - \frac{2M(\alpha)}{\rho}\right) n_\rho^2(S) = -1. \quad (5.72)$$

Comparing the last equation with Eq. (5.66), we derive $n_\mu(S)$ to be

$$n_\mu(S) = \left(-\frac{d\rho}{du}, -\frac{dT}{du}, 0, 0\right). \quad (5.73)$$

We can compute Ω from Eq. (5.62) to be

$$\Omega_{ij} = -\frac{1}{2} \frac{1}{\sqrt{g_{rr}}} \partial_r g_{ij}, \quad (5.74)$$

and this equation is valid for any coordinate hypersurface $r = r_0 = \text{constant}$, in an orthogonal coordinate system and parametrised by $x^i = u^i$.

From Eq. (5.69), we obtain the following equation by differentiating with respect to u^i ,

$$\partial_\mu n_\nu(S) \frac{\partial x_S^\mu}{\partial u^i} \frac{\partial x_S^\nu}{\partial u^j} = -n_\mu \frac{\partial^2 x_S^\mu}{\partial u^i \partial u^j}, \quad (5.75)$$

and we get

$$\Omega_{ij}(S) = \Gamma_{\nu\lambda}^\mu n_\mu \frac{\partial x_S^\nu}{\partial u^i} \frac{\partial x_S^\lambda}{\partial u^j} + n_\mu \frac{\partial^2 x_S^\mu}{\partial u^i \partial u^j}. \quad (5.76)$$

We know that $\Omega_{ij}(S) = \Omega_{ij}(F) = 0$ for $i \neq j$, and for the remaining diagonal components, we have $\Omega_{ij}(S) = \Omega_{ij}(F)$ on Σ , and we get the following three

differential equations:

$$\Omega_{uu}(S) \equiv \Omega_{uu}(F) = \Gamma_{TT}^\rho n_\rho \left(\frac{dT}{du} \right)^2 + \Gamma_{\rho\rho}^\rho n_\rho \left(\frac{d\rho}{du} \right)^2 + 2\Gamma_{T\rho}^T n_T \frac{dT}{du} \frac{d\rho}{du} + n_T \frac{d^2T}{du^2} + n_\rho \frac{d^2\rho}{du^2} = 0, \quad (5.77)$$

$$\Omega_{vv}(S) \equiv \Omega_{vv}(F) = \zeta |a(t)| r_0 = \Gamma_{\theta\theta}^\rho(S) n_\rho, \quad (5.78)$$

$$\Omega_{ww}(S) \equiv \Omega_{ww}(F) = \zeta |a(t)| r_0 \sin^2 \theta = \Gamma_{\phi\phi}^\rho(S) n_\rho, \quad (5.79)$$

where in the Schwarzschild frame, the Christoffel connections are

$$\Gamma_{T\rho}^T = -\Gamma_{\rho\rho}^\rho = \frac{M(\alpha)}{\rho(\rho - 2M(\alpha))}, \quad (5.80)$$

$$\Gamma_{TT}^\rho = \frac{(\rho - 2M(\alpha))M(\alpha)}{\rho^2}, \quad (5.81)$$

$$\Gamma_{\theta\theta}^\rho = -(\rho - 2M), \quad (5.82)$$

$$\Gamma_{\phi\phi}^\rho = \Gamma_{\theta\theta}^\rho \sin^2 \theta, \quad (5.83)$$

and $\zeta \equiv \sqrt{1 - kr_0^2}$. Note that this will also prove that the matching is continuous for the cases where $k \neq 0$, i.e. open and closed cases as well. In retrospect, if we follow the procedure of Hogan[89], we will also obtain the generalization of the Schwarzschild-Tolman metric with the open and closed FRW universes, but their forms will be complicated. By the same physical reasons mentioned in the discussion of the infinite isothermal sphere solution, the open and closed FRW universes would deter the phase transition from happening.

Using Eqs. (5.78), (5.67) and (5.66), we get

$$\frac{dT}{du} = \frac{\zeta \rho}{\rho - 2M(\alpha)} \quad (5.84)$$

$$\left(\frac{d\rho}{du} \right)^2 = \zeta^2 - \left(\frac{\rho - 2M(\alpha)}{\rho} \right). \quad (5.85)$$

Differentiating Eqs. (5.84) and (5.85) gives

$$\frac{d^2T}{du^2} = -\zeta \frac{2M(\alpha)}{(\rho - 2M(\alpha))^2} \frac{d\rho}{du} \quad (5.86)$$

$$\frac{d^2\rho}{du^2} = -\frac{M(\alpha)}{\rho}. \quad (5.87)$$

Because $M(\alpha) = \text{constant}$ for values of α , we can substitute Eqs. (5.84) and (5.85) into (5.77) to show that Eqs. (5.77), (5.78) and (5.79) are consistent. From these solutions, one would realise that both the first and second fundamental forms are continuous on Σ , hence the matching is not piecewise, i.e. it will match for all times rather than just at single instants.

§5.6 Evolution of the Isothermal Universe - A Sequence of Hybrid Solutions

Thus far, we have derived the hybrid metric to describe a generalised isothermal sphere embedded via a “Schwarzschild membrane” in the expanding Einstein-de Sitter universe at any particular cosmic time. Now we consider briefly how such a hybrid model might form and evolve.

Greater than average densities in any volume of an Einstein-de Sitter universe produce local gravitational clustering timescales shorter than the current expansion timescale. This facilitates the growth and merging of a small number of large clusters within an apparent or particle horizon. Collective relaxation [168] could thermalize the velocities of the galaxies on a timescale $\sim (G\bar{\rho})^{-\frac{1}{2}}$ where $\bar{\rho}$ is the average density in a volume containing the merging clusters. Eventually, this would lead to an approximately isothermal virialized cluster. This process would continue indefinitely as other great clusters appear within the horizon and merge.

During periods when one massive isothermal cluster dominates, our idealised hybrid metric would apply. More generally, a much more complicated metric would be needed to describe the periods when two or more great clusters dominate a horizon. However, we may envisage our hybrid metric applying at intervals, for particular values of α and A when one cluster dominates. “Snapshots” of the long term evolution would then be characterized by a discrete sequence of increasing values of α as virialization progresses, and consequently by decreasing values of A , as seen in Fig. 5.4.

How long will it take an isothermal universe to form? We can estimate this timescale and compare it to timescales for several possible competing effects. The timescale for the formation of the isothermal sphere can be estimated from the evolution of N -body galaxy clustering. For clustering in an adiabatically expanding universe this gives [169]

$$a(t) = a_0 \frac{b^{\frac{1}{8}}}{(1-b)^{\frac{7}{8}}}, \quad (5.88)$$

where a is the time-dependent scale factor of the universe and b is defined as the average ratio of the gravitational correlation energy, W , to twice the kinetic energy, K , of peculiar velocities in an ensemble of galaxies. Inverting this gives the time-dependence of $b(t)$ within the limits $b(0) = 0$ (no interaction, perfect gas) and $b(\infty) = 1$ (complete virialization, isothermal). The transition to the isothermal state therefore corresponds to a b close to unity, where the universe is dominated by voids and a small number of very large clusters. We define τ as the time after which the void probability of the universe becomes greater than 0.5. This describes the timescale required for an approximately isothermal cluster to grow to cosmologically significant size. From the galaxy distribution function in

[169], we get the condition

$$e^{-\bar{N}(1-b)} \geq 0.5, \quad (5.89)$$

where \bar{N} is the total number of average mass galaxies in the observable universe. If we assume $\bar{N} \approx 10^{10}$, this allows us to define the condition for transition to the isothermal state as $b_c = 1 - 10^{-10}$. Hence, we find the scale factor $a_c(\tau) = 10^8 a_0$, where a_0 is the present Hubble radius. For an Einstein-de Sitter expansion with $a(t) = t^{\frac{2}{3}}$ this corresponds to

$$t_{exp} \approx 10^{12} t_0 = 3 \times 10^{29} \text{ seconds}, \quad (5.90)$$

where we used an estimate for the present Hubble time $t_0 = 10^{17}$ seconds. Hence, the universe would take approximately 10^{29} seconds to form the isothermal sphere.

The solution permits a sequence of generalised isothermal universes whose radii grow with each step according to

$$r_b = \left(\frac{\alpha^2 C}{D} \right)^{\frac{1+\alpha}{2(1-\alpha)}} = F(\alpha) A^{-\frac{1+\alpha}{4\alpha}}, \quad (5.91)$$

where

$$F(\alpha) \equiv \left(\frac{\alpha^2}{E(\alpha)} \right)^{\frac{1+\alpha}{2(1-\alpha)}} \quad (5.92)$$

and $E(\alpha)$ is defined by Eq. (5.51). The values of r_b increase as α and A change their values with time (discrete steps: for each stage α and A are constant; see Fig. 5.4). We explore next how this constrains the *time-dependence* through discrete steps of the sequence of α and $A = C^2$ values.

We can normalize our metric by finding approximate limits on the sequence of A . These limits can be found by the following approximate argument: $r_b = 0$ at early times requires $\lim_{t \rightarrow 0} A_t \geq 1$ (see Fig. 5.4). We next consider the limit for late times. From the previous discussion we can set $r_b \sim a_c = 10^8 a_0 = O(10^{36}) \text{cm}$ as an approximate scale of the isothermal universe at late times ($t = t_c$).

This allows us to use Eq. (5.91) and find A_{t_c} at $\alpha = (2/3)$,

$$A_{t_c} \sim O(10^{-58}) \text{ cm}^{-\frac{8}{5}}, \quad (5.93)$$

which gives an approximate limit for the time evolution of the sequence of the constants A_t . The proposed time evolution of A_t therefore goes as follows: A starts off at $t = 0$ with $A_0 \geq 1$. At t_c (corresponding to $\alpha(t_c) = 2/3$), $A_{t_c} \sim O(10^{-58}) \text{ cm}^{-\frac{8}{5}}$. For $t > t_c$, A_t decreases further, so that $\lim_{t \rightarrow \infty} A_t \rightarrow 0$ and $\lim_{t \rightarrow \infty} r_b(t) \rightarrow \infty$, meaning that the isothermal sphere grows indefinitely. Fig. 5.4 should therefore be interpreted as a map of the future scale of the isothermal universe for changes in α and A . Note, however, that our present state of the

universe is still very close to $\alpha = 0$, $r_b = 0$. As the universe evolves in the far future, changes of α and A correspond to an increasing scale r_b of the isothermal part of the universe. This evolution as a sequence of quasi-static steps can be characterized by discrete points on the surface of Fig. 5.4.

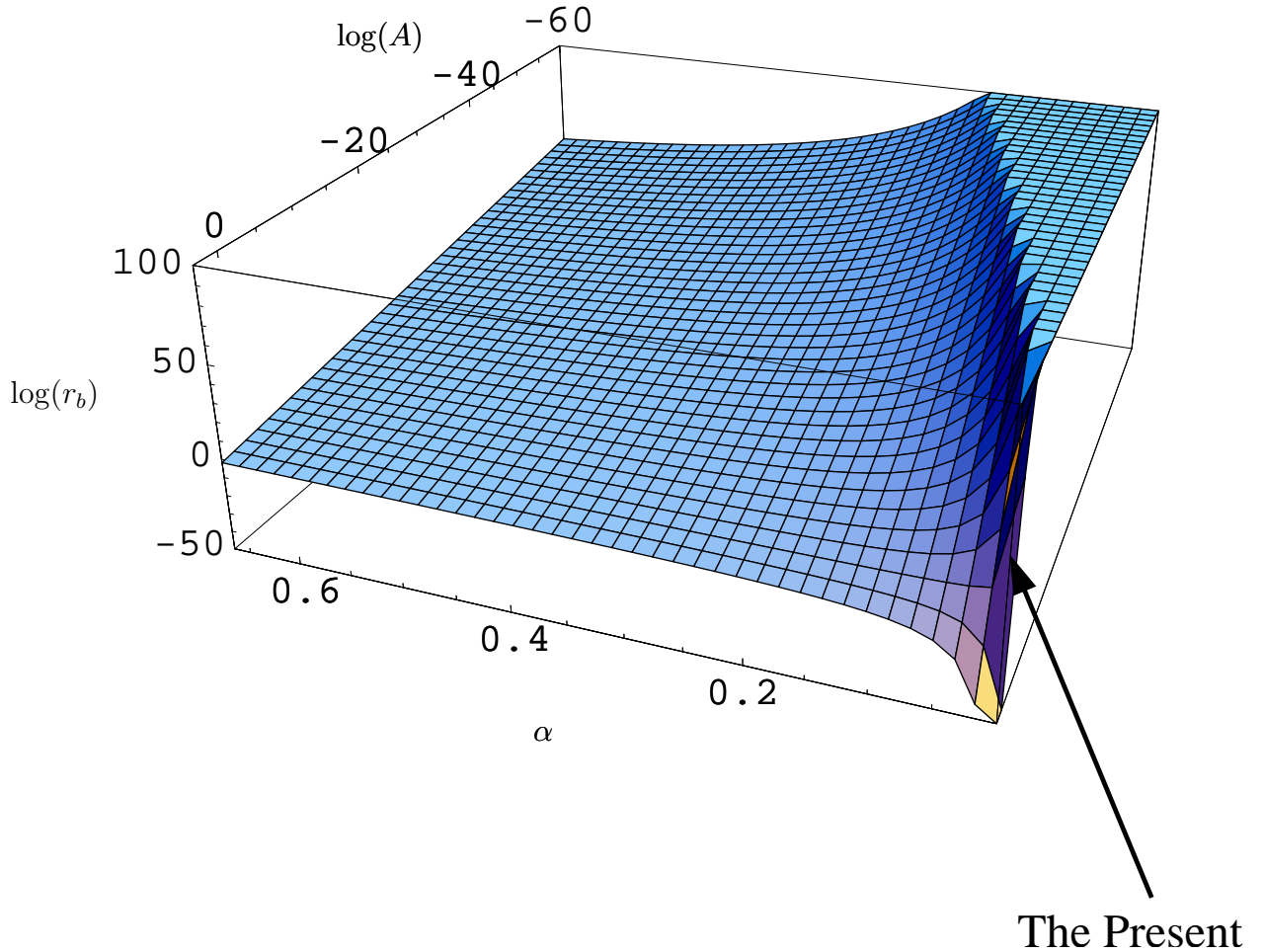


Figure 5.4: Surface plot of r_b – the model’s future laid out before us: It is interpreted as a map of the future scale of the generalised isothermal universe for particular values of α and A . The radius of the generalised isothermal sphere, r_b , is in units of centimeters, A is measured in $[cm^{-\frac{4\alpha}{1+\alpha}}]$ and α is dimensionless. r_b and A are plotted on a logarithmic scale. The hypothetical present size of the isothermal sphere is taken to be $r_b \sim 10^{25}$ cm (the size of the Coma cluster).

There are competing effects, which could inhibit the formation of the generalised isothermal state, namely, (a) the conversion of all the matter into gravita-

tional radiation, (b) Hawking radiation and (c) proton decay and (d) a positive cosmological constant.

Next we estimate the amount of gravitational radiation produced by the interaction between a pair of galaxies. Using the standard quadrupole formula given by Landau and Lifschitz [114] and making reasonable estimates for masses and mean distances of galaxy binaries we find that it would require about 10^{51} seconds for the universe to convert all its mass into gravitational radiation. This is $10^{22}t_{exp}$. The mass which could be evaporated by Hawking radiation of small black holes in the time needed to reach the isothermal phase transition is calculated as 10^{28} grams which is equal to the mass of the Earth and can therefore safely be neglected. The isothermal state is therefore reached long before Hawking radiation could have influenced the mass content of our universe. Some grand unified theories suggest the instability of the proton. Experimentally, however, it was found that the lower limit for the half-life of the proton must be greater than 10^{33} seconds (if not infinity). That leaves us with only one more possibility, a positive non-zero cosmological constant. If we assume $\Omega_\Lambda = 0.7$ in standard big bang cosmology, the cosmological constant would become dominant after the radius of the universe increases to about three times its current value. This is significantly faster than the timescale of the formation of the isothermal sphere. It suggests a possible role for Λ , as a buffer in preventing our universe from undergoing a possible phase transition.

§5.7 Discussion

We have presented a relativistic approach to describe the evolution of the universe from an Einstein-de Sitter expansion with no centre to an isothermal sphere with a centre. We have shown how this changing symmetry of the universe can be incorporated into general relativity. This demonstrates that general relativity permits a changing symmetry on a global scale, a nontrivial result.

Our solution required a Schwarzschild metric to act as an intermediate background to match the static generalised isothermal metric to the FRW metric of the expanding universe. The necessity for this Schwarzschild intermediary can be understood both intuitively and on a formal mathematical basis. The Schwarzschild metric acts as a kind of membrane linking a static space-time region to an expanding space-time. In [68, 143, 144], the general matching of two spherically symmetric spacetimes was investigated in detail. Their results provide a formal basis for understanding the role of the ‘‘Schwarzschild membrane’’. Applying the general matching conditions derived in their paper to the expanding, centrally isothermal universe proves that a direct matching without the ‘‘Schwarzschild membrane’’ between the generalised isothermal and the FRW spacetimes is not possible. An

extension of this idea of a “Schwarzschild membrane” to general spherically symmetric spacetimes other than the isothermal metric might be possible and have interesting implications.

In our hybrid model the field equations are solved for constant pressure/density ratio, α and, as stated, the solution therefore does not incorporate a time-dependent α . We therefore introduced a “sequence of quasi-static stages”. We envisage the universe evolving through a sequence of models with increasing α as its central cluster grows in size and the isothermal approximation becomes better for larger regions. The main physical argument for this is that the local clustering timescale in a nonlinear positive density inhomogeneity in an Einstein-de Sitter model is shorter than the expansion timescale since the average local density is greater than the average global density. Our metric only describes those phases of the evolving universe when it is dominated by one relaxed, static isothermal cluster. As a second large cluster enters the horizon our description breaks down and only applies again after the system has relaxed to a larger static cluster with new values of α and the boundary radius of the cluster. This leads to a sequence of discrete changes which characterize the evolving model. Our solution therefore describes only discrete steps between static intervals and not continuous changes in time. Finding a continuous description remains a problem for the future.

Part IV

Epilogue

Chapter 6

Discussion

"After a lifetime of crabwise thinking, I have gradually become aware of the towering intellectual structure of the world, One article of faith I have about it is that, whatever the end may be for each of us, it cannot be a bad one."

- **Fred Hoyle**

"I do not know what I may appear to the world. But to myself I seem to have been like a boy playing on the seashore, and enjoying myself in now and then finding a smoother pebble, or a prettier shell than ordinary, while the great ocean of truth lay all undiscovered before me."

- **Sir Issac Newton**

From the Beginning to the End

In the epilogue, we summarize the main results of this thesis and discuss possible future directions. We began this thesis with a modest aim to study possible and viable alternatives to the standard inflationary big-bang cosmology, in the hope that we can understand these alternative cosmologies better and search for phenomenological effects if possible. As such, we have explored three interesting alternative themes, namely, spin-torsion theories, extra dimensions and changing global symmetry.

Beginning from chapter 2 for spin-torsion theories, we found new massive, cosmological solutions for the Dirac field coupled self-consistently to gravity with a cosmological constant in a $K = 0$ (flat) universe. In addition to the generalized particle and anti-particle solutions found in [35] with a cosmological constant, we discovered another anti-particle solution which has interesting implications. All these solutions have the presence of a particle horizon but they do not possess

an inflationary phase. Although these spin-torsion solutions are interesting, they are shown not to be viable alternatives to the standard scalar field inflation. It has been shown in [2, 152] that the vacuum polarization terms in the framework of Einstein-Dirac equations would provide an alternative to standard inflationary models. Hence the next step is to reconsider the model with vacuum polarisation terms.

Next, we come to the theme of theories with large extra dimensions. We concentrated on a sector of the braneworld cosmology in chapters 3 and 4, particularly on the study of linear perturbations using the (1+3)-covariant approach and the possible effects on the CMB from the extra dimensions. In chapter 3, we set up the (1+3)-covariant formalism for the study of cosmological perturbations, and provided a complete set of frame-independent equations for the total matter variables, and a partial set of equations for the non-local variables which arise from the projection of the Weyl tensor in the bulk. We also derived the covariant form of the line of sight solution for the CMB temperature anisotropies in braneworld cosmologies. However, our setup still lacks the propagation equation for the non-local anisotropic stress, which appears to be an important ingredient in the study of CMB anisotropies.

In the following chapter, we studied the scalar and tensor perturbations and their implications on the CMB anisotropies. For the scalar perturbations, we provide the equations for the total matter variables with equations for the independent constituents in a cold dark matter cosmology, and supplement solutions in the high and low-energy radiation-dominated phase under the assumption that both the dark energy and non-local anisotropic stress vanish. These solutions reveal an additional pair of non-local isocurvature velocity and density modes which emerge from the two additional non-local degrees of freedom. These mode solutions would be useful in setting up initial conditions for numerical codes (for example, CAMB [126] and CMBFAST [175]) aimed at exploring the effect of braneworld corrections on the cosmic microwave background (CMB) power spectrum. For the tensor perturbations, we set out the framework of a program to compute the tensor anisotropies in the CMB that are generated in braneworld models. In the simplest approximation, we show the braneworld imprint as a correction to the power spectra for standard temperature and polarization anisotropies and similarly show that the tensor anisotropies are also insensitive to the high energy effects.

In principle, future observations can constrain the KK parameter ζ , which controls the generation of 5D modes within our simplified local approximation, Eq. (4.151). The other braneworld parameter λ , the brane tension, is not constrained within our approximation. In practice, the tensor power spectra have not been measured, and the prospect of useful data is still some way off. What is more important is the theoretical task of improving on the simplified local approxima-

tion we have introduced. This approximation has allowed us to encode aspects of the qualitative features of braneworld tensor anisotropies, which we expect to survive in modified form within more realistic approximations. However, a proper understanding of braneworld effects must incorporate the nonlocal nature of the KK graviton modes, as reflected in the general form of Eq. (4.150). A possible direction is to investigate the tensor perturbations in the bulk and determine how it would actually affect the tensor power spectrum.

It is also necessary to investigate the scalar anisotropies, which have a dominant contribution to the measured power spectra. There are a few possible directions for the scalar anisotropies. First, there is the possibility of exciting these nonlocal velocity and density isocurvature modes. Another possibility comes from the fact that the dark radiation, \mathcal{U} is not necessarily zero. It has been shown by Langlois et al [119] that the dark radiation, \mathcal{U}_0 is asymptotically a constant upon reaching the low energy regime, while it is time-dependent as $\mathcal{U} \sim a^4$ at high energies. Hence it would be natural to extend the mode solutions we found for cases $\mathcal{U} \neq 0$ and work out the scalar anisotropies. All these possibilities for both scalar and tensor anisotropies may reveal new braneworld imprints that are more amenable to observational testing.

Finally we come to the last theme of changing global symmetry. In chapter 5, we constructed a possible relativistic description of how an Einstein-de Sitter expansion with no centre would evolve to an isothermal sphere with a centre. We have shown how this changing symmetry of the universe might possibly lead to a phase transition in the future. This construction demonstrates that general relativity permits a changing symmetry on a global scale, a nontrivial result.

The largest galaxy cluster in a flat Einstein-de Sitter universe may grow indefinitely to encompass most of space after an extremely long time. We derive a general relativistic metric for a very large, bounded nearly isothermal cluster of galaxies which is embedded in such a universe. The embedding is done by means of a ‘‘Schwarzschild membrane’’. Pressure is important, unlike previous Tolman-Bondi models of inhomogeneities. The cluster’s expansion, represented by a sequence of models, alters the average global symmetry of an increasing volume of space-time. Initially the metric is homogeneous and isotropic, having translational and rotational symmetry around every point. As the metric evolves, it eventually loses its translational symmetry throughout larger regions and retains rotational symmetry around only one point: the centre of the cluster becomes the centre of the universe. Our sequence of hybrid models transforms between the Einstein-de Sitter and the isothermal cluster limits and illustrates how a changing equation of state of matter can alter the global symmetry of space-time.

Gravitational clustering creates a cosmologically significant pressure, which can feed back into the spacetime structure of the universe. This induces a dynamical

symmetry breaking effected by the redistribution of matter. Is this transition between distinct symmetry states of the universe an actual phase transition? The answer depends on the timescale and the definition of a phase transition. The experimental study of numerous condensed matter systems has demonstrated that transitions, which show a macroscopic discontinuity, might fundamentally be continuous when examined on a microscopic scale (e.g. a ferromagnetic phase transition). This may be analogous to the transition in the isothermal universe in which gravitational clustering provides the continuous, “microscopic” description of what is “macroscopically” a discontinuous phase transition when viewed on a long enough timescale. The different symmetries of the universe simply arise as different limits of the sequence of hybrid solutions. It has also suggested a new role for the cosmological constant, that is to deter the Universe from going into a phase transition in the future.

This possible end of our Universe is conditional on the extremely long term stability of the matter. If the matter decays into radiation before the isothermal metric develops, the expansion can continue and possibly accelerate. Since matter can be converted into radiation in the isothermal universe, the equation of state would change and produce another possible phase transition.

Of course, it is speculative to conceive the end of the simple Einstein-de Sitter Universe without a cosmological constant, just as it is difficult to conceive the beginning of our Universe that might be endowed with spin-torsion or extra-dimensions. It would be appropriate to conclude this thesis along the same thought as [171] that perhaps T. S. Eliot had some intuition of this idea in East Coker, where he said, “*In my beginning is my end.*”

Appendix

Appendix A

Conventions, Units, Sign Manifesto and Table of Symbols

In this thesis, we would like to follow the spirit in [109] and [127] to state the conventions used and provide (i) the units for the conversion factors and fundamental constants and (ii) cosmological parameters, the sign manifesto for the covariant approach (which is useful for the modifying the CAMB code) and the table of symbols adopted throughout this thesis.

§A.1 Conventions

We would like to follow the conventions of the metric signature $(-, +, +, +)$ for Chapters 1,3,4 and 5 and $(+, -, -, -)$ for Chapter 2, and we would adopt the choice of natural units, i.e. we set the fundamental constants $\hbar = c = k_B = 1$, and there is one fundamental dimension, energy, $[E]$ such that

$$[E] = [M] = [T_E] = [L] = [T]^{-1} \quad (\text{A.1})$$

where $[M]$, $[T_E]$, $[L]$ and $[T]$ are the dimensions of mass, temperature, length and time respectively.

The unit of energy is taken to be a $\text{GeV} = 10^3 \text{ MeV} = 10^6 \text{ keV} = 10^9 \text{ eV}$. For the case of braneworlds, the more popular unit for energy is in the TeV scale i.e. $\text{TeV} = 10^3 \text{ GeV}$.

§A.2 Units

§A.2.1 Conversion Factors

Temperature:	$1 \text{ GeV} = 1.1605 \times 10^{13} \text{ K}$
Mass:	$1 \text{ GeV} = 1.7827 \times 10^{-27} \text{ kg}$
Length:	$1 \text{ GeV}^{-1} = 1.9733 \times 10^{-16} \text{ m}$
Time:	$1 \text{ GeV}^{-1} = 6.5822 \times 10^{-25} \text{ s}$
Megaparsec:	$1 \text{ Mpc} = 10^6 \text{ pc} = 3.0856 \times 10^{22} \text{ m} = 1.5637 \times 10^{38} \text{ GeV}^{-1}$

§A.2.2 Fundamental Constants

Planck's constant:	$\hbar = 6.6261 \times 10^{-34} \text{ m}^2 \text{ kg s}^{-1}$
Speed of light:	$c = 29972458 \text{ m s}^{-1}$
Boltzmann's constant:	$k_B = 1.3807 \times 10^{-23} \text{ J K}^{-1}$
Newton's constant:	$G = 6.672 \times 10^{-11} \text{ kg m}^3 \text{ s}^{-2} \equiv m_{Pl}^{-2}$
Planck energy:	$m_{Pl} \equiv \sqrt{\frac{\hbar c^5}{G}} = 1.211 \times 10^{19} \text{ GeV}$
Planck mass:	$m_{Pl} \equiv \sqrt{\frac{\hbar c}{G}} = 2.1768 \times 10^{-8} \text{ kg}$
Planck time:	$t_{Pl} \equiv \sqrt{\frac{\hbar G}{c^5}} = 5.3904 \times 10^{-44} \text{ s}$
Planck length:	$l_{Pl} \equiv \sqrt{\frac{\hbar G}{c^3}} = 1.6160 \times 10^{-35} \text{ m}$
Electron mass:	$m_e = 0.5110 \text{ MeV}$
Neutron mass:	$m_n = 939.566 \text{ MeV}$
Proton mass:	$m_p = 938.272 \text{ MeV}$
Thomas cross section:	$\sigma_T = 6.652 \times 10^{-29} \text{ m}^2$
Solar mass	$M_\odot = 2 \times 10^{30} \text{ kg}$

§A.3 Physical Parameters

§A.3.1 Cosmological parameters

Hubble constant:	$H_0 = 100 h \text{ km s}^{-1} \text{ Mpc}^{-1}$
Present Hubble distance:	$cH_0^{-1} = 2998 h^{-1} \text{ Mpc}$
Present Hubble time:	$H_0^{-1} = 9.78 \times 10^6 h^{-1} \text{ yr}$
Present critical density:	$\rho_{c,0} = 1.88h^2 \times 10^{-32} \text{ kg m}^{-3}$

§A.4 Sign Manifesto

In order to incorporate the equations in the CAMB code, we need to re-write the equations in the convention $(+, -, -, -)$. To do this, we adopt the convention for the change of signs in [31] and expand the range of quantities in this thesis, for the following quantities:

$$\begin{aligned}
 g_{ab} &\rightarrow -g_{ab}, & \nabla_a &\rightarrow \nabla_a & R_{abcd} &\rightarrow R_{abcd} & R_{ab} &\rightarrow R_{ab}, \\
 R &\rightarrow -R, & h_{ab} &\rightarrow -h_{ab}, & \mathcal{R} &\rightarrow -\mathcal{R}, & D_a &\rightarrow -D_a, \\
 u_a &\rightarrow -u_a, & q_a &\rightarrow -q_a, & A_a &\rightarrow -A_a, & \sigma_{ab} &\rightarrow -\sigma_{ab} \\
 \rho &\rightarrow \rho, & P &\rightarrow P, & \Theta &\rightarrow \Theta, & \mathcal{U} &\rightarrow \mathcal{U}, \\
 \Delta_a &\rightarrow -\Delta_a, & \mathcal{Z}_a &\rightarrow -\mathcal{Z}_a, & \eta_a &\rightarrow \eta_a, & \pi_{ab} &\rightarrow \pi_{ab}, \\
 \Upsilon_a &\rightarrow -\Upsilon_a, & \mathcal{Q}_a &\rightarrow -\mathcal{Q}_a, & \mathcal{P}_{ab} &\rightarrow \mathcal{P}_{ab}.
 \end{aligned} \tag{A.2}$$

The above sign manifesto would help to translate equations from the signature of $(-, +, +, +)$ to the other signature $(+, -, -, -)$.

§A.5 Table of Symbols

For all chapters using General Relativity

Symbol	Meaning of Symbol
$a(t)$	Scale Factor of the Universe with respect to cosmic time, t
$a(\tau)$	Scale Factor of the Universe with respect to conformal time, τ
H	Hubble parameter with respect to cosmic time, t
\mathcal{H}	Hubble parameter with respect to conformal time, τ
u^a	4-velocity/tangent vector
∇_a	Covariant derivative

D_a	Projected (spatial) covariant derivative
Λ	Cosmological Constant
λ	Tension of the brane
R_{abcd}	Riemann tensor
R_{ab}	Ricci tensor
R	Ricci scalar
\mathcal{R}	3-curvature scalar in general relativity
K	Constant of curvature in general relativity
G_{ab}	Einstein tensor
T_{ab}	Energy-momentum tensor
ρ	Density of a fluid (or generally energy density)
Δ_a	Spatial gradient in the density (or energy density) of the fluid
P	Pressure of a fluid
q_a	Energy flux of a fluid
π_{ab}	Local anisotropic stress/pressure
η_a	Spatial gradient of the 3-curvature
E_{ab}	Gravito-electric part of the Weyl tensor on the brane
H_{ab}	Gravito-magnetic part of the Weyl tensor on the brane
ω_{ab}	Vorticity tensor
σ_{ab}	Shear
Θ	Comoving expansion
\mathcal{Z}_a	Spatial gradient of the comoving expansion
A_a	Acceleration
Φ	Gravitational Potential
c_s	Adiabatic sound speed
n_e	Electron density

σ_T	Thomson cross section
------------	-----------------------

Brane Worlds

Symbol	Meaning of Symbol
S_{ab}	Symmetric tensor which contains the local quadratic energy corrections from the bulk to brane
\mathcal{E}_{ab}	Symmetric projection of the bulk (5D)-Weyl tensor
\mathcal{U}	Non-local energy density projected from bulk to brane
Υ_a	Spatial gradient in non-local energy from bulk to brane
Q_a	Non-local energy flux projected from bulk to brane
\mathcal{P}_{ab}	Non-local anisotropic stress projected from bulk to brane

For the chapter using Gauge Theory of Gravity

Symbol	Meaning of Symbol
γ_μ	Dirac vectors in Spacetime Algebra (STA)
\mathcal{I}	Pseudoscalar
A_r	Grade- r multivector
∇	Vector derivative
$\bar{h}(a)$	Position gauge field
$\Omega(a)$	Rotation gauge field
\mathcal{D}	Covariant derivative with respect to a multivector

ψ	Spinor in GTG*
$\mathcal{R}(a \wedge b)$	Covariant Riemann tensor in GTG
$\mathcal{R}(a)$	Covariant Ricci tensor in GTG
$\mathcal{G}(a)$	Covariant Einstein tensor in GTG
$\mathcal{T}(a)$	Covariant energy momentum tensor in GTG
$\mathcal{S}(a)$	Covariant spin torsion trivector

*Gauge Theory of Gravity

Appendix B

Identities in Geometric Algebra

In this appendix, we would like to summarize some of the important identities in geometric algebra. A more detailed exposition of the geometric algebra formalism is given in Hestenes et al[85, 86, 87, 88] and Lasenby, Doran and Gull in [121].

§B.1 Multivectors

Let A and B be multivectors of grade r and s , \cdot be the interior product, \wedge be the exterior product and \times be the commutator product, where these operations are defined in Eqs. (2.2), (2.3) and (2.4) respectively in chapter 2, then the following identities hold:

$$A = \langle A \rangle_0 + \langle A \rangle_1 + \dots = \sum_r \langle A \rangle_r, \quad (\text{B.1})$$

$$A_r B_s = \langle A_r B_s \rangle_{|r-s|} + \langle A_r B_s \rangle_{|r-s|+2} + \dots + \langle A_r B_s \rangle_{|r+s|}, \quad (\text{B.2})$$

$$A_r \cdot \lambda = 0, \quad (\text{B.3})$$

$$\langle AB \rangle = \langle BA \rangle, \quad (\text{B.4})$$

$$A_r \cdot (B_s \cdot C_t) = (A_r \wedge B_s) \cdot C_t \quad (\text{for } r + s \leq t \text{ and } r, s > 0), \quad (\text{B.5})$$

$$A_r \cdot (B_s \cdot C_t) = (A_r \cdot B_s) \cdot C_t \quad (\text{for } r + t \leq s), \quad (\text{B.6})$$

$$A \times (B \times C) + C \times (A \times B) + B \times (C \times A) = 0. \quad (\text{B.7})$$

With the pseudoscalar, \mathcal{I} , we have the following identities,

$$A_r \cdot (B_s \mathcal{I}) = A_r \wedge B_s \mathcal{I} \quad (r + s \leq n), \quad (\text{B.8})$$

$$A_r \wedge (B_s \mathcal{I}) = A_r \cdot B_s \mathcal{I} \quad (r \leq s). \quad (\text{B.9})$$

We now specialize to the case for the vector and bivector cases. Let $\{a, b, c\}$ be a set of vectors and $\{A, B, C\}$ be a set of bivectors, and the following identities will hold:

$$a \cdot (b \wedge c) = a \cdot bc - a \cdot cb, \quad (\text{B.10})$$

$$(a \wedge b) \cdot (c \wedge d) = a \cdot db \cdot c - a \cdot cb \cdot d, \quad (\text{B.11})$$

$$a \cdot (b \cdot B) = (a \wedge b) \cdot B, \quad (\text{B.12})$$

$$(a \wedge b) \times (c \wedge d) = b \cdot ca \wedge d - a \cdot cb \wedge d + a \cdot db \wedge c - b \cdot da \wedge c, \quad (\text{B.13})$$

$$(a \wedge b) \times B = (a \cdot B) \wedge b + a \wedge (b \cdot B), \quad (\text{B.14})$$

$$BC = B \cdot C + B \times C + B \wedge C, \quad (\text{B.15})$$

$$CB = B \cdot C - B \times C + B \wedge C, \quad (\text{B.16})$$

$$B \times A_r = \langle B \times A_r \rangle_r, \quad (\text{B.17})$$

$$A \times (BC) = A \times B C + B A \times C. \quad (\text{B.18})$$

§B.2 Geometric Calculus

Let F be an arbitrary function of some multivector argument X , such that $F = F(X)$. The derivative of F with respect to X in the A -direction is defined to be

$$A * \partial_X F(X) = \lim_{x \rightarrow 0} \frac{F(X + xA) - F(X)}{x} \quad (\text{B.19})$$

where we define the multivector derivative ∂_X to be

$$\partial_X \equiv \sum_{i < \dots < j} e^i \wedge \dots \wedge e^j (e_j \wedge \dots \wedge e_i) * \partial_X \quad (\text{B.20})$$

Most of the properties of the multivector derivative follow from the result

$$\partial_X \langle XA \rangle = P_X(A) \quad (\text{B.21})$$

where $P_X(A)$ is the projection of the multivector A onto the graded element contained in X . The multivector derivative acts on the next object to its right unless brackets are present. Denoting the multivector which the derivative acts, we can write Leibniz rule in the form:

$$\partial_X(AB) = \dot{\partial}_X \dot{A}B + \dot{\partial}_X A \dot{B} \quad (\text{B.22})$$

The derivative with respect to the vector a , ∂_a is used to perform linear algebra

operations. The following identities are obtained as follows:

$$\partial_a \dot{b} = b, \quad (\text{B.23})$$

$$\partial_a \dot{a} = n, \quad (\text{B.24})$$

$$\partial_a \wedge a = 0, \quad (\text{B.25})$$

$$\partial_a a = n, \quad (\text{B.26})$$

$$\partial_a a^2 = 2a, \quad (\text{B.27})$$

$$(B \cdot \partial_a) \wedge a = 2B, \quad (\text{B.28})$$

$$\partial_a \wedge \partial_b (b \wedge a) \cdot B = 2B, \quad (\text{B.29})$$

$$\partial_a A_r a = (-1)^r (n - 2r) A_r, \quad (\text{B.30})$$

$$\partial_a a \cdot A_r = r A_r, \quad (\text{B.31})$$

§B.3 Linear Algebra

Let a, b, c be vectors, $\underline{f}(A)$ be the linear function with the multivector A in its argument and $\bar{f}(A)$ be its adjoint, from the definition in Eq. (2.9), it follows that

$$\bar{f}(a) = \partial_b \langle \underline{h}(b)a \rangle \quad (\text{B.32})$$

Eq. (B.32) is frequently employed perform algebraic manipulations of linear functions. The advantage is that all manipulations are frame-frame. We note that the ∂_a and a vectors can be replaced by the sum over a set of constant frame vectors and their reciprocals, if required.

Linear functions extend to act on multivectors via

$$\underline{f}(a \wedge b \wedge \dots \wedge c) \equiv \underline{f}(a) \wedge \underline{f}(b) \wedge \dots \wedge \underline{f}(c) \quad (\text{B.33})$$

so that \underline{f} is a grade-preserve linear function mapping multivectors to vectors.

In particular, since the pseudoscalar \mathcal{I} is unique to a scale factor, we define

$$\det(\underline{f}) = \underline{f}(\mathcal{I})\mathcal{I}^{-1} \quad (\text{B.34})$$

From the Eq. (B.33) and (B.34), the following identities hold:

$$f(a \wedge b \wedge \dots \wedge c) = f(a) \wedge f(b) \wedge \dots \wedge f(c) , \quad (\text{B.35})$$

$$f(\mathcal{I}) = \det(f)\mathcal{I} , \quad (\text{B.36})$$

$$\bar{f}(b) = \partial_a f(a) \cdot b , \quad (\text{B.37})$$

$$f(A_r) \cdot B_s = f[A_r \cdot \bar{f}(B_s)] \quad (r \geq s) , \quad (\text{B.38})$$

$$A_r \cdot \bar{f}(B_s) = \bar{f}[f(A_r) \cdot B_s] \quad (r \leq s) , \quad (\text{B.39})$$

$$f^{-1}(A) = \det(f)^{-1} \mathcal{I} \bar{f}(\mathcal{I}^{-1} A) , \quad (\text{B.40})$$

$$\bar{f}^{-1}(A) = \det(f)^{-1} \mathcal{I} f(\mathcal{I}^{-1} A) , \quad (\text{B.41})$$

$$\partial_{\bar{h}(a)} \det \underline{h}^{-1} = -\det \underline{h}^{-1} \underline{h}^{-1}(a) , \quad (\text{B.42})$$

$$\partial_{\bar{h}(a)} \underline{h}^{-1}(b) \cdot v = -\underline{h}^{-1}(a) \cdot v \underline{h}^{-1}(b) . \quad (\text{B.43})$$

Appendix C

Identities in Cosmological Perturbation Theory

§C.1 Differential Identities in the PSTF Approach

We will summarize the following covariant linearized identities on a Friedmann background used in [31, 134, 135, 137, 138], which are useful for the derivation of the propagation and evolution equations in chapter 3.

The following linearized identities with the operation of curl and div, which is valid for any arbitrary first order PSTF vector, V_a , tensor, S_{ab} , and arbitrary

scalar f with first order projected gradients are summarized as follows:

$$\text{curl}D_a f = -2\dot{f}\omega_a , \quad (\text{C.1})$$

$$D^2(D_a f) = D_a(D^2 f) + \frac{2K}{a^2}D_a f + 2\dot{f}\text{curl}\omega_a , \quad (\text{C.2})$$

$$(D_a f)^\cdot = D_a \dot{f} - HD_a f + \dot{f}A_a , \quad (\text{C.3})$$

$$(aD_a V_b \dots)^\cdot = aD_a \dot{V}_b \dots , \quad (\text{C.4})$$

$$(D^2 f)^\cdot = D^2 \dot{f} - 2HD^2 f + \dot{f}D^a A_a , \quad (\text{C.5})$$

$$D_{[a}D_b]V_c = \frac{K}{a^2}V_{[a}h_{b]c} , \quad (\text{C.6})$$

$$D_{[a}D_b]S^{cd} = \frac{2K}{a^2}S_{[a}{}^{(c}h_{b]}{}^{d)} , \quad (\text{C.7})$$

$$D^a \text{curl}V_a = 0 , \quad (\text{C.8})$$

$$\text{curl}\text{curl}V_a = D_a(D^b V_b) - D^2 V_a + \frac{2K}{a^2}V_a , \quad (\text{C.9})$$

$$(\text{curl}S_{ab})^\cdot = \text{curl}\dot{S}_{ab} - \frac{1}{3}\Theta \text{curl}S_{ab} , \quad (\text{C.10})$$

$$(D^a S_{ab})^\cdot = D^a \dot{S}_{ab} - \frac{1}{3}\Theta D^a S_{ab} , \quad (\text{C.11})$$

$$D^a(\text{curl}S_{ab}) = \frac{1}{2}\text{curl}(D^a S_{ab}) , \quad (\text{C.12})$$

$$\text{curl}(\text{curl}S_{ab}) = -D^2 S_{ab} + \frac{3}{2}D_{\langle a}D^c S_{b\rangle c} + \frac{3K}{a^2}S_{ab} , \quad (\text{C.13})$$

where the vectors and tensors vanish in the background, i.e. $S_{ab} = S_{\langle ab \rangle}$ and all the identities except (C.1) are linearized.

The identities in [31] are also useful for the evaluation of the curl quantities for parity tensor harmonics are also summarized here:

$$\text{curl}Q_{ab} = \frac{k}{a} \left(1 + \frac{3K}{k^2}\right)^{1/2} \bar{Q}_{ab}^{(k)} , \quad (\text{C.14})$$

$$\text{curl}\bar{Q}_{ab} = \frac{k}{a} \left(1 + \frac{3K}{k^2}\right)^{1/2} Q_{ab} . \quad (\text{C.15})$$

§C.2 The identities for the harmonics

§C.2.1 Scalar Harmonics

As in [22, 79, 108], we define the scalar harmonics as being eigenfunctions of the covariantly Laplace-Beltrami operator.

$$D^2 Q \equiv D_a D^a Q = - \left(\frac{k}{a} \right)^2 Q, \quad (\text{C.16})$$

where we have dropped the index k from the Q s. One can use the scalar harmonic to expand scalars, and with this we define the following vector which correspond to the definition in [108].

$$Q_a = - \frac{a}{k} D_a Q, \quad (\text{C.17})$$

and a trace-free symmetric tensor,

$$Q_{ab} = \left(\frac{a}{k} \right)^2 D_b D_a Q + \frac{1}{3} h_{ab} Q. \quad (\text{C.18})$$

These harmonics are defined to have the following feature:

$$\dot{Q} = \dot{Q}_a = \dot{Q}_{ab} = 0, \quad (\text{C.19})$$

and by the above property, we can apply the commutations in [66] to get

$$D_{[a} D_{b]} Q = -\omega_{ab} \dot{Q} = 0, \quad (\text{C.20})$$

$$D_{[a} D_{b]} Q_c = - \frac{K}{2a} (h_{ac} Q_b - h_{bc} Q_a), \quad (\text{C.21})$$

$$D_{[a} D_{b]} Q_{cd} = \frac{K}{2a^2} [(h_{ac} Q_{bd} - h_{bc} Q_{ad}) + (h_{ad} Q_{bc} - h_{bd} Q_{ac})]. \quad (\text{C.22})$$

We derive the properties of the scalar harmonics, by making use of the projected

(spatial) covariant derivative, D^a ,

$$D_a Q^a = \left(\frac{k}{a}\right) Q, \quad (\text{C.23})$$

$$D^2 Q_a = -\left(\frac{k^2 - 2K}{a^2}\right) Q_a, \quad (\text{C.24})$$

$$D_b Q_a = -\frac{k}{a} \left(Q_{ab} - \frac{1}{3} h_{ab} Q\right), \quad (\text{C.25})$$

$$Q^a{}_a = 0, \quad (\text{C.26})$$

$$D^b Q_{ab} = \frac{2}{3} \left(\frac{1}{ka}\right) (k^2 - 3K) Q_a, \quad (\text{C.27})$$

$$D^a D^b Q_{ab} = \frac{2}{3} \left(\frac{1}{a^2}\right) (k^2 - 3K) Q, \quad (\text{C.28})$$

$$D_b D^c Q_{ac} = \frac{2}{3} \left(\frac{1}{a^2}\right) (3K - k^2) \left(Q_{ab} - \frac{1}{3} h_{ab} Q\right), \quad (\text{C.29})$$

$$D^2 Q_{ab} = \left(\frac{6K - k^2}{a^2}\right) Q_{ab}. \quad (\text{C.30})$$

§C.2.2 Vector Harmonics

These harmonics are defined as eigenfunctions of the Helmholtz equation:

$$D^2 Q_a = -\left(\frac{k}{a}\right)^2 Q_a, \quad (\text{C.31})$$

with Q_a being the solenoidal vector, i.e.

$$D_a Q^a = 0. \quad (\text{C.32})$$

From this, we can construct a symmetric trace-free tensor,

$$Q_{ab} = -\frac{a}{2k} (D_b Q_a + D_a Q_b), \quad (\text{C.33})$$

and we note that both these harmonics are covariantly constant along the flow lines

$$\dot{Q}_a = \dot{Q}_{ab} = 0. \quad (\text{C.34})$$

The following relations hold for the defined tensor Q_{ab} (equation (C.33)) from

Q_a in this section:

$$Q^a{}_a = 0 , \tag{C.35}$$

$$D^b Q_{ab} = \frac{1}{2} \left(\frac{1}{ka} \right) (k^2 - 2K) Q_a , \tag{C.36}$$

$$D_b D^c Q_{ac} + D_a D^c Q_{bc} = - \left(\frac{k^2 - 2K}{a^2} \right) Q_{ab} , \tag{C.37}$$

$$D^2 Q_{ab} = - \left(\frac{k^2 - 4K}{a^2} \right) . \tag{C.38}$$

Note that Q_a and Q_{ab} also satisfy relations (C.21) and (C.22) respectively.

§C.2.3 Tensor Harmonics

For tensor harmonics, we define again

$$D^2 Q_{ab} = - \left(\frac{k}{a} \right)^2 Q_{ab} , \tag{C.39}$$

and $\dot{Q}_{ab} = 0$. The tensor is also trace-free and divergenceless,

$$Q^a{}_a = 0 , \tag{C.40}$$

$$D^b Q_{ab} = 0 . \tag{C.41}$$

Bibliography

- [1] ABEL, S., & RUSSELL, J. M. 2000. The Search for Extra Dimensions. *Physics World*, **Nov**, 39.
- [2] ALÉ, M.G., & CHIMENTO, L.P. 1995. Self-Consistent Solutions of the Semi-classical Einstein-Dirac equations with Cosmological Constant. *Class. Quan. Grav.*, **12**, 101.
- [3] ALBRECHT, A., & STEINHARDT, P.J. 1982. Cosmology for Grand Unified Theories with Radiatively Induced Symmetry Breaking. *Phys. Rev. Lett.*, **48**, 1220.
- [4] ANCHORDOQUI, L., NUNEZ, C., & OLSEN, K. 2000. Quantum Cosmology and ADS/CFT. *JHEP*, **10**, 50.
- [5] ANTONIADIS, I., ARKANI-HAMED, N., DIMOPOULOUS, S., & DVALI, G. 1998. New Dimensions at a Millimeter to a Fermi and Superstrings at a TEV. *Phys. Lett. B*, **436**, 257.
- [6] ARKANI-HAMED, N., DIMOPOULOUS, S., & DVALI, G. 1998. The Hierarchy Problem and New Dimensions at a Millimeter. *Phys. Lett. B*, **429**, 263.
- [7] BANKS, T., & FISCHLER, W. 2001. An Holographic Cosmology. *hep-th/0111142*.
- [8] BARDEEN, J. 1980. Gauge-Invariant Cosmological Perturbations. *Phys. Rev. D*, **22**, 1882.
- [9] BARROW, J., & MAARTENS, R. 2002. Kaluza-Klein Anisotropy in the CMB. *Phys. Lett. B*, **532**, 153.
- [10] BAUMANN, D., LEONG, B., & SASLAW, W. 2003. Universes that change their global symmetry. *MNRAS*, **345**, 552.
- [11] BERTSCHINGER, E. 1993. Cosmological Dynamics. *Les Houches Lectures on Cosmology and Large Scale Structure*, **60**, 273.

- [12] BINETRUY, P., DEFFAYET, C., ELLWANGER, U., & LANGLOIS, D. 2000. Brane cosmological evolution in a bulk with cosmological constant. *Phys. Lett. B*, **477**, 285.
- [13] BOJOWALD, M. 2002. Inflation from Quantum Geometry. *gr-qc/0206054*.
- [14] BOND, J., & ET AL. 2000. CMB Analysis of BOOMERANG & MAXIMA and the Cosmic Parameters, Ω_{TOT} , Ω_B , H^2 , Ω_{CDM} , H^2 , Ω_Λ , N_S . *astro-ph/0011378*.
- [15] BONDI, H. 1947. Spherically Symmetrical Models in General Relativity. *MNRAS*, **107**, 410.
- [16] BONNOR, W., & VICKERS, P. 1981. Junction Conditions in General Relativity. *Gen. Rel. Grav.*, **13**, 29.
- [17] BRANDENBERGER, R., & VAFA, C. 1989. Superstrings in the Early Universe. *Nucl. Phys. B*, **316**, 391.
- [18] BRATT, J., GAULT, A., SCHERRER, R., & WALKER, T. 2002. Big Bang Nucleosynthesis Constraints on Brane Cosmologies. *astro-ph/0208133*.
- [19] BRAX, P., VAN DE BRUCK, C., & DAVIS, A. 2001. Brane-World Cosmology, Bulk Scalars and Perturbations. *JHEP*, **10**, 26.
- [20] BRIDGMAN, H., MALIK, K., & WANDS, D. 2002. Cosmological Perturbations in the Bulk and on the Brane. *Phys. Rev. D*, **65**, 043502.
- [21] BRUNI, M., & DUNSBY, P. 2002. Singularities on the Brane aren't isotropic. *hep-th/0207189*.
- [22] BRUNI, M., DUNSBY, P., & ELLIS, G. 1992a. Cosmological Perturbations and the Physical Meaning of Gauge Invariant Variables. *ApJ*, **395**, 34.
- [23] BRUNI, M., ELLIS, G., & DUNSBY, P. 1992b. Gauge-Invariant Perturbations in a Scalar Field Dominated Universe. *Class. Quan. Grav.*, **9**, 921.
- [24] BUCHER, M., MOODLEY, K., & TUROK, N. 2000. The General Primordial Cosmic Perturbation. *Phys. Rev. D*, **62**, 083508.
- [25] CARR, B. 2000. A Classification of Spherically Symmetric Self-Similar Dust Models. *Phys. Rev. D*, **62**, 044022.
- [26] CARR, B., & COLEY, A. 2000. A Complete Classification of Spherically Symmetric Perfect Fluid Similarity Solutions. *Phys. Rev. D*, **D62**, 044023.
- [27] CARROLL, S. 2000. The Cosmological Constant. *astro-ph/0004075*.

- [28] CARTAN, E. 1922. Sur un généralisation de la notion de courbure de Riemann et les espaces à torsion. *C. R. Acad. Sci. (Paris)*, **174**, 593.
- [29] CHALLINOR, A. 1998. Applications of Geometric Algebra in Physics and Cosmology. *Ph.D. Thesis, Cambridge*.
- [30] CHALLINOR, A. 2000a. The Covariant Perturbative Approach to Cosmic Microwave Background Anisotropies. *Gen. Rel. Grav.*, **32**, 1059.
- [31] CHALLINOR, A. 2000b. Microwave Background Anisotropies from Gravitational Waves: the (1+3) Covariant Approach. *Class. Quan. Grav.*, **17**, 871.
- [32] CHALLINOR, A. 2000c. Microwave Background Polarization in Cosmological Models. *Phys. Rev. D*, **62**, 043004.
- [33] CHALLINOR, A., & LASENBY, A. 1998. A Covariant and Gauge-Invariant of CMB anisotropies from scalar perturbations. *Phys.Rev. D*, **58**, 023001.
- [34] CHALLINOR, A., & LASENBY, A. 1999. Cosmic Microwave Background Anisotropies in the Cold Dark Model : A Covariant and Gauge Invariant Approach. *ApJ*, **513**, 1.
- [35] CHALLINOR, A., LASENBY, A., DORAN, C., & GULL, S. 1997. Massive Non-Ghost solutions for the Dirac field coupled self-consistently to Gravity. *Gen. Rel. Grav.*, **29**, 1527.
- [36] CHANDRASEKHAR, S. 1972. A Limiting Case of Relativistic Equilibrium. *General Relativity edited by L. O’Raifeartaigh, Oxford University Press*.
- [37] CHIMENTO, L., JAKUBI, A., & PENSA, F. 7. Cosmological solutions of the semiclassical Einstein-Dirac equations. *Class. Quan. Grav.*, **1561**, 1990.
- [38] CHO, Y. 2000. Gauge Theory of Poincaré symmetry. *Phys. Rev. D*, **62**, 043004.
- [39] CLIFFORD, W. 1878. Applications of Grassmann’s extensive algebra. *Am. J. Math*, **1**, 350.
- [40] C. MISNER, THORNE, K., & WHEELER, J.A. 1973. *Gravitation*. Freeman Press.
- [41] COPELAND, E., LIDDLE, A., & LIDSEY, J. 2001. Steep inflation: ending braneworld inflation by gravitational particle production. *Phys. Rev. D*, **64**, 023509.

- [42] DADHICH, N. 1996. A Conformal Mapping and Isothermal Perfect Fluid Model. *Gen. Rel. Grav.*, **28**, 1455.
- [43] DE BEAUREGARD, O. COSTA. 1963. Translational Inertia Spin Effect. *Phys. Rev.*, **129(1)**, 466.
- [44] DEFFAYET, C. 2002. On Brane World Cosmological Perturbations. *hep-th/0205084*.
- [45] DERUELLE, N., DOLEZEL, T., & KATZ, J. 2001. Perturbations of Brane Worlds. *Phys. Rev. D*, **63**, 083513.
- [46] DIMAKIS, A., & MÜLLER-HOISSEN, F. 1982. Massive Ghost Dirac fields in Einstein-Cartan theory. *Phys. Lett. A*, **92**, 431.
- [47] DIMAKIS, A., & MÜLLER-HOISSEN, F. 1985. Solutions of the Einstein-Cartan-Dirac equations with vanishing energy-momentum tensor. *J. Math. Phys.*, **26**, 1040.
- [48] DORAN, C., LASENBY, A., GULL, S., & SOMAROO, S. 1996. Spacetime Algebra and Electron Physics. *Adv. Imag. and Elect. Phys.*, **95**, 271.
- [49] DORAN, C., LASENBY, A., CHALLINOR, A., & GULL, S. 1998. Effects of Spin-Torsion in Gauge Theory Gravity. *J. Math. Phys.*, **39(3)**, 3303.
- [50] DORCA, M., & VAN DE BRUCK, C. 2001. Cosmological Perturbations in Brane Worlds: Brane Bending and Anisotropic Stresses. *Nucl. Phys. B*, **605**, 215.
- [51] DUNSBY, P. 1991. Gauge Invariant Perturbations in Multi-Component Fluid Cosmologies. *Class. Quan. Grav.*, **8**, 1785.
- [52] DUNSBY, P. 1997. A Fully Covariant Description of CMB Anisotropies. *Class. Quan. Grav.*, **14**, 3391.
- [53] DUNSBY, P., & BRUNI, M. 1994. General conserved quantities in perturbed inflationary universes. *International Journal of Modern Physics*, **D3**, 443.
- [54] DUNSBY, P., BASSETT, B., & ELLIS, G. 1997. Covariant Characterisation of Gravitational Waves in Cosmology. *Class. Quan. Grav.*, **14**, 1215.
- [55] DYER, C., & OLIWA, C. 2000. The "Swiss cheese" Cosmological Model has no Extrinsic Curvature Discontinuity: A comment on the paper by G.A. Baker, Jr. *astro-ph/0004090*.

- [56] EGUCHI, T., GILKEY, P., & HANSON, A. 1980. Gravitation, Gauge Theories and Differential Geometry. *Phys. Rep.*, **66(6)**, 213.
- [57] EHLERS, J. 1993. Contributions to the Relativistic Mechanics of Continuous Media. *Gen. Rel. Grav.*, **25**, 1225.
- [58] EINSTEIN, A., & STRAUSS, E. 1945. The Influence of the Expansion of Space on the Gravitational Fields surrounding the Individual Stars. *Rev. Mod. Phys.*, **17**, 120.
- [59] ELLIS, G. 1971. Relativistic Cosmology. *General Relativity and Cosmology. Proceedings of the International School of Physics, "Enrico Fermi", Course XLVII*, Academic Press, 104.
- [60] ELLIS, G. 1973. Relativistic Cosmology. *Cargèse Lectures in Physics, Gordon and Breach, New York*, **6**.
- [61] ELLIS, G., & BRUNI, M. 1989. Covariant and Gauge Invariant Approach to Cosmological Density Fluctuations. *Phys. Rev. D*, **40**, 1804.
- [62] ELLIS, G., & ELST, H. VAN. 1998. Cosmological Models. *Cargèse Lectures in Physics, gr-qc/9812046*.
- [63] ELLIS, G., MATRAVERS, D., & TRECIOKAS, R. 1983a. Anisotropic solutions of the Einstein-Boltzmann equations 1: General Formalism. *Ann. Phys.*, **150**, 455.
- [64] ELLIS, G., TRECIOKAS, R., & MATRAVERS, D. 1983b. Anisotropic solutions of the Einstein-Boltzmann equations 2: Some Exact Properties of the equations. *Ann. Phys.*, **150**, 487.
- [65] ELLIS, G., HWANG, J., & BRUNI, M. 1989. Covariant and Gauge-Independent Perfect-Fluid Robertson-Walker Perturbations. *Phys. Rev. D*, **40**, 1819.
- [66] ELLIS, G., BRUNI, M., & HWANG, J. 1990. Density-Gradient-Vorticity relation in Perfect-Fluid Robertson-Walker Perturbations. *Phys. Rev. D*, **42**, 1035.
- [67] EMDEN, R. 1907. *Gaskugeln*. Leipzig, Teubner.
- [68] FAYOS, F., SENOVILLA, J., & TORRES, R. 1996. General Matching of Two Spherically Symmetric Space-times. *Phys. Rev. D*, **54**, 4862.

- [69] FUKUDA, Y., & THE SUPER-KAMIONKANDE COLLABORATION. 1998. Evidence for Oscillation of Atmospheric Neutrinos. *Phys. Rev. Lett.*, **81**, 1562.
- [70] GARECKI, J. 2001. Is Torsion needed in Theory of Gravity? *gr-qc/0103029*.
- [71] GARRIGA, J., & SASAKI, M. 2000. Braneworld Creation and Black Holes. *Phys. Rev. D*, **62**, 043523.
- [72] GASPERINI, M., & VENEZIANO, G. 2002. The Pre-Big Bang Scenario in String Cosmology. *hep-th/0207130*.
- [73] GEBBIE, T., & ELLIS, G. 1998. 1+3 Covariant Cosmic Microwave Background Anisotropies I: Algebraic Relations for Mode and Multipole Representations. *astro-ph/9804316*.
- [74] GEBBIE, T., DUNSBY, P., & ELLIS, G. 1999. 1+3 Covariant Cosmic Microwave Background Anisotropies I: The Almost Friedmann-Lemaitre Model. *astro-ph/9904408*.
- [75] GIUDICE, G., KOLB, E., LESGOURGUES, J., & RIOTTO, A. 2002. Trans-dimensional Physics and Inflation. *hep-ph/0207145*.
- [76] GORBUNOV, D., RUBAKOV, V., & SIBIRYAKOV, S. 2001. Gravity Waves from Inflating Brane or Mirrors moving in AdS₅. *JHEP*, **10**, 15.
- [77] GORDON, C., & MAARTENS, R. 2001. Density Perturbations in the Brane World. *Phys. Rev. D*, **63**, 044022.
- [78] GUTH, A. 1981. The Inflationary Universe: A Possible Solution to the Horizon and Flatness problems. *Phys. Rev. D*, **23**, 347.
- [79] HAWKING, S. 1966. Perturbations of an Expanding Universe. *ApJ*, **145**, 544.
- [80] HAWKING, S., HERTOG, T., & REALL, H. 2000. Brane New World. *Phys. Rev. D*, **62**, 043501.
- [81] HAYASHI, T., & SHIRAFUJI, T. 1980. Gravity from Poincaré Symmetry I. *Prog. Theor. Phys.*, **64(3)**, 866.
- [82] HEHL, F., VON DER HEYDE, P., & KERLICK, G. 1961. General Relativity with Spin and Torsion and its deviations from Einstein's theory. *Phys. Rev. D*, **12**, 212.
- [83] HEHL, F., VON DER HEYDE, P., KERLICK, G., & NESTER, J. 1976. General Relativity with Spin and Torsion: Foundations and Prospects. *Rev. Mod. Phys.*, **48**, 393.

- [84] HENNEAUX, M. 1980. Bianchi type-I Cosmologies and Spinor fields. *Phys. Rev. D*, **21**, 857.
- [85] HESTENES, D. 1966. *Space-Time Algebra*. Gordon and Breach, New York.
- [86] HESTENES, D. 1975. Observables, operators, and complex numbers in the Dirac theory. *J. Math. Phys.*, **16(3)**, 556.
- [87] HESTENES, D. 1999. *New Foundations for Classical Mechanics, 2nd Ed.* Kluwer Press.
- [88] HESTENES, D., & SOBCZYK, G. 1984. *Clifford Algebra to Geometric Calculus*. Kluwer Press.
- [89] HOGAN, P. 1990. McVittie's Mass Particle in an Expanding Universe and related solutions of Einstein's equations. *ApJ*, **360**, 315.
- [90] HOLLANDS, S., & WALD, R. 2002. An Alternative to Inflation. *Gravity Research essay, gr-qc/0205058*.
- [91] HORAVA, P., & WITTEN, E. 1996. Heterotic and Type I String Dynamics from Eleven Dimensions. *Nucl. Phys. B*, **460**, 506.
- [92] HU, W. 1996. Wandering in the Background: A CMB Explorer. *Ph.D. Thesis, UC Berkeley, astro-ph/9508126*.
- [93] HU, W., SUGIYAMA, N., & SILK, J. 1997. The Physics of CMB Anisotropies. *Nature*, **386**, 37.
- [94] HUBBLE, E., & HUMASON, M. 1931. The Velocity-Distance Relation among Extra-Galactic Nebulae. *Chicago*.
- [95] HUEY, G., & LIDSEY, J. E. 2002. Inflation and Braneworlds: Degeneracies and Consistencies. *astro-ph/0205236*.
- [96] ISHAM, C., & NELSON, J. 1974. Quantization of a coupled Fermi field and Robertson-Walker metric. *Phys. Rev. D*, **10(10)**, 3226.
- [97] IVANENKO, D., & SARDANASHVILY, G. 1983. The Gauge Treatment of Gravity. *Phys. Rep.*, **94(1)**, 1.
- [98] IVANOV, E., & NIEDERLE, J. 1982. Gauge Formulation of Gravitation theories I: The Poincaré, de Sitter, and Conformal cases. *Phys. Rev. D*, **25(4)**, 976.

- [99] KALUZA, T. 1921. On the Problem of Unity in Physics. *Sitzungsber. Preuss. Akad. Wiss. Berlin (Math.Phys.)*, **K1**, 966.
- [100] KANNO, S., & SODA, J. 2002a. Brane World Effective Action at Low Energies and AdS/CFT. *hep-th/0205208*.
- [101] KANNO, S., & SODA, J. 2002b. Radion and Holographic Brane Gravity. *hep-th/0207029*.
- [102] KERLICK, G. 1975. Cosmology and Particle Pair production via Gravitational Spin-Spin Interaction in the Einstein-Cartan-Sciama-Kibble theory of Gravity. *Phys. Rev. D*, **12**, 212.
- [103] KERLICK, G. 1976. "Bouncing" of Simple Cosmological Models with Torsion. *Ann. Phys.*, **99**, 127.
- [104] KHOURY, J., OVRUT, B., STEINHARDT, P., & TUROK, N. 2001. The Ekpyrotic Universe : Colliding Branes and the Origin of Hot Big Bang. *Phys. Rev. D*, **64**, 123522.
- [105] KIBBLE, T. 1961. Lorentz invariance and the gravitational field. *J. Math. Phys.*, **2(3)**, 212.
- [106] KLEIN, O. 1926. Quantum Theory and Five-Dimensional Theory of Relativity. *Z. Phys.*, **37**, 895.
- [107] KODAMA, H. 2000. Behavior of Cosmological Perturbations in the Brane-World Model. *hep-th/0012132*.
- [108] KODAMA, H., & SASAKI, M. 1984. Cosmological Perturbation Theory. *Prog. Theor. Phys.*, **78**, 1.
- [109] KOLB, E., & TURNER, M. 1993. *The Early Universe*. Perseus Publishing.
- [110] KOYAMA, K. 2002. Radion and Large Scale Anisotropy on the Brane. *gr-qc/0204047*.
- [111] KOYAMA, K., & SODA, J. 2002. Bulk Gravitational Field and Cosmological Perturbations on the Brane. *Phys. Rev. D*, **65**, 023514.
- [112] KRAMER, D., STEPHANI, H., MACCALLUM, M., & HERTL, E. 1980. *Exact Solutions of Einstein's Field Equations*. Cambridge University Press.
- [113] KRANSINSKI, A. 1997. *Inhomogeneous Cosmological Models*. Cambridge University Press.

- [114] LANDAU, & LIFSHITZ. 1975. *The Classical Theory of Fields*. Pergamon Press.
- [115] LANGE, A., & ET AL. 2000. Cosmological Parameters from the first results of BOOMERANG. *Phys. Rev. D*, **62**, 084023.
- [116] LANGLOIS, D. 2000. Brane Cosmological Perturbations. *Phys. Rev. D*, **62**, 126012.
- [117] LANGLOIS, D., MAARTENS, R., & WANDS, D. 2000. Gravitational Wave from Inflation on the Brane. *Phys. Lett. B*, **489**, 259.
- [118] LANGLOIS, D., MAARTENS, R., SASAKI, M., & WANDS, D. 2001. Large Scale Cosmological Perturbations on the Brane. *Phys. Rev. D*, **63**, 084009.
- [119] LANGLOIS, D., SORBO, L., & RODRIGUEZ-MARTINEZ, M. 2002. Cosmology of a Brane radiating gravitons into the Extra Dimension. *hep-th/0206146*.
- [120] LASENBY, A., DORAN, C., & GULL, S. 1993. A Multivector Derivative Approach to Lagrangian Field Theory. *J. Math. Phys.*, **34(8)**, 3642.
- [121] LASENBY, A., DORAN, C., & GULL, S. 1998. Gravity, Gauge Theories and Geometric Algebra. *Phil. Trans. R. Soc. Lond. A*, **356**, 487.
- [122] LASENBY, A., DORAN, C., HOBSON, M., DABROWSKI, Y., & CHALLINOR, A. 1999. Microwave background anisotropies and non-linear structures - I. Improved Theoretical Models. *MNRAS*, **302**, 748.
- [123] LEONG, B., DUNSBY, P., CHALLINOR, A., & LASENBY, A. 2002a. 1+3 Covariant Dynamics of Scalar Perturbations in Brane-worlds. *Phys. Rev. D*, **65**, 104012.
- [124] LEONG, B., CHALLINOR, A., MAARTENS, R., & LASENBY, A. 2002b. Braneworld Tensor Anisotropies in the CMB. *Phys. Rev. D*, **66**, 104010.
- [125] LEWIS, A. 2000. Geometric Algebra and Covariant Methods in Physics and Cosmology. *Thesis, University of Cambridge*.
- [126] LEWIS, A., CHALLINOR, A., & LASENBY, A. 2000. Efficient Computation of CMB Anisotropies in Closed FRW models. *ApJ*, **538**, 473.
- [127] LIDDLE, A., & LYTH, D. 2000. *Cosmological Inflation and Large-Scale Structure*. Cambridge University Press.
- [128] LIDDLE, A., & TAYLOR, A. 2002. Inflaton Potential Reconstruction in the Braneworld Scenario. *Phys. Rev. D*, **65**, 041301.

- [129] LINDE, A. 1982. A New Inflationary Universe Scenario: a Possible Solution of the Horizon, Flatness, Homogeneity, Isotropy and Primordial Monopole Problems. *Phys. Lett. B*, **108**, 389.
- [130] LINDE, A. 1983. Chaotic Inflation. *Phys. Lett. B*, **129**, 177.
- [131] LONGAIR, M. 1998. *Galaxy Formation*. Springer Verlag.
- [132] LYTH, D., & WANDS, D. 2002. Generating the Curvature Perturbation without an Inflation. *Phys. Lett. B*, **524**, 5.
- [133] MA, C., & BERTSCHINGER, E. 1995. Cosmological Perturbation theory in the Synchronous and Conformal Newtonian Gauges. *ApJ*, **455**, 7.
- [134] MAARTENS, R. 1998. Covariant Velocity and Density Perturbations in Quasi-Newtonian Cosmologies. *Phys. Rev. D*, **58**, 124006.
- [135] MAARTENS, R. 2000. Cosmological Dynamics on the Brane. *Phys. Rev. D*, **62**, 084023.
- [136] MAARTENS, R. 2001. Geometry and Dynamics of The Brane World. *gr-qc/0101059*.
- [137] MAARTENS, R., & BASSETT, B. 1998. Gravitoelectromagnetism. *Class. Quan. Grav.*, **15**, 705.
- [138] MAARTENS, R., & TRIGINER, J. 1997. Density Perturbations with Relativistic Dynamics. *Phys. Rev. D*, **56**, 4640.
- [139] MAARTENS, R., ELLIS, G., & STOEGER, W. 1995. Limits on Anisotropy and Inhomogeneity from the Cosmic Background Radiation. *Phys. Rev. D*, **51**, 1525.
- [140] MAARTENS, R., GEBBIE, T., & ELLIS, G. 1999. Cosmic Microwave Background Anisotropies: Nonlinear Dynamics. *Phys. Rev. D*, **59**, 083506.
- [141] MAARTENS, R., WANDS, D., BASSETT, B., & HEARD, I. 2000. Chaotic Inflation on the Brane. *Phys. Rev. D*, **62**, 041301.
- [142] MANSOURI, F., & CHANG, L. 1976. Gravitation as a Gauge Theory. *Phys. Rev. D*, **13(12)**, 3192.
- [143] MARS, M. 1998. Axially Symmetric Einstein-Straus Models. *Phys. Rev. D*, **57**, 3389.

- [144] MATRAVERS, D., & HUMPHREYS, N. 2001. Matching Spherical Dust Solutions to Construct Cosmological Models. *Gen. Rel. Grav.*, **33**, 531.
- [145] MCVITTIE, G. 1933. The Mass Particle in an Expanding Universe. *MNRAS*, **93**, 326.
- [146] MCVITTIE, G. 1984. Elliptic Functions in Spherically Symmetric Solutions of Einstein's equations. *Ann. Inst. Poincare*, **40**, 235.
- [147] MUKOHYAMA, S. 2000. Gauge Invariant Gravitational Perturbations of Maximally Symmetric Spacetimes. *Phys. Rev. D*, **62**, 084015.
- [148] MUKOHYAMA, S. 2001. Integro-Differential Equation for Brane-World Cosmological Perturbations. *Phys. Rev. D*, **64**, 064006.
- [149] NERONOV, A., & SACHS, I. 2001. On Metric Perturbations in Brane-World Scenarios. *Phys. Lett. B*, **513**, 173.
- [150] NOERDLINGER, P., & PETROSIAN, V. 1971. The Effect of Cosmological Expansion on Self-Gravitating Ensembles of Particles. *ApJ*, **168**, 1.
- [151] NOLAN, B. 1993. Sources for McVittie's mass particle in an expanding universe. *J. Math. Phys.*, **34**, 1.
- [152] OCHS, U., & SORG, M. 1995. Non-singular, cosmological solutions for the coupled Dirac Einstein equations. *J. Phys. A*, **28**, 7263.
- [153] PADMANABHAN, T. 1993. *Structure Formation in the Universe*. Cambridge University Press.
- [154] PADMANABHAN, T. 1996. *Cosmology and Astrophysics-through Problems*. Cambridge University Press.
- [155] PEACOCK, J. 1999. *Cosmological Physics*. Cambridge University Press.
- [156] PEEBLES, P. 1993. *Principles of Physical Cosmology*. Princeton University Press.
- [157] PENZIAS, A., & WILSON, R. 1965. A Measurement of Excess Antenna Temperature at 4080-MC/S. *ApJ*, **142**, 419.
- [158] PULLIN, J. 1989. Massive Solutions to Einstein-Cartan-Dirac theory. *Ann. Physik., Leipzig*, **45**, 559.
- [159] RADFORD, C., & KLOTZ, A. 16. An Exact Solution of the Einstein-Dirac equations. *J. Phys. A*, **317**, 1983.

- [160] RANDALL, L., & SUNDRUM, R. 1999. An Alternative to Compactification. *Phys. Rev. Lett.*, **83**, 4690.
- [161] RAYCHAUDHURI, A. 1979. *Theoretical Cosmology*, p. 96. Clarendon Press.
- [162] RIAZUELO, A., VERNIZZI, F., STEER, D., & DURRER, R. 2002. Gauge invariant cosmological perturbation theory for braneworlds. *hep-th/0205220*.
- [163] RUBAKOV, V. 2001. Large and Infinite Extra Dimensions. *hep-ph/0104152*.
- [164] RUBINO-MARTIN, JOSE ALBERTO, *et al.* . 2002. First results from the Very Small Array. IV: Cosmological parameter estimation. *Submitted to MNRAS*.
- [165] SAGO, N., HIMEMOTO, Y., & SASAKI, M. 2002. Quantum fluctuations in Brane-World Inflation without Inflaton on the Brane. *Phys. Rev. D*, **65**, 024014.
- [166] SAHNI, V., SAMI, M., & SOURADEEP, T. 2002. Relic Gravity Waves from Braneworld Inflation. *Phys. Rev. D*, **65**, 023518.
- [167] SASAKI, M., SHIROMIZU, T., & MAEDA, K. 2000. Gravity, Stability, and Energy Conservation on the Randall-Sundrum Brane World. *Phys. Rev. D*, **62**, 024008.
- [168] SASLAW, W. 1987. *Gravitational Physics of Stellar and Galactic Systems*. Cambridge University Press.
- [169] SASLAW, W. 2000a. *The Distribution of the Galaxies : Galaxy Clustering in Cosmology*. Cambridge University Press.
- [170] SASLAW, W. 2000b. Phase Transitions and Galaxy Clustering. *Phase Transitions in the Early Universe: Theory and Observations, NATO Science Series*, edited by H. Vega, M. Khalatnikov and N. Sanchez, Kluwer Press, **40**, 373.
- [171] SASLAW, W. 2000c. The Ultimate Phase Transition. *Phase Transitions in the Early Universe: Theory and Observations, NATO Science Series*, edited by H. Vega, M. Khalatnikov and N. Sanchez, Kluwer Press, **40**, 389.
- [172] SASLAW, W., MAHARAJ, S., & DADHICH, N. 1996. An Isothermal Universe. *ApJ*, **471**, 571.
- [173] SCIAMA, D. 1964. The Physical Structure of General Relativity. *Rev. Mod. Phys.*, **36**, 463.
- [174] SEITZ, M. 1985. On solutions of Einstein-Cartan-Dirac theory. *Class. Quan. Grav.*, **2**, 919.

- [175] SELJAK, U., & ZALDARRIAGA, M. 1996. A Line of Sight Approach to Cosmic Microwave Background Anisotropies. *ApJ*, **469**, 437.
- [176] SHIROMIZU, T., MAEDA, K., & SASAKI, M. 2000. The Einstein Equation on a 3-brane World. *Phys. Rev. D*, **62**, 024012.
- [177] SMOOT, G., & THE COBE TEAM. 1992. Structure in the COBE DMR First Year maps. *ApJ Lett.*, **396**, L1.
- [178] SODA, J., & KOYAMA, K. 2002. Cosmological Perturbations in Brane World - Brane view v.s. Bulk view. *hep-th/0205208*, *proceedings of the workshop "Braneworld - Dynamics of spacetime with boundary"*.
- [179] STAROBINSKY, A. 1985. Cosmic Background Anisotropy Induced by Isotropic, Flat Spectrum Gravitational-Wave Perturbations. *Sov. Astron. Lett.*, **11**, 3.
- [180] STOEGER, W., MAARTENS, R., & ELLIS, G. 1995. Proving almost-homogeneity of the Universe: an almost Ehlers-Geren-Sachs theorem. *ApJ*, **443**, 1.
- [181] TASGAS, C., & BARROW, J. 1997. A Gauge-Invariant Analysis of Magnetic Fields in General Relativistic Cosmology. *Class. Quan. Grav*, **14**, 2539.
- [182] TASGAS, C., & BARROW, J. 1998. Gauge-Invariant Magnetic Perturbations in Perfect fluid Cosmologies. *Class. Quan. Grav*, **15**, 3523.
- [183] TASGAS, C., & MAARTENS, R. 2000. Magnetized Cosmological Perturbations. *Phys. Rev. D*, **61**, 083519.
- [184] TOLMAN, R. 1939. Static Solutions of Einstein's Field Equations for Spheres of Fluid. *Phys. Rev.*, **55**, 365.
- [185] UTIYAMA, R. 1956. Invariant Theoretical Interpretation of Interaction. *Phys. Rev.*, **101**(5), 1597.
- [186] VAN DE BRUCK, C., & DORCA, M. 2000. On Cosmological Perturbations on a brane in an Anti-de Sitter Bulk. *hep-th/0012073*.
- [187] VAN DE BRUCK, C., DORCA, M., MARTINS, C., & PARRY, M. 2000a. Cosmological Consequences of the Brane/Bulk interaction. *Phys. Lett. B.*, **495**, 183.
- [188] VAN DE BRUCK, C., DORCA, M., BRANDENBERGER, R., & LUKAS, A. 2000b. Cosmological Perturbations in Brane World Theories : Formalism. *Phys. Rev. D*, **62**, 123515.

- [189] WEINBERG, S. 1972. *Gravitation and Cosmology*. Wiley, New York.
- [190] WESSON, P. 1989. A Class of Solutions in General Relativity of Interest for Cosmology and Astrophysics. *ApJ*, **336**, 58.
- [191] WESSON, P., & DE LEON, J. PONCE. 1988. Cosmological Solution of Einstein's equations with uniform density and non-uniform pressure. *Phys. Rev. D*, **39**, 2.
- [192] WEYL, H. 1950. A remark on the coupling of Gravitation and Electron. *Phys. Rev*, **77(5)**, 699.
- [193] WEYSSENHOFF, J., & RAABE, A. 1947. Relativistic Dynamics of Spin Fluids and Spin Particles. *Acta Phys. Pol.*, **9**, 7.
- [194] WOLF, C. 1995. The Effects of Spin Torsion generated Torsion on the early Universe's evolution. *Gen. Rel. Grav.*, **27**, 1031.